Universität für Bodenkultur Wien

University of Natural Resources and Life Sciences, Vienna

Department for Agrobiotechnology, IFA- Tulln

Institute for Environmental Biotechnology

INCREASING THE REACTIVITY OF KRAFT LIGNIN BY IMPLEMENTING BIOBASED PROCESSES

Master Thesis

Submitted by

Mohammed Faraaz Ali
11824416
Vienna, 2020

Supervisors

Univ. Prof. DI Dr.techn. Georg Gübitz

Priv. Doz. Dr. Gibson Stephen Nyanhongo

ACKNOWLEDGEMENT

Firstly, I am thankful to God Almighty for his grace, wisdom and knowledge which has immensely helped me to complete the master thesis.

I would like to thank the following people, without whom I would not have been able to complete this research, and without whom I would not have made it through my masters degree.

The BET group at IFA, Tulln, especially my main supervisors, Doctor Georg Gübitz and Doctor Gibson Stephen Nyanhongo for their support, insights and scientific guidance during the master thesis. I would especially like to thank my tutor, Sebastian Alois Mayr whose support, patience, dedication, encouragement and assistance has been invaluable throughtout this research project. I am also thankful to BOKU university for giving me this wonderful opportunity to acquire deeper knowledge in the field of biotechnology.

Finally, I would like to thank my family and friends for their unconditional support, advice, understanding and encouragement in this very intense academic year.

ABSTRACT

Lignin, the most abundant natural aromatic biopolymer is highly heterogeneous with a complex structure. Although it comes along with certain limitations, it can potentially be used to produce various high value chemical products and serves as a raw material in industrial applications. In this master thesis, two processes were developed to increase the reactivity of both soft and hardwood kraft lignin samples. The first approach was fractionation through membrane filtration and the second one was microbial demethylation. The reactivity of the thus modified samples was tested by polymerization with a fungal laccase. The characterization of the samples by different analytical methods demonstrated differences in their reactivity. The fractionated samples showed higher phenol content compared to the demethylated samples. The highest phenol content after modification was obtained for both the retentate fractions which indicates higher reactivity due to higher phenolic group content. The decrease in fluorescence intensity of lignin moieties were significant for the fractionated samples validating higher reactivity to laccase mediated oxidation. The demethylation reaction intended to increase the phenolic group content in kraft lignin samples did not work as expected as the phenol content after modification was lower compared to the fractionated samples. The enzyme profile determined by SDS PAGE did not contain enzymes responsible for higher degree of demethylation. The differences in the chemical composition of the modified samples were determined by FTIR spectrum analysis. The results indicate that the fractionation process was more effective in increasing the reactivity of kraft lignin samples compared to the microbial demethylation process aimed at demethylation of the samples. The hardwood retentate fraction was more susceptible to modification compared to the softwood retentate fraction and thus was identified as the most reactive fraction.

KURZFASSUNG

Lignin ist das am häufigsten natürlich vorkommende, aromatische Biopolymer. Es ist sehr heterogen und besitzt eine komplexe Struktur. Obwohl es dadurch mit gewissen Einschränkungen verbunden ist, kann es potenziell zur Herstellung verschiedener, hochwertiger, chemischer Produkte verwendet werden. In dieser Masterarbeit wurden zwei Verfahren entwickelt, um die Reaktivität von sowohl Weich- als auch Hartholz Kraft Lignin Proben zu erhöhen. Der erste Ansatz war die Fraktionierung durch Membranfiltration und der zweite war die mikrobielle Demethylierung. Die Reaktivität der dadurch modifizierten Proben wurde durch Polymerisation mit einer durch einen Pilz erzeugten Laccase getestet. Die Charakterisierung der Proben mit verschiedenen Analysemethoden zeigte Unterschiede in ihrer Reaktivität auf. Die fraktionierten Proben zeigten im Vergleich zu den demethyliert Proben einen höheren Phenolgehalt. Der höchste Phenolgehalt nach der Modifikation wurde für beide Retentat Fraktionen erhalten, was auf eine höhere Reaktivität hinweist. Die Abnahme der Fluoreszenzintensität der Lignin Proben war für die fraktionierten Proben signifikant, was eine höhere Reaktivität bestätigte. Die Demethylierungsreaktion zur Erhöhung des Phenolgruppengehalts funktionierte nicht wie erwartet, da der Phenolgehalt nach der mikrobielle Demethylierung im Vergleich zu den fraktionierten Proben niedriger war. Das durch SDS-PAGE bestimmte Enzymprofil enthielt keine Enzyme, die für einen höheren Demethylierungsgrad verantwortlich waren. Die Unterschiede in der chemischen Zusammensetzung der modifizierten Proben wurden durch FTIR-Spektrumanalyse bestimmt. Die Ergebnisse zeigen, dass der Fraktionierungsprozess die Reaktivität von Kraft Lignin Proben wirksamer erhöhte als der mikrobielle Demethylierung. Die Hartholz Retentat Fraktion war im Vergleich zur Weichholz Retentat Fraktion besser für Modifikationen geeignet und wurde daher als die reaktivste Fraktion identifiziert.

TABLE OF CONTENTS

ABBREVIATIONS

^{13}C NMR *Carbon-13 nuclear magnetic resonance*
µL *microliter*
2D-NMR *Two dimensional nuclear magnetic resonance*
4CL *4-coumarate:CoA ligase*
ABTS *2,2'-azino-bis(3-Ethylbenzothiazoline-6-Sulfonic acid)*
AC *Activated carbon*
ATP *Adenosine tri phosphate*
CAD *cinnamyl alcohol dehydrogenase*
CAZy *carbohydrate-active enzymes*
CB *Carbon black*
CCR *cinnamoyl-CoA reductase*
CCoAMT *caffeoyl-CoA O-methyltransferase*
cm *centimeter*
COMT *caffeic acid O-methyl transferase*
C3H *p-coumarate-3-hydroxylase*
C4H *cinnamate-4-hydroxylase*
Da *Dalton*
DMSO *dimethylsulfoxide*
DSH *1-dodecanethiol*
F5H *ferulate 5-hydroxylase*
FC *Folin-Ciocalteu*
FT *Fischer-Tropsch*
FTIR *Fourier transform infrared spectroscopy*
FU *Fluorescence units*
g *gram*
GH *glycoside hydrolases*
G guaiacyl
h *hour*
H *p-hydroxyphenyl*
HMW h*igh molecular weight*
HBT *1-hydroxybenzotriazole*
HCT *p-hydroxycinnamoyl-CoA-quinate/shikimate p-hydroxy-cinnamoyltransferase*
HPLC *High performance liquid chromatography*
HWKL *Hardwood kraft lignin*
Kat *katal*
kDa *kilo Dalton*
L *liter*
LMS *Laccase mediator system*
LMW *low molecular weight*
Li *lithium*
M *molar*
mg *milligram*
min *minute*
mL *milliliter*
mm *millimeter*
mmol *milli mol*
mPa.s *millipascal-seconds*
MtL *Myceliophthora thermophila* laccase
MWCO *molecular weight cutoffs*
M_w *mass average molar mass*
MWD *molecular weight distribution*
nm *nanometer*
NIR *near InfraRed*

NMR *nuclear magnetic resonance spectroscopy*
Pa *pascal*
PAHs *polycyclic aromatic hydrocarbons*
PAL *phenylalanine ammonia lyase*
PAN *polyacrylonitrile*
PAGE *polyacrylamide gel electrophoresis*
PDI *polydispersity*
PE *polyethylene*
PF *phenol formaldehyde*
Phe *phenylalanine*
PP *polypropylene*
PVDF *poly vinylidene fluoride*
RID *Refractive index detector*
rpm *revolutions per minute*
s *second*
S *syringyl*
SWKL *Softwood kraft lignin*
SDS *sodium dodecyl sulfate*
ThL *Trametes hirsuta laccase*
TNC *tri-nuclear copper*
TGS *tris glycine SDS*
UDP *uridine diphosphate*
UV *Ultraviolet*
V *Volt*

1. INTRODUCTION

1.1 Lignin

Lignin is the second most abundant naturally occurring biopolymer on earth [1]. This multi-substituted phenolic polymer accounts for up to 30% organic carbon on earth [2]. The term lignin is derived from the Latin word *lignum* which means wood. Lignin was discovered during treatment of dried woods with nitric acid (HNO_3) and sodium hydroxide (NaOH) in 1839 by French chemist, Anselme Payen (1795-1871). Lignin was at first characterized as the encrusting substance in wood consisting of cellulose. Subsequently, the term lignin was defined by Schulze in 1857 [3].

Lignin is an essential component of the plant structure and they are involved in the formation of principal elements of the plant cell wall [3]. Lignin and its related metabolism confer to the function of multiple types of cells in plant tissues and organs. The rigidness of the plant cell wall is improved by lignin and the metabolic products of lignin are involved in insect resistance and plant disease resistance mechanisms. Lignin metabolism also confers stress tolerance which are induced by external factors such as heat, heavy metals and salts [4]. Additionally, lignin protects the woody tissues from microbial and fungal attack by altering the polysaccharide network in cells. The hydrophobicity of lignin alters the permeability of cell wall facilitating water transport through the vascular bundles in plants [3]. In some plants, lignin accumulation is important for seed propagation protecting the seeds from external adverse factors [4].

Lignin content is highly variable within plant tissues and differs from species to species. Within a plant, lignin content is higher in wood, but very low in young shoots. The lignin content can vary from 15% to 40% between different species. Additionally, the lignin content in wood depends on mechanical stress imparted on the plant or gravitropic stimulation leading to increased or decreased synthesis of lignin. For example, in softwoods (gymnosperms), compression wood fibers contain up to 40% lignin, but tension wood fibers in hardwoods (angiosperms) are almost devoid of lignin. Lignin composition is also highly variable between species. The lignin in softwoods are derived from G (guaiacyl) units, whereas a mixture of G and S (syringyl) units are typical of hardwood lignins. The lignin composition and content of wood is greatly influenced by the genetic factors and the environmental conditions [5].

Lignin is abundant in the biosphere, with its quantity exceeding 300 billion tons. The annual growth rate of lignin is around 20 billion tons [6]. Lignin is primarily obtained as a by product of pulping processes in the paper and pulp industry. Even though the production capacity of the pulp and paper industry is around 70 million tons per year, only 2% of the total extracted lignin is used in commercial applications. The majority of the extracted lignin is incinerated for energy generation [1]. The limited low exploitation of lignin for industrial applications is attributed to its huge physicochemical heterogeneity caused by different pulping processes such as kraft, sulfite, solvent or soda process leading to variations in the structure and properties due to the harsh pulping conditions. Other reasons for limited applications of lignin are variations of lignin from species to species such as hardwood and softwood, extent of cooking during lignin extraction and variations in distribution of polar and non-polar groups such as hydroxyl, methoxyl and carbonyl groups etc [1]. In addition, the poor solubility of lignin is a major hurdle in valorization of lignin [7]. These structural and chemical variations result in a highly complex immiscible heterogeneous polymer with high polydispersity, high interfacial tension and low reactivity which limits the industrial application of lignin [1].

Lignin can be utilized for the production of various high value industrial products. These products include carbon fibers, hydrocarbons and syngas. Lignin can also be used in the production of phenolic compounds which are primarily produced from petroleum derived

processes. Lignin derived materials are fuel efficient, cost effective, of low weight and possess an environmental edge over petroleum derived products and processes [8]. Widely known applications of lignin are as binders, surfactants, fillers, resins, deflocculants, vanillin production, dispersants, chelators and antioxidants [1].

1.1.1 Biosynthesis and structure of lignin

Lignin is one of the most essential secondary metabolites in plant cells. Lignin is synthesized by the phenylalanine/tyrosine biosynthetic pathway. The complex synthesis is divided into three processes namely biosynthesis of lignin monomers, transportation to cell wall and polymerization [4].

Biosynthesis of lignin monomers

Lignins are complex racemic aromatic heteropolymers derived mainly from three different hydroxycinnamyl alcohol monomers called monolignols [9]. The three monolignols namely, sinapyl alcohol, *p*-coumaryl alcohol and coniferyl alcohol differ only in their degree of methoxylation on the aromatic ring. The methoxy groups reduces the number of reactive sites on the aromatic ring. This reduction in reactive sites on the aromatic ring decreases the degree of cross linking during polymerization. The monolignols are toxic and unstable compounds that require stabilization reactions in order to accumulate within plant cells at high concentrations. Monolignols are stabilized to monolignol glycosides by enzymatic glycosylation of the phenolic hydroxyl groups of monolignols [10]. The enzyme UDP-glucose coniferyl alcohol glucosyltransferase (EC 2.4.1.111) catalyses the formation of monolignol glucosides *p*-hydroxycinnamyl alcohol glucoside, coniferin and syringin, respectively [11]. This stabilization reaction renders the monolignols non-toxic and the resulting monolignol glycosides serve as storage and transport forms of monolignols in plant cells [10].

Monolignols are derived from phenylalanine through the general phenylpropanoid and monolignol specific pathway. The precursor phenylalanine (Phe) is derived from shikimate biosynthetic pathway which occurs in plastids [11]. In the first step of the phenylpropanoid pathway, the enzyme phenylalanine ammonia lyase (PAL) catalyses the conversion of phenylalanine to cinnamic acid and ammonia. The formation of *p*-coumaric acid from cinnamic acid is catalysed by the enzyme cinnamate-4-hydroxylase (C4H). Aldehyde intermediates of the respective monolignols are formed from *p*-coumaric acid catalysed by different enzymes. The aldehyde intermediates undergo dehydrogenation catalysed by the enzyme cinnamyl alcohol dehydrogenase (CAD) to form the respective monolignols in the endoplasmic reticulum [11]. The monolignol biosynthesis pathway and the enzymes involved in the formation of monolignols are shown in figure 1.

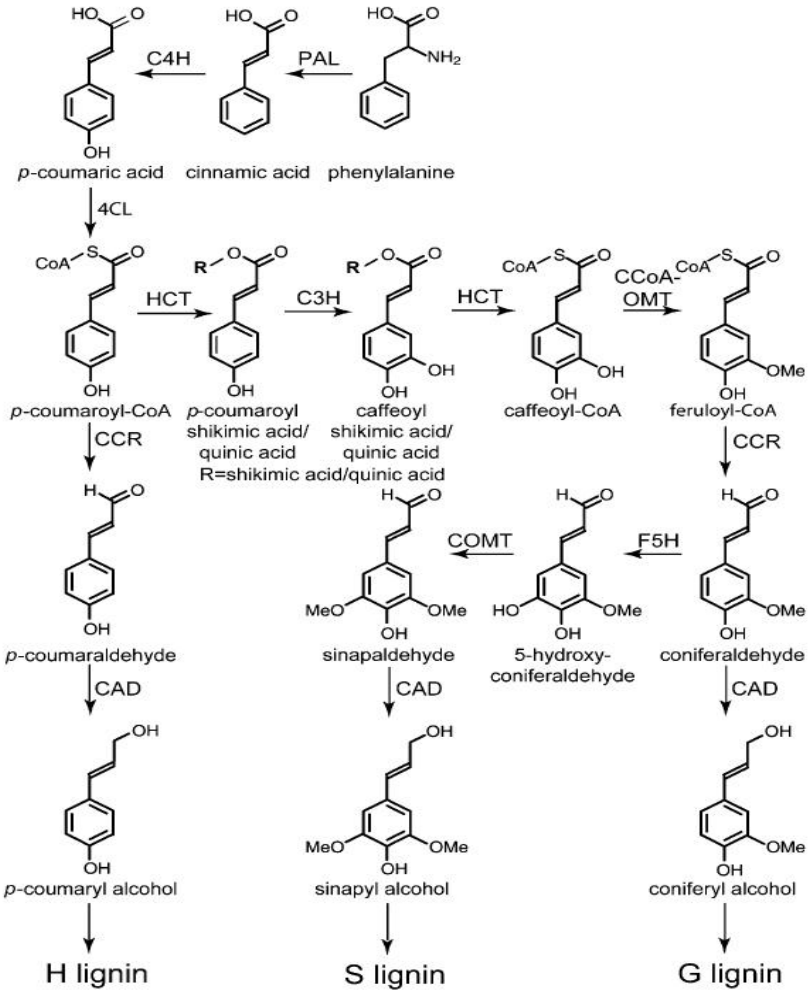

Figure 1: The principle biosynthetic pathway of the monolignols *p*-coumaryl, coniferyl, and sinapyl alcohol. Phenylalanine ammonia-lyase (PAL), cinnamate-4-hydroxylase (C4H), 4-coumarate:CoA ligase(4CL), *p*-coumarate-3-hydroxylase (C3H), *p*-hydroxycinnamoyl-CoA-quinate/shikimate *p*-hydroxy-cinnamoyltransferase (HCT), caffeoyl-CoA O-methyltransferase (CCoAMT), cinnamoyl-CoA reductase (CCR), ferulate 5-hydroxylase (F5H), caffeic acid O-methyl transferase (COMT) , cinnamyl alcohol dehydrogenase (CAD) [11].

Transportation and polymerization

The synthesized monolignols are then transported to the cell wall where lignin polymerization occurs. Only when the respective monolignols are incorporated into the lignin polymer, they are known as guaiacyl (G), syringyl (S) and *p*-hydroxyphenyl (H) units. The polymerization of lignin occurs by oxidative radicalization of phenols followed by combinatorial radical coupling. During the oxidative radicalization of monolignols, the phenol groups are oxidized leading to the formation of stabilized radicals. Then the two stabilized radicals undergo a coupling reaction to form a dimer establishing a covalent bond between the subunits. The coupling is favourable at the β position, resulting in β-β, β-O-4 and β-5 dimers. The probability of radical-radical coupling for the formation of favoured dimers depends on the conditions of the cell wall and the chemical nature of the monomeric radicals involved such as presence of methylated groups [11].

The chain elongation proceeds when the dimer is dehydrogenated to a phenolic radical in order to undergo radical-radical coupling with another oxidized monomeric radical. This type of coupling where a monomer radical is added to the growing polymer chain is known as

endwise coupling. Two oxidized radicals are consumed during each coupling reaction in which a single electron from each radical contributes to the formation of a new bond [11]. This type of intrinsic radical polymerization in lignin is different from the radical polymerization that occurs in several industrial polymers, such as polystyrene, polypropylene and polyethylene [11]. The dehydrogenation of monolignol and subsequent polymerization is performed by the action of intracellular plant peroxidases or laccases. Peroxidases utilize hydrogen peroxide for oxidation of monolignols, whereas laccases utilize oxygen for monolignol oxidation. However, the exact mechanism of these enzymes and the enzymology of lignin polymerization is still not fully understood [10].

Many covalent linkages are formed during the coupling reaction between two oxidized monomeric radicals. The most common linkage found in lignin motifs is the β-aryl ether (β-O-4) linkage which can be chemically cleaved easily. The other common linkages are phenylcoumaran (β-5), pinoresinol (β-β), diphenyl ether (4-O-5), 5-5, dibenzodioxin and diphenyl methane β-1 linkages [13]. The relative abundance of different linkages depends largely on the relative contribution of a particular monomer to the lignification process. Polymerization by endwise coupling differs substantially from dimerization of monolignols in which only three dimers are produced. The coupling of a new monomer to the growing chain of polymer by polymerization results in the formation of more β-linked ethers leading to the structural variation in lignin. These structural unit variations with different frequencies are responsible for the non-uniform structure and heterogeneity of lignin [9]. The dimerization of oxidized monolignols followed by subsequent radical polymerization and the common linkages found in lignin are shown in figure 2.

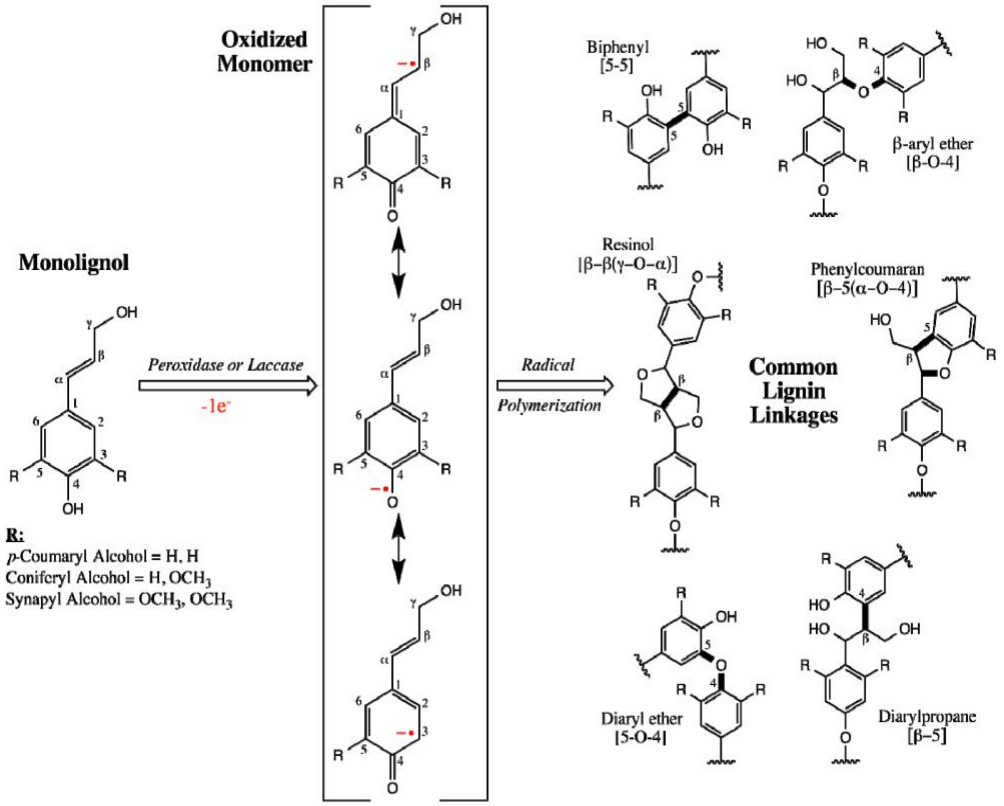

Figure 2: Radical dimerization and most common linkages found in lignin [12].

Different spectroscopic methods can be utilized to analyze the complex structures of lignin. Spectroscopic analysis can give information about the structural bonds and functional groups present in lignin, both quantitatively and qualitatively. Methods such as nuclear magnetic resonance (NMR) and Fourier-transform infrared (FTIR) spectroscopy are extensively used

for structural analysis of lignin. Other commonly used spectroscopic methods are Raman and ultraviolet spectroscopy. Among these methods, quantitative ^{13}C NMR and various 2D NMR techniques provide detailed structural information of lignin with high resolution and precision and they are regarded as an ideal method for the structural characterization of lignin [13].

1.1.2 Fluorescence of lignin

Wood cell walls possess a natural fluorescence due to the presence of lignin. Lignin exhibits a wide range of fluorescence emission when excited by ultraviolet and visible light. Lignin can also be localised with fluorescent stains such as safranine, berberine sulphate, basic fuchsin and acriflavin. These stains are brighter but lack specificity compared to lignin autofluorescence [14]. The blue-green fluorescence of leaves originates from ferulic acid present in the cell walls and most of the fluorescing structures on the leaf surface are lignified. The fluorescence intensity is much stronger when lignin is excited by UV compared to visible light excitation [15]. Coniferyl alcohol, biphenyl, stilbene and phenylcoumarone structural elements are the main fluorophores which emit in the range between 300-450 nm [16]. The shape and intensity of emission spectra varies with the excitation wavelength due to the fact that the multifunctional phenyl-propanoid units have different side groups and are excited to a different extent when the excitation wavelength is varied. This structural complexity of lignin makes the interpretation of fluorescence spectra (emission spectra and excitation spectra) of lignin difficult [15].

Albinsson et al proposed that, when excited lignin chromophores transfer non-radiative energy to an acceptor, fluorescent light is emitted. The acceptor, also known as "energy sink" structure in lignin could be of aryl conjugated carbonyl (phenyl coumarone, cinnamyl alcohol) and stilbene structure. The fluorescence intensity from the energy sink structure increased when the carbonyl groups in lignin were reduced by borohydride. The emission spectra of technical lignins such as kraft lignin (pH dependent) exhibits a maximum at 400nm on excitation at wavelengths ranging between 240-350 nm [17]. It has been observed that the fluorescence intensity of lignin decreases when treated with laccases. The fluorophore functional groups are modified and the extent of modification depends on the redox potential of the laccase. When lignin is polymerized by laccase, the increase in molecular weight correlates with the decrease in fluorescence intensity [18].

1.1.3 Extraction and types of technical lignins

The potential of lignin in high-value added applications can be unlocked by using technological processes to produce technical lignins [19]. Technical lignins are the by-products of the pulping process or cellulosic ethanol production process and are used as bulk feed-stocks due to large scale availability [20]. Naturally, lignin contains a higher amount of inter-unit C-O bonds. Depending on the pulping process, formation of C-C linkages occurs in the respective technical lignins. This is due to condensation reactions between the compounds cleaved from native lignin and the remaining oligomer chains. As such, all technical lignins differ in physicochemical properties such as molecular weight, polydispersity, moisture, ash content, homogeneity and impurity content [21].

The presence of impurities especially sulphur is one of the major challenges in processing of technical lignins. Based on the presence of sulphur, the lignin extraction process is classified as sulphur free process and sulphur based process. The sulphur free processes are Soda pulping and Organosolv pulping. The sulphur based lignins are kraft lignin, lignosulphonates, hydrolysis lignin and ionic liquid lignin [21]. The classification of the extraction processes, technical lignins and the average sulphur content of sulphur based processes is shown in figure 3.

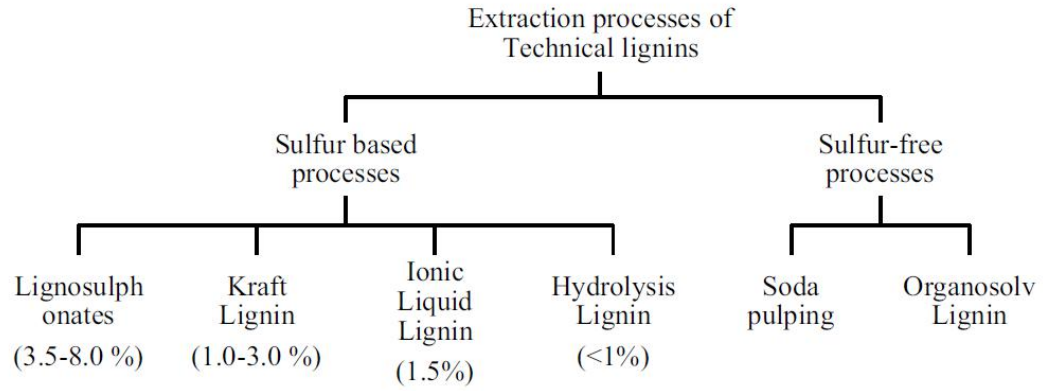

Figure 3: Classification of the extraction process and types of technical lignins. Sulphur content in % for sulphur based processes is given within brackets [21].

Sulphur free lignin

Soda lignin is produced as the by-product of the soda pulping process. The soda pulping process is utilized primarily for crops such as straws and flax. Soda lignin is sulphur free as the cooking liquor does not contain sulphur, which relates to the chemical composition and structure of soda lignin being closer to that of natural lignin. Soda lignin from non wood plants have higher nitrogen content and higher silicate content compared to wood lignins [19].

Organosolv process employs cooking liquor consisting of a mixture of organic solvents and water in the pulping process. The most commonly used solvents are acetic acid, ethanol and formic acid. The separation process involves solubilization which modifies lignin to a smaller extent leading to high homogeneity in organosolv lignins [19]. As such, the structure of organosolv lignin is closest to native lignin compared to other technical lignins [13]. Organosolv lignins have a high purity, low molecular weight, are sulphur free and poorly soluble in water [19].

Sulphur based lignin

Lignosulphonates are obtained as by products of the sulphite pulping process which is used primarily for delignification of wood. During the process, the lignocellulosic material is cooked in a liquor containing HSO_3^{2-} or SO_3^{2-} ions and a pH dependent base. The Sulphite process can be divided into Acid sulphite process (pH 1–2), Neutral Sulphite Semi Chemical Process (pH 5–7) and Alkaline Sulphite Process (pH 9–13.5) [20]. Lignosulphonates are water soluble anionic polyelectrolytes that contain a variety of functional groups such as carboxylic groups, phenolic hydroxyl groups and sulphur containing groups. Lignosulphonates have a relatively high molecular weight with a broad distribution of molecular weights and high ash content [19].

Hydrolysis lignin can be produced by enzymatic hydrolysis and the acid hydrolysis processes. It contains a high amount of condensed structures with a high molecular weight. Enzymatic hydrolysis lignin exhibits a higher activity compared to kraft lignin and lignosulphonates. Ionic liquid lignins are obtained by fractionating lignin with ionic liquids such as alkylbenzenesulfonate and dimethylsulfoxide (DMSO). Lignin can be recovered from ionic liquids by precipitation with non solvents such as water and acetonitrile. The lignin obtained exhibits similar properties as the organosolv lignin. However, ionic liquid lignin is not completely regarded as a technical lignin but considered as a promising alternative [19].

The Kraft or sulphate cooking process are potentially the largest sources of technical lignins [20]. Kraft lignin obtained from kraft pulp accounts for about 85% of total lignin production in the world [19]. During kraft cooking, lignocellulose is digested in white liquor consisting of aqueous solutions of sodium hydroxide (NaOH) and sodium sulfide (Na_2S) at high temperatures (150-180°C) [20]. Lignin is broken down into smaller fragments of different molecular weights which are soluble in alkali solutions [19]. Cellulose is removed by filtration and black liquor consisting of hemicellulose and lignin is obtained [20].

The most important feature of kraft pulping is the recovery of all chemicals used for pulping. The recycling process involves concentration of weak black liquor by evaporation to heavy black liquor. The heavy black liquor is then subjected to combustion during which thermochemical sulphur reduction takes place forming a green liquor and sodium carbonate (Na_2CO_3) is formed as a by-product. The next step involves treatment of the green liquor with lime (CaO). During the treatment, the by-product sodium carbonate reacts with lime resulting in the formation of calcium carbonate ($CaCO_3$). Sodium hydroxide is also formed during this reaction. White liquor is regenerated by precipitating $CaCO_3$ from the liquid and $CaCO_3$ is converted back to CaO by heating. The surplus energy generated during kraft pulping is utilized for extracting lignin from the black liquor. The extracted lignin can be further processed into valuable products [20].

Kraft lignin contains an increased amount of free phenolic hydroxyl groups compared to native lignin and other technical lignins. The extensive degradation of β-aryl linkages during pulping is responsible for the high amounts of free phenolic OH groups. In addition, kraft lignin also contains an increased amount of carboxyl groups and condensed structures such as biphenyl, quinine and catechol structures. The molecular weight of kraft lignin obtained from kraft pulp varies within the range of 200-200000 grams per mole. Kraft lignin has a high ash content whereas the sulphur content is quite low in comparison to lignosulphonates [19]. Kraft lignin is generally soluble in water under alkaline conditions but insoluble under acidic conditions. For this reason, commercial kraft lignin is sulfonated to increase solubility in water [29]. The properties of kraft lignin depend on the lignocellulose source used in the delignification process [19].

1.1.4 Softwood lignin

Softwoods are gymnosperms (mostly conifers), generally needle leaved evergreen trees. For example pines (*Pinus* spp.) and spruces (*Picea* spp.). The lignin content in softwoods varies between 25 and 35% and consists almost exclusively of guaiacyl units (G) with a low proportion of *p*-hydroxyphenyl units (H). The methoxyl content of softwood is between 15-16% and in the compression wood of softwoods, lignin is enriched in condensed structures such as H units and G units depending on species [22].

The most abundant linkage in softwood is the β-O-4 (arylglycerol-β-aryl ether) linkage accounting for more than 50% of the linkages in lignin. The β-O-4 substructure side chain contains both *erythro* and *threo* stereoisomers and each stereoisomer has a pair of enantiomers [23]. The β-O-4 structure in the compression wood lignin of softwoods exists dominantly in the *erythro* form due to the presence of H units [24]. The other linkages in softwood lignin are β-5, 5-5, 4-O-5 and β-β units which are more resistant to chemical degradation compared to the weak β-O-4 linkage [25]. The structural representation of a section of softwood lignin along with linkages found in softwood lignin are shown in figure 4.

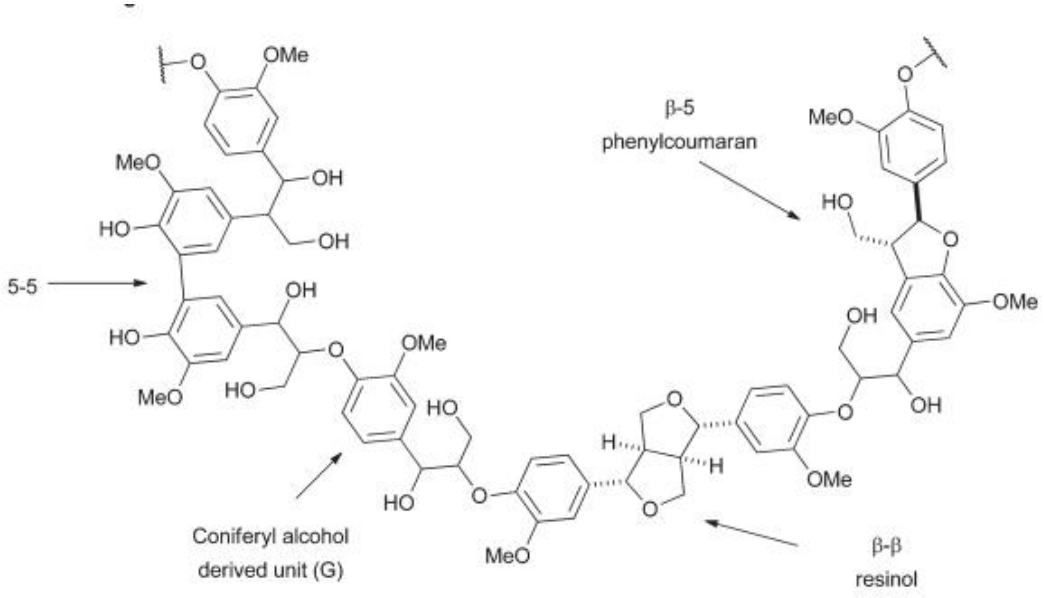

Figure 4: Structural representation of a section of softwood lignin [26].

During the pulping delignification process, the G based structural network is more resistant to cleavage leading to a lower degree of lignin depolymerization during pulping. The C-5 position of the benzene ring in G units is unoccupied. This renders the G units susceptible to condensation reactions. The free C-5 position in G units also leads to the formation of C-C linkages resulting in lignin re-polymerization. The main reason for higher frequency of the C-C linkages between aromatic rings in softwood lignin is due to resistant linkages of C-5 of aromatic nuclei such as β-5, 5-5 and 4-O-5 linkages [25].

1.1.5 Hardwood lignin

Hardwoods belong to angiosperms and are typical of broadleaf deciduous trees such as *Eucalyptus*, *Acacia*, *Fagus sylvatica* (European beech) and *Tectona* (teak). The lignin content in hardwoods varies between 15 and 25% and is constituted mainly by guaiacyl units (G) and syringyl units (S). The methoxy content of hardwood is 21 % and the S/G ratio is higher compared to softwoods [22].

The most common linkage in hardwood lignin is β-O-4 linkage with a proportion of 71% or higher of the inter-monomeric linkages [22]. The β-O-4 bond of syringyl type lignin can be easily cleaved by chemicals compared to softwoods [23]. The other linkages in hardwood lignin are β-β, 5-5 with a low amount of β-5 (phenylcoumaran) units [26]. The presence of additional methoxy groups in hardwood lignin inhibits the formation of 5-5 bonds. For this reason, the polymer structures of hardwood lignin have more linearity compared to the polymer structures of softwood lignin [27]. The inter-unit connectivity of hardwood lignin is simpler than that of softwood lignin [26]. The structural representation of a section of hardwood lignin with the linkages are shown in figure 5.

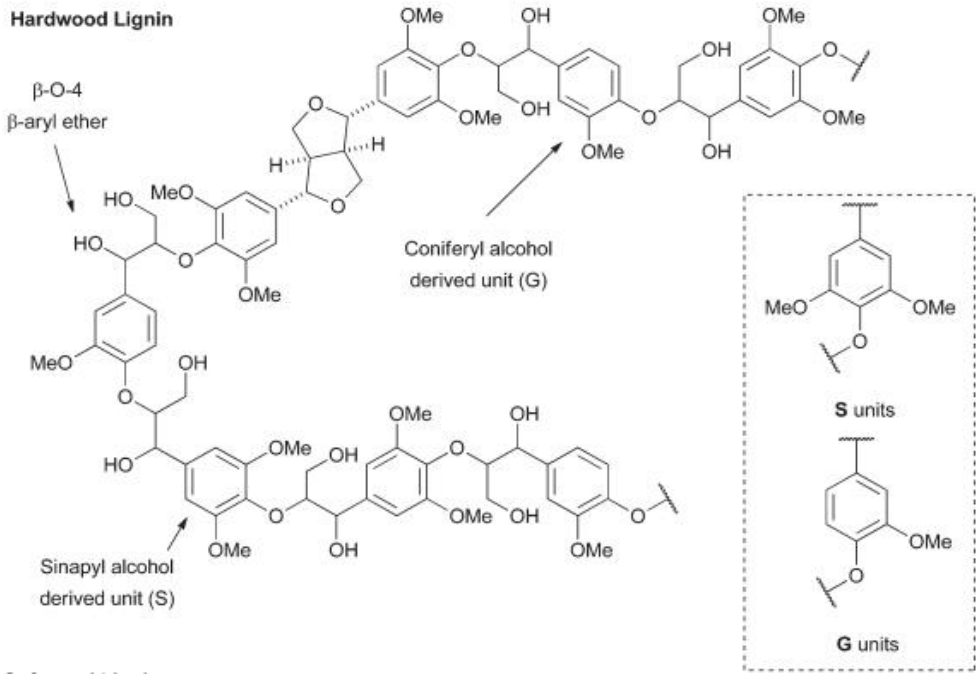

Figure 5: Structural representation of a section of hardwood lignin [26].

The pulping efficiency depends on the quantity of S units in lignin. The resistance to degradation during pulping is low for hardwood lignins due to the presence of S units. This results in higher degree of polymerization in hardwood lignins during the pulping reaction. In hardwood lignin, the frequency of C-C bond formation between aromatic rings is less compared to the rate of formation of C-C bond in softwood lignin [25].

1.1.6 Fractionation of lignin

The widely used industrial kraft pulping process alters the native lignin structures significantly by fragmentation and condensation [28]. Depending on the process variables of the pulping process, the chemical structure of lignin differs significantly from the native lignin structure in plants in terms of molecular weight (M_w), cross linking density and functional groups such as OH and COOH groups [29]. The most abundant aryl-alkyl ether linkages such as β-O-4, are susceptible to fragmentation resulting in the formation of large amounts of phenolic hydroxyl groups. New linkages such as enol ethers, stilbenes and carbon-carbon linkages are formed which alters the structure of lignin. As such, lignins are inherently heterogeneous, exhibit high polydispersity and have complex and variable functional group distributions which affect the reactivity, nature and functionality of lignin for the use in value added applications [28].

The diversity of various functional groups present in lignin makes its utilization quite challenging [30]. It has been reported that the content of certain functional groups and the chemical structure of lignin vary with molecular weight to some extent [30]. Fractionation methodologies can enhance the properties of lignin such as polydispersity, homogeneity and reactivity and make it suitable for industrial applications [31]. Commonly applied fractionation methods are sequential organic solvent extraction, selective precipitation based on pH and membrane ultrafiltration [28]. In 1986, Mörck, Yoshida, and Kringstad illustrated that fractionation could be achieved by successively extracting kraft lignin with organic solvents. Organic solvents such as dichloromethane, methanol, n-propanol and methanol/dichloromethane were used as fractionation reagents. Mörck et.al adopted a series of solvents to extract both hardwood and softwood kraft lignin. The approach for selective

precipitation is to dissolve lignin in an organic solvent followed by precipitation with non-polar or aqueous solvents. Lignin fractions can be directly isolated from black liquor by stepwise reduction of the pH value as described by Toledano, Serrano, Garcia, Mondragon and Labidi (2010) [31].

Membrane ultrafiltration involves the application of membranes with differing molecular weight cut-offs (MWCO) for fractionation of lignin into a high molecular weight fraction and a low molecular weight fraction. Ceramic membranes are the most suitable membranes for lignin fractionation due to their temperature and pH resistance [31]. Polymer membranes are also used for lignin fractionation [32]. Fractionation using membranes with differing MWCO yields lignin fractions with desired properties such as low polydispersity and distinct molecular mass. Therefore, fractionation of kraft lignin by membrane ultrafiltration can improve the desired properties of lignin and make it suitable for industrial production of high value added products [28].

The molecular weight distribution is an important factor that determines solubility, viscosity and thermal stability of lignin molecules. The molecular weight of lignin varies from species to species and also depends on the pulping process. The average molecular weight of kraft lignin can vary between 600 and 180000 Da. Separation of lignin fractions by ultrafiltration results in a low molecular weight fraction (LMW) and a high molecular weight fraction (HMW) containing insoluble solid residues due to a lower degree of polymerization and intact ether bonds. The relative carbon content of lignin samples increases from HMW to LMW fractions accompanied by an increase in hydrogen content and a decrease in oxygen content. These elemental compositions are related to the distribution of OH groups within the fractions [31].

The mass distribution (yield) is higher in the HMW fraction (40-70%) and the LMW fraction has the lowest yield. The molecular weight (M_w) and average molecular weight (M_n) decreases from the HMW to the LMW fraction accompanied by a simultaneous decrease in polydispersity and aliphatic hydroxyl groups. However, the number of carboxylic hydroxyl groups and phenolic hydroxyl groups increases when the molecular weight decreases. This results in lower aliphatic to phenolic OH ratio in the LMW fraction. The number of aliphatic and phenolic OH groups are important for the reactivity of lignin and essential for the subsequent reactions on the existing OH groups in order to incorporate various functional groups into the lignin molecule [31].

However, each of the three fractionation methods have their own limitations. The disadvantages of membrane fractionation are high cost, low purity and membrane fouling. The fractions obtained by solvent extraction are of low purity and the method is limited by economic considerations [30]. Therefore, an efficient and economical method for lignin fractionation still needs to be developed.

1.1.7 Modifications and applications of lignin

The complex structural network of the highly heterogeneous lignin restricts its application as a raw material for the synthesis of chemicals and production of polymers. The most reactive site in lignin is the α- position of the phenylpropene subunits. This reactive α-site can either be occupied by ether bonds or sterically hindered by other interunit linkages which lower the reactivity of lignin [33]. Therefore, modification of lignin is required which includes physical, chemical, biological and enzymatic approaches.

Physical methods such as ultrasonication have been applied to synthesize lignin based nanoparticles for textile fiber treatments. Ultrasound energy was used to increase the lignin extraction yield and purity or to polymerize high molecular weight lignin. The majority of the

ether bonds can be homolytically cleaved to some extent by sonication. The application of nanotechnology allowed chemical, biological and physical effects on nano scale which are environmentally friendly in comparison to inorganic materials. The treated textile fibers acquired antistatic, antibacterial and ultraviolet radiation absorbing properties [34].

Chemical modification of kraft lignin includes fragmentation, hydroxyl groups chemical modification and creation of new active sites. In order to increase the reactivity of kraft lignin, various methods which modifie the lignin structure have been studied. These methods include demethylation, oxidation, phenolation, hydrolysis, reduction and hydroxymethylation [33].

Polyurethane (PU) polymers exhibit remarkable flexibility for material design. They are formed by polymerization of diisocyanates with polyols via carbamate linkage. Kraft lignin derived rigid PU foams exhibit low thermal conductivity and possess high strength to weight ratio. These rigid polyurethane foams are utilized as insulating agents in the transportation and construction industry. The mechanical properties of rigid polyurethane foams can be improved by replacing a portion of polyol with kraft lignin. Kraft lignin can be converted into liquid polyol monomers by oxypropylation and the viscosity of the lignin polyol can be rapidly increased. The higher OH group content and low polydispersity of lignin polyol can increase the reactivity of modified kraft lignin for polyurethane synthesis. The rigid polyurethane product with lignin polyols exhibits better mechanical properties compared to the commercial rigid foam [20].

In polymer industry, kraft lignin can be utilized for the production of novel plastics with desirable properties. Kraft lignin can be used in lignin-polymer blends such as plastic bends, as an UV and thermal stabilizer, and to improve mechanical properties. Depolymerized kraft lignin has high antioxidant activity, decreased aliphatic OH content and increased compatibility with polymers such as polyethylene (PE) and polypropylene (PP). The decrease in the polarity of lignin during the chemical modifications does not alter the mechanical properties of the polymer such as polyethylene. The thermostability, elastic modulus and impact strength of biodegradable thermoplastic polylactic acid (PLA) increases upon the addition of kraft lignin. In addition to bioplastics, esterified softwood kraft lignin when used as coating along with PLA increased the efficacy of nitrogen fertilizer (urea). Kraft lignin can be used as a barrier for fiber based packaging materials [33].

The adhesives based on phenol formaldehyde (PF) resins are used as binders in the production of wood based composites such as plywood, particle board, waferboard fiberboard, glue laminated timber and laminated veneer lumber [33]. PF resins formation involves reaction of formaldehyde with phenol at ortho or para position to give methylol groups which crosslink with other phenols via methylene bridges. The mechanical properties of the resin could be increased by aromatic substitution of lignin moieties with formaldehyde. However, due to low reactivity of aromatic units in kraft lignin, modifications such as demethylation and methylolation were able to increase the active sites in aromatic units for the reaction with formaldehyde [20]. Base catalyzed depolymerization of pine kraft lignin yielded oligomeric lignin units which could substitute 70% phenols in PF resins without changing the mechanical properties of PF resin [33]. The mechanical properties of the plywood did not change when 20% of the PF resin was substituted with pine kraft lignin [20].

Activated carbon (AC) is widely used as adsorbent in gas separation, catalyst supports, filtration systems and electrochemical applications. AC possesses desirable properties such as thermochemical stability, good structural porosity and high adsorption capacity. The production process of AC involves carbonization, physical and chemical activation. AC derived from kraft lignin has high area surface and is produced as a potential sorbent for sediment remediation. In addition, lignin based carbon black (CB) is a renewable substitute for ordinary CB. Carbon black is used as a reinforcement filler in rubber products, plastic

products and in ink and paints. Kraft lignin can potentially reduce the dependence on oils for the production of technical carbons [33].

Li-ion batteries possess desirable properties such as long shell life, high energy densities and environmentally friendly mode of operation. Li-ion batteries are extensively utilized as power source for battery operated emission-less electric vehicles and portable electronics. The commercial electrode binder material poly vinylidene fluoride (PVDF) can easily deteriorate the cycling performance of batteries and its preparation procedure involves toxic organic solvents which are harmful to both humans and environment. Application of lignin as an alternative binding material for Li-ion battery electrodes provides an inexpensive, non-fluorinated and environmentally friendly approach. Pretreatment of lignin by leaching is required in order to remove soluble, low molecular weight fractions. The electrodes based on pretreated lignin exhibited good stability and high specific capacity. Usage of lignin based composites for preparation of carbon based materials for Li-ion batteries resulted in the improvement of electrochemical performance of the battery. These lignin based carbon fibers can be used for high power and high energy applications [36].

Depolymerized or crude lignins form cross-linkages with anhydrides and amines functional group to form thermoset resins. Thermosets cannot be melted again by increasing temperature because of formation of a rigid network of polymer chains after crosslinking. Lignin based thermosets such as phenol-formaldehyde (PF) and epoxy resins are used as adhesives for wood, composite boards, films and aerogels [13]. Diverse applications of lignin can be seen in figure 6.

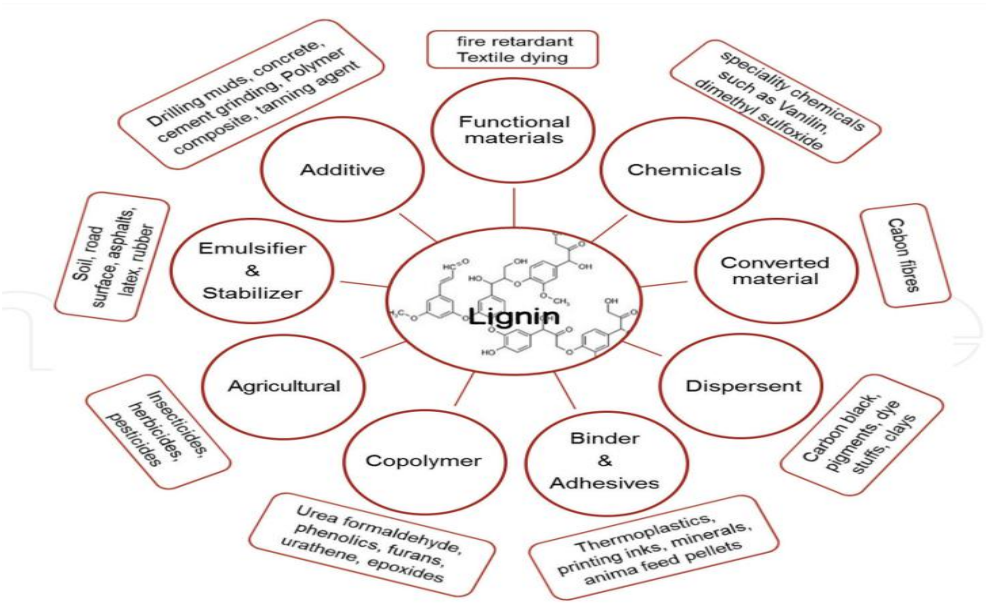

Figure 6: Potential and current applications of lignin [38].

Bacteria and fungi produce lignocellulosic enzymes for their growth and metabolic activities.. These enzymes naturally modify lignin by the process of oxidative depolymerization. Demethylation by these microorganisms has been reported but the responsible enzymes have not yet been fully characterized. Enzymes such as lignin peroxidase, manganese peroxidase and laccase from microbes can depolymerize lignin, generating phenoxy radicals. Therefore, biological treatment and enzymatic modification enhances the potential of kraft lignin for application in various value added products [41].

The application of kraft lignin for the production of renewable biofuels and aromatic compounds has led to an increased sustainability and reduced the dependence on fossil fuels

[35]. Kraft lignin is fragmented by thermochemical and biological processes. The two different thermochemical approaches are depolymerization of kraft lignin to yield aromatics and hydrocarbons; and gasification for syngas generation followed by conversion to Fischer-Tropsch (FT) synthetic fuels, synthetic alcohols and hydrogen. The FT process produces conventional fuels such as diesel, gasoline, kerosene and various hydrocarbons. The depolymerization techniques include pyrolysis, supercritical water, alkaline oxidation and catalytic hydrogenolysis. These techniques produce low molecular weight substances such as vanillin, aldehydes and aliphatic acids [33].

Carbon fibers containing 92% carbon are used in sporting goods, composites, wind turbine blades, automotive and aerospace industries. The commercial carbon fibers production from petroleum synthetic polymer polyacrylonitrile (PAN) limits the application of carbon fibers due to high cost of PAN. Using lignin as an alternate precursor for carbon fiber production due to low cost, availability, high carbon content and high carbon yield resulted in faster thermostabilization and reduction in production time. Several approaches have been developed for lignin-carbon fiber production, one of these involved fractionation of kraft lignin followed by oxidative polymerization by laccase-mediator system. The insoluble fraction when used with PAN in 1:1 ratio resulted in better spinning ability of carbon fibers and the elastic modulus of lignin PAN-carbon fiber was similar to that of several commercial carbon fibers [33].

Lignin based hydrogels due to their biocompatibility, low toxicity, environment friendliness and biodegradability are widely used for controlled release of water and functional materials which include biomaterial release, drug delivery and enzyme immobilization. Lignin based hydrogels with antibacterial and antioxidant agents have great potential in applications such as water treatment, separation films, biosensors and tissue engineering. The smart biomaterial, lignin based hydrogels are also used for stimuli response, pesticide delivery and electrodes [37].

Lignosulfonates are used as additives in concrete admixtures, animal feed binders, vanillin production and soil stabilizers. Their surface stabilizing properties are widely applicable in agrochemicals, dyes, pigments, detergent formulations and textile lubricants [25]. Lignosulfonates are also used for other minor applications such as components of linoluem paste, dispersant in oil drilling mud, metal sequestrant for the treatment of cooling system, flocculants and metal absorbents [20].

Organosolv lignin is utilized as a formulating agent in the production of varnishes and paints. Soda lignin is used for the production of phenolic resins, animal nutrition and dispersants. Ionic liquid lignin has similar applications as soda lignin and organosolv lignin. Hydrolysis lignin is used as sorbent and in the preparation of polymeric materials including grafting polymers [19].

Small market applications of lignin include carbon black, emulsifiers, cleaning chemicals, leather tanning, battery expanders water treatment and rubber additives. Non traditional high value applications of lignin include production of lignin based carbon fiber, usage of upgraded technical lignins in polymer composites and production of valuable oxygenated aromatic compounds and olefins [38].

1.2 Demethylation of lignin

Lignin is a highly methylated, recalcitrant complex biopolymer with high heterogeneity [39]. The relative abundance of *p*-hydroxyphenyl (H), guaiacyl (G) and syringyl (S) structural units is variable among plant species. In all lignins, the *para* position to the OH group is occupied by partially hydroxylated propyl chains. The *ortho* positions to the OH group are either free (H) or dimethoxylated (S) or monomethoxylated (G) [41]. The methoxy groups on the benzene ring sterically hinder the phenolic OH groups on the benzene ring of the monolignols. The phenolic OH groups on the benzene ring are essential for the formation and elongation of the polymer chain during lignin biosynthesis. Increase in steric hindrance due to methoxy groups lowers the amount of cross linking in lignin structures. This internal cross linking affects the lignin molecule as well as the properties of the lignin based materials [42]. Therefore, development of modified lignins by chemical, biological or enzymatic means is required for broader application in value added products such as fine chemicals, phenol formaldehyde resins and plastic applications [39].

Demethylation activates different lignin structures by removing methoxy groups (-OCH_3) and liberating the phenolic hydroxyl groups, thereby increasing the reactivity of lignin [41]. Chemical demethylation of lignin can be achieved using various nucleophilic reagents such as hydroiodic acid (HI) and hydrogen bromide (HBr) and thiols such as iodocyclohexane (ICH) and 1-dodecanethiol (DSH). Complete demethylation of lignin was achieved with the very strong nucleophile HI, which is generally used for quantitative determinations of lignin methoxy contents [40]. Biological demethylation is accomplished by means of microorganisms such as bacteria, and various fungi [39].

1.2.1 Microbial demethylation of kraft lignin

1.2.1.1 Bacterial demethylation

The degree of methoxylation in kraft lignin is high, containing more than 50 % of methoxylated reactive aromatic hydroxyls [41]. Lignin demethylation is facilitated by enzymes called O-demethylases which strip-off the methoxy groups to release methanol as the end product and renders lignin more phenolic [39]. O-demethylases catalyse the conversion of lignin and lignin derived compounds into their respective diol intermediates leading to central carbon catabolism. These enzymes play a vital role in aromatic catabolic pathways, which are important mechanisms of natural carbon cycle [74].

The O-demethylases catalyze the removal of O-methyl groups at C3 position of benzene ring in softwood lignin and at C3 and C5 positions of the benzene ring in hardwood lignin [41]. These enzymes are produced by several bacteria such as *Nocardia corallina* A81, *Pseudomonas putida*, *Rhodococcus jostii* RHA1, *Desulfifitobacterium hafniense* strain DCB-2 and *Sphingomonas sp.* SYK6. These bacteria secrete various O-demethylases such as veratrate O-demethylase, vanillate O-demethylase, syringate O-demethylase, *p*-anisate-O-demethylase, vanillate O-demethylase oxidoreductase, tetrahydrofolate (THF) dependent O-demethylase. However, lignin demethylation by these enzymes is not understood adequately [39].

Bacteria secrete different kinds of ligninolytic enzymes which are involved in various degradation pathways. The bacterial demethylation occurs by intracellular action during which a hydroxyl group is introduced in the form of hydroxylate. The demethylation of lignin and non-phenolic compounds requires NADH, ATP, CO_2, O_2 and electron donors or acceptors to produce a highly reactive lignin. For example, *Pseudomonas fluorescens* requires NADH and O_2 for oxidative demethylation reactions and oxidizes vanillate resulting in the accumulation of protocatechuate and generation of formaldehyde. This reaction was catalyzed by O-demethylase and it was later demonstrated that ATP is also required for O-demethylase

activity. Another bacterium *Sphingobacterium* sp. T2 manganese superoxide dismutase (SpMnSOD) catalyzed aryl-Ca oxidative cleavage, alcohol oxidation, alkene dihydroxylation and demethylation that produced 20-40% increase in phenolic and aliphatic OH content [39].

1.2.1.2 Fungal demethylation

Various fungi have the ability to demethylate lignin, which include *Penicillium simplicissimum*, *Penicillium cinnabarinus* A-360, *Chaetomium piluliferum*, *Haplographium* sp., *Hormodendrum* sp., *Phanerochaete chrysosporium*, *Aspergillus* sp. and *Galerina autumnalis*. Wood rot fungi are also involved in demethylation of lignin along with the natural delignification process. Ligninolytic enzymes such as laccase and manganese peroxidase catalyze the mineralization of lignin to methanol (CH_3OH). During this reaction, these enzymes produce vicinal hydroxyl in polyphenylpropanoid units of lignin. However, the removal of methoxyl groups by these ligninolytic enzymes leads to damage of the polymer structure. Very few wood rot fungi secrete enzymes that can demethylate methoxy groups at C3 (3-O-demethylase), C4 (4-O-demethylase) or C5 (5-O-demethylase) positions in phenyl propanoid units of lignin and lignin model compounds [39]. The catalytic reactions of these enzymes are represented in figure 7.

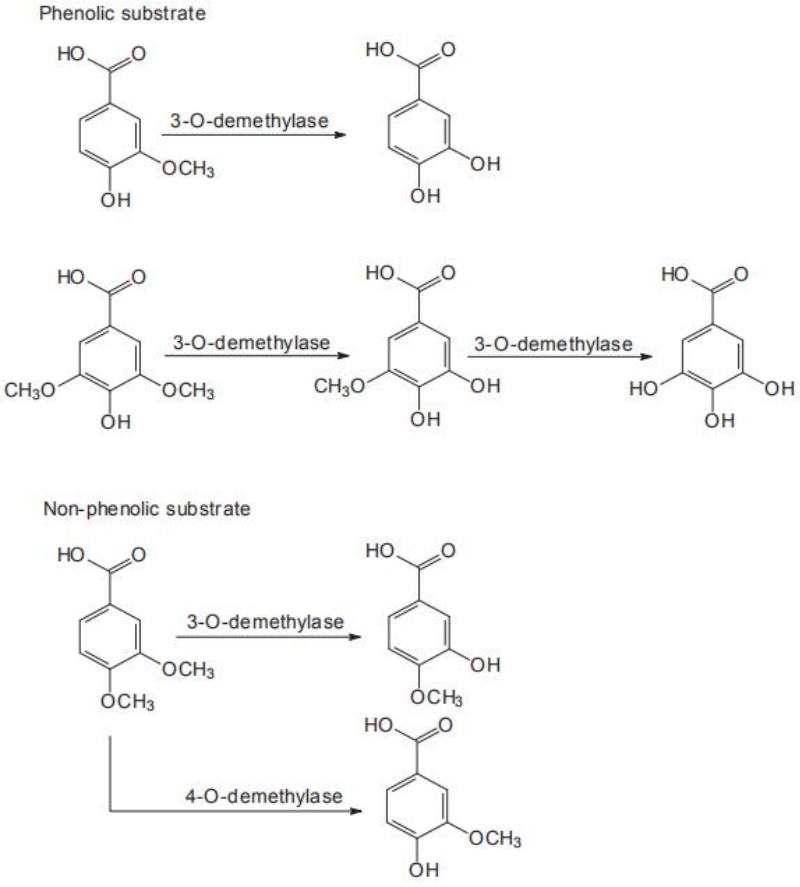

Figure 7: Enzymatic demethylation of lignin model compounds by different types of O-demethylases [39].

The efficacy of white rot fungal decay of spruce lignin, monitored by ^{13}C NMR analysis demonstrated the demethylation process of the aromatic methoxy group. The activity of the oxidoreductases of the basidiomycete-mediated radical system has been reported. In addition, it was found that the reactive oxygen species (ROS) were involved in the removal of methoxy groups on the benzene ring of lignin. The brown rot decay process initiated by Fenton chemistry, produced demethylated lignin as a residue while degrading cellulose. The O-demethylases secreted by *Basidiomycetes* and *Ascomycetes* were proven very difficult to isolate due to their oxygen sensitivity and their tendency to bind to the cellular membranes [39]. Hence, more studies focussing on the isolation and characterization of O-demethylases secreted by wood rot fungi has to be done.

1.2.1.2.1 The ascomycete *Aspergillus niger*

The ascomycete *Aspergillus niger* is a filamentous fungus that is ubiquitously present in the environment. The genome size of *Aspergillus niger* is estimated to be between 35.5 and 38.5 megabases (Mb) divided among eight chromosomes that vary in size from 3.5- 6.6 Mb [43]. *Aspergillus niger* belongs to the section *Nigri* in the subgenus *Circumdati* which are taxonomically placed in the genus *Aspergillus* [44]. It is naturally found in soil, litter, compost and decaying plant material. The growth of the ascomycete is favourable at various temperatures ranging from 6 °C to 47°C and at pH ranging from 1.4 to 9.8. The water activity limit of *Aspergillus niger* is higher than the other members of the *Aspergillus* species. These characteristics along with profuse production of conidiospores secure the ubiquitous occurrence of the species in warm and humid places [45]. The colonies of *Aspergillus niger* are fast growing, flat granular which gradually change from white to black. The conidiosphores are very long (1.5-3.0 mm), thick walled, smooth with large round vesicle and the conidia are brown, thick walled and spherical in shape with ridges [44].

The ascomycete *Aspergillus niger* is one of the most significantly utilized microorganism in biotechnology. It is widely known for industrial production of citric acid which is regarded as one of the most efficient, highest yield bioprocesses [43]. In addition to citric acid, *Aspergillus niger* is widely used for the production of enzymes such as cellulases, amylases, proteases, lipases and pectinases. The efficient secretion system of *Aspergillus niger* is well suited for large scale industrial production [44]. *Aspergillus niger* is an significant model microorganism for numerous research studies and substantially contributes to global carbon cycling. The research studies includes protein secretion in eukaryotes, mechanisms relating to morphology of fungi and crucial development of fermentation processes. The ascomycete *Aspergillus niger* is considered as a harmless fungal microorganism, despite of reports of involvement in human infections [45].

Generally, the ascomycete *Aspergillus niger* is responsible for soft degradation of wood. Therefore, their potential for lignin degradation is limited [46]. The ligninolytic enzymatic potential of *Aspergillus niger* has not yet been fully explored.

1.3 Laccases

The enzyme Laccase (EC 1.10.3.2, benzenediol oxygen oxidoreductase) is a member of the blue multi-copper oxidase family with a molecular mass of about 70 kDa. Laccase was first isolated more than one century ago from the Japanese lacquer tree *Rhus venicifera* and is widely distributed among plants where they are involved in lignin synthesis and wounding response [47]. The versatile oxidoreductase enzyme possesses the capability to oxidize a wide range of phenolic, non-phenolic compounds, aromatic and non-aromatic compounds by converting an oxygen molecule to water on concomitant four electron reduction. In addition, laccases can oxidize amines substituted with different functional groups. Laccases are glycoproteins which are ubiquitous in nature and are found in many kingdoms, ranging from various fungi to plants of higher order [48]. The intensively studied fungal laccases play important roles in fungal physiological processes. These processes include pigmentation. delignification and morphogenesis. Among the fungal species, ascomycetes, dueteromycetes and basidiomycetes are known to produce laccases. The basidiomycete, white rot fungi is regarded as the most efficient laccase producer and lignin modifier. White rot fungi secrete laccases along with other ligninolytic enzymes such as manganese peroxidase, lignin peroxidase and versatile peroxidase. Two model organisms, *Pleurotus ostreatus* and *Trametes versicolor* are extensively used in basic and applied laccase research [49].

Plant laccase families are even larger than fungal families and the plant laccases are involved in lignin synthesis as opposed to fungal laccases which are involved in delignification. In relation to fungal and plant laccases, the bacterial laccases were discovered comparatively at a later stage [49]. The first bacterial laccase was isolated from *Azospirillum lipoferum* in 1993 from rice rhizosphere. Gram positive bacteria such as *Bacillus, Geobacillus, Streptomuces, Aquisalibacillus, lysinibacillus* and *azosprillum* secrete laccases [48]. Bacterial laccases exhibits high temperature stability and high tolerance to halogens. The activity of bacterial laccases is optimal at high pH [49]. Moreover, bacterial laccases have additional advantages over fungal laccases because of their cost effective use in industrial applications, which include broad substrate specificity and enzyme production in short time. Bacterial laccases mediate delignification and are also useful in applications such as pulp and paper bio-bleaching, decoloration and degradation of textile dyes and biosensor development [48]. The insect laccases are not well characterized compared to fungal, bacterial and plant laccases. However, insect laccases are significantly involved in insect physiological processes such as cuticle sclerotization and melanization [49].

1.3.1 Mechanism and structure of laccase

Laccases contain three different types of copper and their catalytic functions depend on copper atoms that are distributed at the three copper centers [50]. Type 1 copper center which gives the characteristic blue colour is paramagnetic and absorbs at 610nm. This copper center is trigonally coordinated with two histidines, one cysteine and one variable axial ligand position. The typical blue colour results from the intense electron absorption caused by covalent copper-cysteine bond. The two amino acids, histidines and cysteine are conserved as equatorial ligands in the trigonal coordination. The variable axial position is occupied by either leucine or phenylalanine in fungal laccases. The axial position ligand strongly influences the oxidation potential of the laccase, regulating the enzyme activity. The oxidation potential and the activity of fungal laccase was shown to significantly decrease when phenylalanine was mutated to methionine. Type 1 copper center has high redox potential due to which substrate oxidation takes place in this site [51].

The reduction of dioxygen to water occurs in the trinuclear cluster (TNC), which is formed by type 2 and type 3 copper centers. Type 2 copper center is paramagnetic and shows no absorption in the visible spectrum. Type 2 copper center is coordinated by two histidine residues and is located close to the type 3 copper center. Type 3 copper center is a binuclear copper coupled pair with diamagnetic spin which adsorbs electron at 330 nm and is coordinated by six histidine residues. The hydroxyl bridge maintains the strong anti-ferromagnetic coupling between the type 3 copper atoms [51]. The eight histidine ligands of the TNC of the laccase occur in a extremely conserved pattern of four HXH motifs. In one motif, cysteine (X) is bound to type 1 copper and each of the histidine ligands is bound to one of the type 3 copper atom [52].

Type 1 copper center catalyzes the oxidation of the organic substrate and the three copper centers drive electrons to molecular oxygen without releasing toxic peroxide intermediates [51]. The mononuclear Type 1 copper center functions as the primary electron acceptor extracting electrons from the reducing substrate and shuttling the electrons to the trinuclear cluster, where reduction of molecular oxygen to water takes place along with the regeneration of the oxidized form of the enzyme [50]. This results in the formation of four reactive radicals and two water molecules. The four reactive radicals are formed by the oxidation of four molecules of substrate, whereas the reduction of one oxygen molecule produces two water molecules. These reactive radicals undergo non-enzymatic covalent coupling reactions resulting in the formation of dimers and polymers. Other non-enzymatic reactions include polymer degradation yielding monomers and ring opening reactions of aromatic compounds [54].

Figure 8 depicts the structure of the coordination network of the three different types of copper centers in laccase which are involved in the catalytic function. Type 1 copper center is coordinated with one cysteine, one methionine and two histidine molecules. The reaction mechanism of oxidation of substrate coniferyl alcohol by laccase can be seen in figure 9.

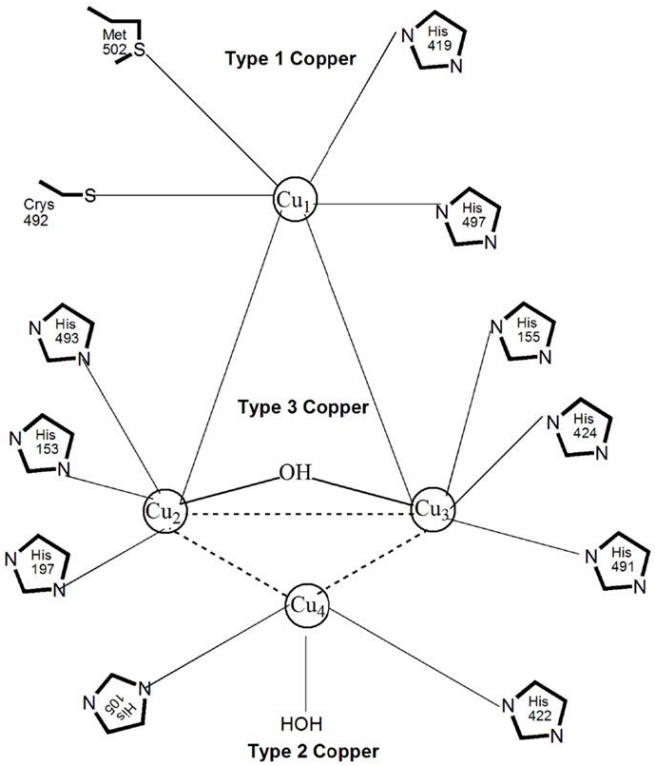

Figure 8: Schematic representation of three different types of copper centers in laccase [53].

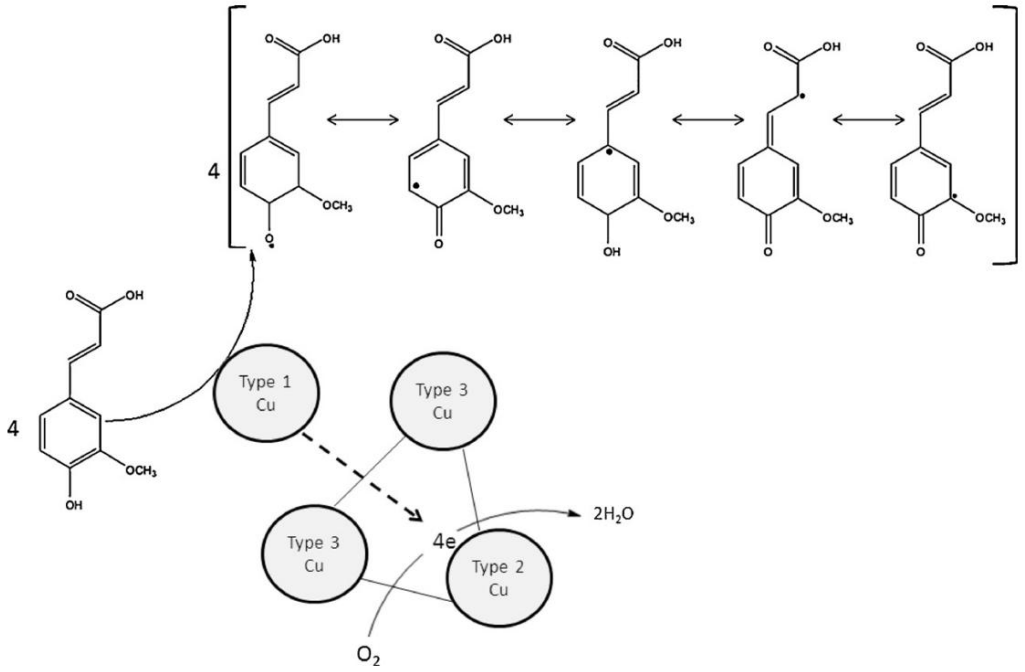

Figure 9: Reaction mechanism of laccase oxidation of substrate. Coniferyl alcohol is used as an example in this reaction [54].

The reduction of type 1 copper center is a rate limiting step in reactions catalysed by laccase which depends on the redox potential of the type 1 copper center [55]. Laccases can be classified into high potential and low potential laccases, based on the properties and structure of the copper center. Low potential laccases are widely distributed in bacteria, insects and molds whereas high redox potential laccases are found mainly in fungi mainly in the division of basidiomycetes [56]. The redox potential of laccase influences the substrate selectivity. Low redox potential laccases exhibit higher substrate selectivity whereas substrate selectivity is low for laccases having high redox potential [57].

Laccases can oxidize non-phenolic lignin residues in the presence of mediators whose redox potential is usually higher than 0.9 V. A mediator is a low molecular weight chemical compound which undergoes continuous laccase oxidation and subsequent substrate reduction reactions. The size of the substrate is responsible for the effect of steric hindrance, due to which the substrate is not able to reach the active site of the enzyme. The mediator overcomes this hindrance effect by carrying electrons between the substrate and the laccase. The reactivity of laccase to oxidize lignin decreases with the increase of the substrate size. Laccase mediators can be utilized to overcome this restricted accessibility of substrates. In the initial reaction step, oxidation of mediator by laccase to stable intermediates with high redox potential occurs. Then, the oxidized mediator due to its small size diffuses into the lignin substrate. As a result, the substrate is oxidized by the mediator intermediates, which could be not oxidized directly by laccase. The oxidized mediator is reduced to its initial form and the recycled mediator can oxidize another substrate molecule. An ideal redox mediator must be non-toxic in nature and possess the ability to maintain continuous cyclic redox transformations. The ideal mediator should be cost efficient and the intermediate forms must be stable so that inhibition of catalytic reactions does not occur [53].

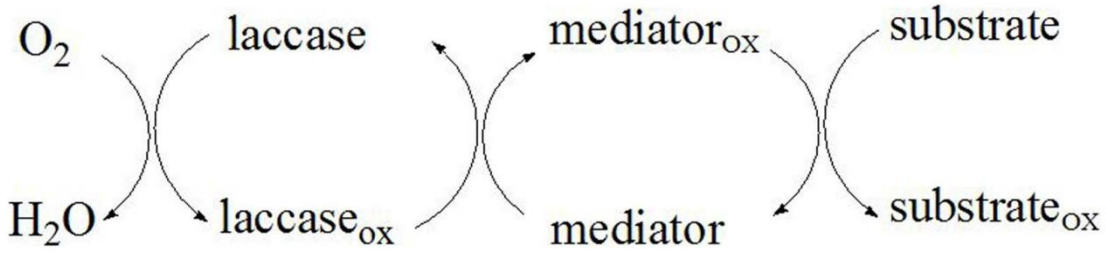

Figure 10: Reaction mechanism of substrate oxidation by laccase-mediator systems [53].

Common synthetic mediators used in laccase-mediator systems are ABTS (2,2' -azino-bis (3-ethylbenzothiazoline-6-sulfonic acid)) and HBT (1-Hydroxybenzotriazole). The laccase-ABTS system was able to oxidize, demethylate and delignify kraft pulps. Synthetic mediators are expensive, toxic and difficult to reuse, because of formation of by-products and the mediator intermediates are unstable resulting in poor substrate oxidation or incomplete redox cycles. To overcome these problems associated with synthetic mediators, naturally occurring mediators which are cost effective and environmentally friendly are gaining importance. Phenolic compounds produced by white rot fungi during delignification are potential sources of natural mediators. Examples of natural mediators include acetosyringone, syringaldehyde, vanillin, acetovanillone, hydroquinone, phenolsulfonphthalein. LMS has gained importance in applications such as soil bioremediation, manufacturing of pharmaceuticals, cosmetic products, textile dye bleaching and detoxification of industrial effluents [53].

Laccases are significant biocatalysts in fungal biotechnology due to their properties such as flexibility and broad substrate specificity [56]. In the textile industry, laccases are used in the modification of textile fibers, producing materials with many desired properties. Laccases are also utilized to degrade azo dyes which are extensively used in dyestuff and textile industries. In the food and beverage industry, laccases are used to remove undesired polyphenols which causes turbidity, color intensification and alters flavor in wine and fruit juices [54]. Laccase treatment exhibits delignification capacities providing a cleaner alternative to harmful chlorine based delignification and bleaching treatments in pulp and paper industry and are also capable of targeted modification of wood fibers to produce fiber based products. In soil remediation, laccases are utilized to degrade polycyclic aromatic hydrocarbons (PAHs) [58].

1.3.2 *Myceliophthora thermophila* (MtL) laccase

The thermophilic filamentous fungus *Myceliophthora thermophila* possesses a broad capacity for degradation of biomass. The fungus constitutes a potential cell machinery of novel enzymes that can be utilized for production of valuable products [59]. *Myceliophthora thermophila* is classified as an ascomycete and is also known as *Sporotrichum thermophile*. The isolation of the fungus from soil was first reported in eastern Russia. The exceptionally powerful microorganism synthesizes all cellulolytic enzymes required for cellulose degradation. The genome size of *Myceliophthora thermophila* is 38.7 Mbp which comprises about 9500 genes. A large number of genes was found to putatively encode industrially important enzymes such as carbohydrate-active enzymes (CAZy), lipases, proteases and oxidoreductases. More than 200 sequences of enzymes involved in plant wall degradation have been identified. These enzymes comprises a extensive number of polysaccharide lyases and glycoside hydrolases (GH) which are involved in plant wall degradation. To increase the feasibility in commercial applications, the fungus was developed into a trademarked mature enzyme production system called C1 strain. The C1 strain exhibits high production levels up to 100 g/L protein. The C1 strain also maintains low viscosity levels leading to very high density levels of the proteins of the fermentation processes [60]. *Myceliophthora thermophila* also represents a potential cell machinery for the production of biofuels from renewable lignocellulosic biomass [59].

MtL is a thermostable and heavily glycosylated protein with high solubility [61]. The molecular mass of native MtL is 80 kDa and the activity is optimal at pH 7 [62]. The overall architecture of MtL consists of three tightly associated cupredoxin like domains and the secondary structural elements of the three domains. The overall architecture of MtL can be seen in figure 11. In figure 11, the three domains A (blue), B (green) and C (yellow) and the four catalytic copper ions (orange spheres) are shown. The Type 1 Copper site is located in domain C while residues from the A and C domain form the tri-nuclear copper (TNC) site. The superimposed ligands displayed as black spheres represent the location of the Type 1 copper binding pocket and the cyan spheres illustrate an alternative substrate binding site in the type 1 copper center [61].

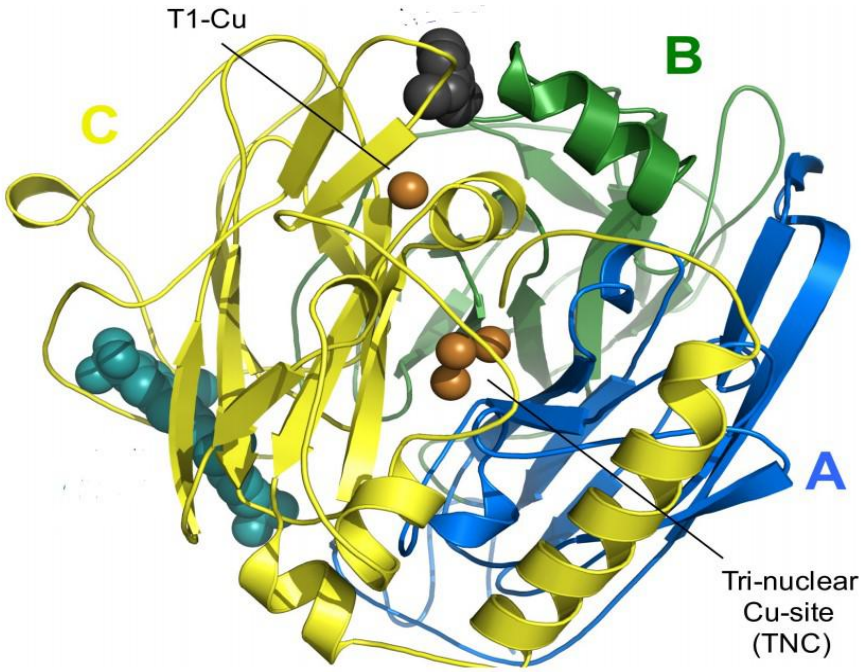

Figure 11: Overall architecture of MtL laccase [61].

The phenolic lignin substrate interacts directly with the type 1 copper histidine residues which are the primary electron acceptors. The axial ligand facilitates proton abstraction during the oxidation of phenolic substrates. These negatively charged ligands along with bridging water molecules form a polar residue for phenol recognition. MtL forms dimers with lignin substrates which seals the binding pocket of type 1 copper center suggesting that the active form of the enzyme is monomeric. MtL has a low redox potential of 0.45V and exhibits high substrate specificity [61].

1.4 Polymerization reaction

By increasing the molecular weight, the usability of lignin in particular valuable products can be enhanced [63]. The molecular weight can be increased by the introduction of radicals on the phenolic end groups of lignin which subsequently undergo coupling reactions leading to cross linking of lignin molecules. The formation of radicals during the pulping process exhibits low or zero selectivity. The radicals formed during oxidation of lignin phenols by manganese (III) ions under mild conditions have high selectivity and form coupled products. However, the formation of manganese (IV) oxide precipitate renders the method undesirable for large scale applications [64].

Enzymatic polymerization is a sustainable and environmental friendly approach to increase the molecular weight of lignin. The enzymes involved in the intrinsic polymerization during lignin formation are suitable for increasing the molecular weight of technical lignins [63]. The enzymes, peroxidases and laccases can oxidize the phenolic end groups of lignin and produce water as a by-product mimicking the natural lignification process. These enzymes exhibit high specificities in radical generation, can operate in mild reaction conditions and do not produce any undesired by-products. Laccases utilize dioxygen (O_2) for polymerizing lignin whereas peroxidases require hydrogen peroxide (H_2O_2) as their oxidants. The utilization of O_2 as oxidant is advantageous because of high stability, low cost and absence of decomposition reactions which could inactivate the enzyme. Hence, laccases are preferred in industrial applications [64].

The enzymatic activity of laccases involves the unit electron oxidation of four hydrogen donating substrates coupled with four electron reduction of dioxygen to water. The net result is the reduction of one molecule of oxygen to two molecules of water and oxidation of four molecules of substrate to produce four radicals. These reactive radicals can either degrade lignin releasing monomeric units or undergo covalent coupling to form lignin oligomers and polymers [54]. Efficient lignocellulose decomposers such as basidiomycetes produces radicals by laccase oxidation which leads to a production of different reactive species by various reactions [55]. These reactions can lead to productive and unproductive coupling. The predominant reactions in lignin oxidation by laccase is the formation of 5-5' and 4-O-5' bonds. If the 5- position is blocked, other reactions such as coupling at 1-position and oxidation of α-position occurs, leading to cross-linking of lignin molecules (productive coupling). An example of unproductive coupling is the coupling at 1-position in lignin when the 5-position in lignin is occupied for example by S units in hardwood lignin. As such, phenol OH group is only transferred from one end to another end group. Therefore, cross linkages between the lignin molecules are not formed leading to unproductive coupling [65].

Laccases can oxidize any substrates with characteristics similar to a *p*-diphenol [54]. However, the low oxidation potential of laccase limits the capacity of laccase to oxidation of only phenolic end groups in substrates like lignin. The non-phenolic end groups are not oxidized by laccase [64]. This can be due to the high redox potential of non-phenolic aromatic groups of substrates or due to the steric hindrance which inhibits the enzyme activity of oxidation of non-phenolic end groups [54].

Laccases are capable of polymerization as well as depolymerization of lignin. If the degree of depolymerization is high, the cross linking between lignin molecules decreases and other low molecular weight products are formed leading to a decrease in molecular weight. The degree of polymerization should predominate the degree of depolymerization for increase in molecular weight. Therefore, research must be done to increase the redox potential of laccases for broader substrate specificity and to reduce lignin degradation reactions.

2. AIMS

The aim of this study was to develop biobased processes for the modification of kraft lignin and make it suitable for industrial applications. In order to achieve this, two different approaches aimed at increasing the reactivity of lignin were carried out. The first approach includes the development of a kraft lignin filtration system for the isolation of highly reactive fractions from kraft lignin solutions. The second approach includes microbial demethylation of kraft lignin samples with the soft rot fungus *Aspergillus niger.* The aim of the microbial demethylation was to increase the reactivity of kraft lignin samples and improve their solubility. The phenol content can be increased by removing the methoxy groups on the benzene ring from the kraft lignin samples. This increase in the phenol content of lignin samples is thought to increase the reactivity of samples. The reactivity of the microbially demethylated and fractionated samples was tested by polymerization with a laccase from the fungus *Myceliophthora thermophila*. After the polymerization, the reaction products were characterized to monitor the changes in the functional groups which influence the reactivity of lignin. The herein used MtL enzyme is environmentally friendly and operations can be done at mild conditions with water as the only byproduct.

During the polymerization reaction, the fractionated and microbially demethylated kraft lignin samples were treated with the laccase. The samples were aerated with steady supply of external oxygen and a constant temperature was maintained during the reaction. The polymerized products of kraft lignin samples were then analyzed by different methods in order to determine changes in the functional properties and success of polymerization of the kraft lignin samples. These methods were determination of phenolic group content as well as measurement of fluorescence and viscosity. Spectral analysis by Fourier transform infrared spectroscopy revealed additional information about the chemical composition and functional properties of the kraft lignin samples before and after polymerization. Additionally, insights into the demethylation mechanism by *Aspergillus niger* such as sugar consumption for metabolism and secreted enzymes for kraft lignin modification were determined by high performance liquid chromatography and SDS PAGE respectively.

The presence of methoxylated reactive aromatic hydroxyls potentially affects the usability of kraft lignin in value added products and industrial applications. Modification of kraft lignin enhances the reactivity for broader industrial applications and also for the development of novel applications of the heterogeneous biopolymer. Additionally, comparison between the reactivity of SWKL and HWKL samples from different wood sources were done.

3. MATERIALS AND METHODS

3.1 Enzyme

The laccase from the organism *Myceliophthora thermophila* was kindly supplied by Novozymes (Bagsveard, Denmark).

3.2 Chemicals

All of the chemicals utilized were of analytical grade quality and purchased from Sigma-Aldrich, VWR, Merck, Roth, Roche, Serva, Zeller GmbH, Fluka and BioRad (Table 1).

Table 1: List of chemicals used.

CHEMICAL	MANUFACTURER
Vanillin	Sigma-Aldrich
Sodium hydroxide	Zeller GmbH
Folin-Ciocalteu reagent	VWR
2- Methoxyethanol	Sigma-Aldrich
Sodium carbonate	Sigma-Aldrich
Hydrochloric acid	Sigma-Aldrich
Ethanol	Sigma-Aldrich
Azino-Bis(3-Ethylbenzothiazoline-6-Sulfonic acid)	Roche
Disodium hydrogen phosphate	Sigma-Aldrich
Sodium dihydrogen phosphate	Roth
Peptone extract	Fluka
Yeast extract	Sigma-Aldrich
Glucose	Sigma-Aldrich
Sulphuric acid	VWR
Trihydrate Potassium ferrocyanide	Sigma-Aldrich
Zinc sulfate heptahydrate	Sigma-Aldrich
Sodium nitrate	Roth
Sodium azid	Roth
Sodium dodecyl sulfate	Sigma-Aldrich
Coomassie brilliant blue R250	Sigma-Aldrich
Protein marker IV	VWR
Crystal violet	Sigma-Aldrich
TGS buffer	BioRad
Acetone	Sigma-Aldrich

3.3 Lignin samples

The samples were received in a dried state and were further milled and characterized. The properties and the findings for the characterization are summarized in Table 2.

Table 2: Properties of the kraft lignin samples.

	SWKL	HWKL
Ash content	Low	Low
Kind	Spruce softwood	Hardwood
pH	2	3.0
M_w [kDa]	20.6	3.2
PDI	4.9	3.6
S/G ratio	0.35	1.05
Phenol [mg/mL]	49.200	57.697

3.4 Determination of the enzyme activity

The MtL activity was measured spectrophotometrically at the wavelength of 420 nm using a plate reader (Infinite M200, Tecan, Switzerland). The substrate ABTS (Azino-Bis(3-Ethylbenzothiazoline-6-Sulfonic acid)) is oxidized by MtL to its green blue colored cation radical and the concentration of the colored radical corresponds to the MtL activity [53]. The laccase activity was measured in units per millilitre (U mL^{-1}). One U (µmol min^{-1}) corresponds to the laccase amount that catalyses the conversion of 1 µmol of substrate per minute.

The enzyme activity of MtL was measured at pH 7 with 0.05 M Disodium hydrogen phosphate (Na_2HPO_4) buffer. 0.01 M ABTS solution was prepared by the dissolution of relative amount of ABTS (mg) in ultrapure water. Serial dilutions upto the final dilution (1:30000) of the enzyme in Na_2HPO_4 was performed. The reaction mixture contained 50 µL of 0.01 M ABTS solution and 170 µL of enzyme diluted 1:30000. The blank used for the assay was 170 µL Na_2HPO_4 buffer. In the 96 well plate (Carl Roth, Germany), triplicates of the blank and enzyme diluted in Na_2HPO_4 buffer was added first followed by the addition of 50 µL of 0.01 M ABTS solution and the measurement of the absorbance values was done immediately at 420 nm in the plate reader.

The activity was determined from the linear range of the curve obtained when the absorbance (ordinate) was plotted against the time (abscissa). The slope is defined as the change in absorbance per minute and the mean activity is calculated from the formula given below.

$$[\mu kat/mL] = \frac{Slope[1 \times min^{-1}] \times \text{total volume}\,[mL] \times \text{dilution factor} \times 1.6 \times 10^{-2}}{pathlength[cm] \times \text{sample volume}\,[mL] \times \text{molar extinction coefficient}\,[1 \times cm^{-1} \times mmol^{-1}]}$$

Formula 1: Determination of the activity of the enzyme [53].

$1\ U.mL^{-1} = 1.6 \times 10^{-2}\ \mu kat.\ mL^{-1}$

The path length used in this formula is 0.61 cm and the molar extinction coefficient at pH 7 is 12.07 $mmol^{-1}cm^{-1}$.

3.5 Dissolving of lignin samples

Hardwood kraft lignin (HWKL) and softwood kraft lignin (SWKL) are soluble in high pH values. Hence, lignin solutions were prepared by dissolving samples in ultrapure water and the pH is set to 9.0 by the addition of 2M NaOH.

3.6 Fractionation of lignin by crossflow filtration

Fractionation of HWKL and SWKL samples is performed in order to characterize the lignin fractions in terms of phenol content, fluorescence, fourier transform infrared spectroscopy, viscosity and oxygen consumption during polymerization with MtL. The principle method for fractionation is crossflow filtration of lignin samples through the pump head driven by the rotor.The pump head was kindly supplied by Masterflex®,United states of America. The rotor of the Masterflex® Easy load model 07514-10 is constructed of stainless steel. The reusable crossflow cassette Vivaflow 50 R for concentrating the lignin samples was supplied by Sartorius, United Kingdom. The cassette features a unique, low-binding regenerated cellulose membrane Hydrosart® with a membrane area of 50 cm^2.

Forty grams of HWKL and SWKL samples are dissolved in 400 mL of ultrapure water. The pH is set to 10 by adding 2M NaOH. For the HWKL sample, a membrane with a cut-off of 5000 Da and for SWKL sample a membrane with a cut-off of 10000 Da is used. Before concentrating the sample, ultrapure water is run through the cassette to remove ethanol. Then, air is passed through the module to remove the ultrapure water. The sample is then run through the cassette and the pressure is maintained at 2 bar. The sample is run for 6 h and the resultant retentate and the filtrate are collected and dried in the oven at 70℃ for 3 to 4 days.

3.7 Microbial demethylation of lignin

FUNGAL STRAIN: The ascomycete fungus *Aspergillus niger* is able to metabolize the aromatic compounds in lignin. *Aspergillus niger* is used to increase the reactivity of lignin by demethylating the aromatic structures of lignin. The filamentous fungus *Aspergillus niger* (DSM: 1957) was supplied by the German Collection of Microorganisms and Cell Cultures GmbH (DSMZ), Leibniz, Germany.

Media preparation

Pre-culture medium: 5 g/L Yeast extract
10 g/L Peptone extract
Carbon source: 2 g/L Glucose

The pH of the pre-culture medium was set to 4.0 with 0.5 M HCl and then autoclaved. The carbon source was autoclaved separately and added into the flask shortly before inoculation.

Demethylation culture medium: 5 g/L Yeast extract
10 g/L Peptone extract
Lignin: 5 g/L HWKL and SWKL
Carbon source: 5 g/L Glucose

The pH of the culture medium was set to 4.0 with 0.5 M HCl and then autoclaved. The carbon source was autoclaved separately.

3.7.1 Pre-culture

For the pre-culture, three 500 mL flasks with baffles containing 150 mL of pre-culture medium and 50 mL glucose were used. The flasks were then inoculated with 500 µL of a cryostock of *Aspergillus niger*. The pre-cultures were then incubated at 30°C and 150 rpm for 4 to 5 days.

3.7.2 Spore counting

After incubation, the morphology and the density of the fungal spores are checked in order to determine the number of spores required for microbial demethylation with HWKL and SWKL samples. For visualization, 12 µL of the pre-culture medium was stained with crystal violet under aseptic conditions. The chamber of the haemocytometer was filled with 10 µL of the stained medium containing spores and the morphology was checked under the microscope. The number of spores in two different 4 x 4 grids were counted to determine the average number of spores per mL.

N_1 = (Total number of spores in 16 squares of first 4 x 4 grid)/16
N_2 = (Total number of spores in 16 squares of second 4 x 4 grid)/16
$N_A = (N_1 + N_2)/2$
$N = N_A * 10^5$

Where,N_1 and N_2 are the average number of spores in a single square of the first and second 4x4 grid respectively; N_A is the average of N_1 and N_2; N is the average number of spores in 1 mL of pre-culture medium.

3.7.3 Microbial demethylation

For the microbial demethylation, 1 L flasks with baffles containing 400 mL culture medium were used. HWKL and SWKL samples (5g/L) were dissolved in 150 mL ultrapure water. The samples are then autoclaved, and three different combinations were performed for each lignin sample, each combination was done in three replicates. The combinations were as follows:

Medium + Lignin (M+L): Under sterile conditions, 390 mL of culture medium is added to the flasks. To the culture medium, 10 mL glucose and 50 mL lignin solution is added. This serves as a control for microbial demethylation as there is no *Aspergillus niger* present.

Medium + Organism (M+O): Under sterile conditions, 390 mL of culture medium is added to the flasks. To the culture medium, 10 mL glucose is added followed by inoculation with 10^5 spores/mL from the pre-culture.

Medium + Organism + Lignin (M+O+L): Under sterile conditions, 390 mL of culture medium is added. To the culture medium, 50 mL lignin solution is added and then inoculated with 10^5 spores/mL of the pre-culture. The sugars formed during microbial demethylation in the lignin sample serves as a substrate for *Aspergillus niger* and therefore addition of glucose is not necessary.

The M+O+L sample is the demethylated sample and both the M+O, M+L samples are the demethylation control samples. Samples of 10 mL were taken under sterile conditions (time point 0). The cultures are then incubated at 30°C at 150 rpm. Every 48 hours samples were taken under sterile conditions. This is done for five time points. The collected samples of all the time points are centrifuged at 3700 rpm for 6 minutes at room temperature. The supernatant obtained is used for determination of sugar content by HPLC and secreted fungal enzymes by SDS-PAGE.

3.7.4 Determination of sugar content by HPLC

High Performance Liquid Chromatography (HPLC) separates compounds in a mixture based on the compounds partition properties between a stationary phase and a mobile phase. The sugar content of lignin samples is determined by anion exchange chromatography. The principle mechanism is separation of negatively charged analyte ions based on their differential affinity to the cationic stationary phase and aqueous based mobile phase. The signal generated by elution of analyte is captured by refractive index detection method. The principle of detection is based on the measurement of the variation in refractive index of eluent relative to the aqueous based mobile phase. The greater the refractive index difference between the mobile phase and the eluent, the greater is the signal [69].

SAMPLE PREPARATION: For every time point, 200µL from the supernatant of a sample is used for HPLC analysis. To each sample, 760 µL of 0.05 M sulfuric acid is added followed by Carrez precipitation with 20 µL $K_4[Fe(CN)_6].3H_2O$ (Trihydrate Potassium ferrocyanide) and 20 µL $ZnSO_4.7H_2O$ (Zinc sulfate heptahydrate). The precipitated samples were centrifuged at 14000 rpm at room temperature. 40µL of the supernatant from each sample (1mg/mL) is then injected through a 0.45 µm sterile filter into glass vials. The samples are analysed for glucose concentration.

Glucose concentration was measured using HPLC. An ion exchange column ION 300 (Transgenomic, Omaha, USA) heated to 45°C was used in a separation module equipped with a refractive index detector (Agilent 1100, Santa Clara, USA). Elution was performed using 0.005 mol/L sulfuric acid as the mobile phase, at a flow rate of 0.325 mL/min. The column and refractive index detector were maintained at 45°C with a sample run time of 70 minutes. For data analysis, Agilent ChemStation software was used.

3.7.5 Determination of molecular weight of secreted proteins by SDS PAGE

Sodium dodecyl sulfate polyacrylamide gel electrophoresis (SDS PAGE) has been an important method since 1950 for molecular weight estimation and analytical separation of protein mixtures. The most popular SDS PAGE procedure was described by Laemmli in 1970. The technique is based on the basic principle that protein having net electrical charge in a medium will migrate when subjected to an electric field. In order to separate proteins solely based on molecular weight, an anionic detergent sodium dodecyl sulfate (SDS) denatures protein molecules and imparts a net negative charge to the SDS-protein complex which allows them to migrate through the gel depending solely on their molecular weight [70].

Solutions for SDS PAGE

Destaining solution: 600 mL ultrapure water + 300ml 96% (v/v) ethanol + 100mL 99% (v/v) acetic acid

Staining solution (1.25g/L): Destaining solution + 0.125% Coomassie brilliant blue R250

Running buffer: 1 x TGS buffer

The sample supernatant obtained after centrifugation is used to determine the extracellular enzymes secreted by the fungal organism *Aspergillus niger.* At each time point, 400 µL of the sample supernatant was collected and stored at -20°C. 1.2 mL ice cold acetone was added to each sample supernatant and the samples were stored overnight on ice. The samples were then centrifuged at 4°C at 14000 rpm for 30 minutes. The acetone supernatant was discarded, and

the cell pellets were denatured with 20 to 40 µL Laemmli buffer containing β-mercaptoethanol at 99°C for 10 minutes at 300 rpm in the thermomixer.

PeqGold prestained protein marker IV was used as a molecular weight standard to estimate the molecular weight of extracellular fungal enzymes separated by SDS-PAGE. The marker contains a mixture of 10 recombinant highly purified proteins with molecular weights ranging from 10kDa to 170kDa. The loading buffer used was 1 x TGS Buffer and the denatured samples were then loaded into the pockets of the polyacrylamide gel.

The run time of polyacrylamide gel electrophoresis was 60 minutes at 100 V. After 60 minutes, coomassie brilliant blue R-250 staining solution was added to the gels and the gels were kept on the shaker for 30 minutes. The staining solution was removed and the destaining solution was added to the stained gels. The gels were kept on the shaker overnight. The gels were again destained for 1 hour and the gels were visualized (BIO-RAD ChemiDoc™ MP Imaging System) for the bands.

3.8 Biochemical analysis of lignin

3.8.1 Lignin polymerization reaction

Oxygen supply is critical for the polymerization of lignin by laccase. To monitor and measure the change in dissolved oxygen concentration over time during polymerization, a fiber optic multifunctional oxygen meter called FireSting O_2 is used. The device FireSting O_2 is manufactured by *Pyroscience* GmbH (Aachen, Germany). The measuring principle of the fiber optic oxygen meter is based on red light excitation and detection of the phase shifted sinusoidally modulated emission in the near infrared (NIR) region using luminescent oxygen indicators. The measured phase shift is then converted into oxygen units. The oxygen unit measured is % O_2.

Before connecting to the oxygen supply, empty bottles with sensor spots are calibrated (two point) at 0% (N_2) and 100% oxygen (air). The sensor was excited at 610 nm and the emission was measured at 760 nm. The flow rate of the pure oxygen supply channel was adjusted to 30 cm^3 min^{-1} to ensure adequate concentration of pure oxygen in the lignin solution during polymerization.

The temperature for polymerization of both HWKL and SWKL samples by MtL is set to 33°C. The respective reaction volume of the sample, containing 10% (w/v) dry substance (DS) is added to the bottle connected to the sensor of the FireSting device. Before connecting the oxygen supply, 2 mL of the sample were taken for viscosity measurement and 1 mL for determination of phenol content and fluorescence. This point is time point 0 (TP0).

The volume of enzyme required for polymerization is derived from the activity determined by ABTS assay (section 3.4). The needed volume of the enzyme to reach an activity of 10 U/mL is calculated. The activity of MtL measured is 792.905 U/mL. For the activity of 10 U, the volume is 0.01261 mL. For example, the volume of crude lignin solution used is 100 mL. The volume of the enzyme needed for polymerization of crude sample is 0.01261 mL × 100 mL = 1.26 mL.

After TP0, the oxygen supply is connected to the lignin solution and stirred at 500 rpm at 33°C. The dissolved oxygen content of the lignin solution was monitored until a steady oxygen level is reached. Then the respective amount of enzyme was added to the lignin solution. Upon the addition of enzyme, the dissolved oxygen content drops slowly and approaches 0% oxygen. Afterwards an increase in oxygen content can be observed again until a saturation level is reached.

Three samples (TP1, TP2 and TP3) were collected at an interval of 1 h. The overall polymerization run time is 3 h and a total of 4 samples were collected to monitor the progress of the reaction in terms of phenol content, fluorescence and viscosity.

Polymerization was done for crude HWKL and SWKL samples; fractionated HWKL and SWKL samples (retentate and filtrate fraction); demethylated (M+O+L) and demethylation control (M+O, M+L) HWKL and SWKL samples.

3.8.2 Fluorescence measurements

Fluorescence is an intrinsic property of lignin that can be used to monitor lignin polymerization. The fluorescence intensity during the lignin polymerization was measured to monitor the reaction [18]. The reaction mixture consists of 100 µL of the diluted polymerized lignin sample (1:5000) mixed with 120 µL of a water solution of 2-methoxyethanol (2:1 v/v). The reaction mixture was then transferred into a 96 well plate (Greiner Bio-One, Austria). As blank, 100 µL of water is used instead of the sample. The excitation wavelength of the sample was 355 nm and the emitted light was measured at 400 nm using a plate reader (Infinite M200, Tecan, Switzerland).

3.8.3 Determination of phenol content

The content of phenolic groups was determined using the Folin-Ciocalteu (FC) method. The method is based on the formation of blue phosphotungstic-phosphomolybdenum complex during the reaction of FC reagent with phenol groups. This blue complex can be quantitatively measured by visible light spectrophotometry [66].

The samples from the polymerization reaction are serially diluted in ultrapure water to 1: 5000. For phenol content determination, 1:50 diluted lignin samples are used. The reaction mixture consists of 20 µL lignin sample and 60 µL FC reagent filled up to a final volume of 680 µL with ultrapure water. The blank contains 60 µL FC reagent with 620 µL ultrapure water and is treated like the samples. The samples are vortexed and incubated at 21°C for 8 minutes in the thermomixer (Eppendorf, VWR, Austria). Afterwards, 200 µL sodium carbonate 20% (w/v) and 120 µL ultrapure water were added. The samples are then incubated for 2 h at 21°C at 800 rpm in the thermomixer (Eppendorf, VWR, Austria) and then 200 µL of the samples were transferred into a 96 well plate (Carl Roth, Germany). The absorbance of the samples was determined at the wavelength of 760nm using a plate reader (Infinite M200, Tecan, Switzerland). The phenol concentration in the lignin samples was calculated using the calibration curve which is generated using vanillin as standards in concentrations ranging from 0.05 $g.L^{-1}$ to 1 $g.L^{-1}$. All samples were measured in triplicates.

3.8.4 Viscosity measurements

To measure the viscosity a MCR 302 Rheometer (Anton Paar GmbH, Austria) was used. The device was equipped with the CP 50-1 measuring system, a measuring plate with a diameter of 50 mm and an angle of 1º. The principle of measurement of a rheometer is based on the viscosity law which is derived from the ratio of the shear stress (τ) and shear rate (γ). The principle of operation is based on controlled shear rate and the rheometer determines the required shear stress and the change in defined torque [67].

The rheometer runs on the RheoCompass software (version 1.24). The device is calibrated at zero gap width and the water bath is set to 20°C. The shear rate is kept constant at 200 s^{-1} throughout the measurements. The samples are loaded on to the device and 10 measuring points are taken in a period of 10 seconds. Each sample is measured twice and the data is exported for analysis. The measured data consists of shear stress [Pa], Torque [mN*m] and viscosity [mPa*s] for each measurement.

3.8.5 FTIR spectrum analysis

FTIR was performed on a PerkinElmer Spectrum 100 spectrometer equipped with an universal ATR (attenuated total reflectance) attachment. FTIR works on the principle of Fourier transformation which determines the interferogram experimentally. The molecules on absorbing IR radiation excite to a higher vibrational state and the absorbed IR frequency interacts with the molecule at a certain frequency. The transformation is carried out automatically and provides fingerprint information on the chemical composition of the sample [68].

A few milligrams of dried HWKL and SWKL samples were analyzed in triplicates between 600 and 4000 cm^{-1} with a 4 cm^{-1} resolution and 30 scans. Baseline correction of each sample spectrum followed by normalization between 1000 and 1600 cm^{-1} was done. The average spectra from the normalized triplicates of each sample were then determined. The system was managed by Spectrum Express™ software (version 10).

4. RESULTS AND DISCUSSIONS

4.1 Results

4.1.1 Enzyme activity

The activity of MtL was determined on a consistent basis. The maximum activity obtained was 792.905 U/mL at pH 7 at room temperature. The activity of the MtL enzyme decreased with time. The enzyme activity depends for example on the molarity of the buffer (Na_2HPO_4) used.

4.1.2 Fractionation of lignin samples

4.1.2.1 Oxygen consumption during polymerization

The Firesting device was used to monitor the oxygen consumption during oxidation of lignin samples. The behaviour of oxygen content is similar for all lignin samples. Initially, the oxygen content is constant for all lignin samples and after the addition of MtL during which oxygen supply was discontinued, a slow decrease in oxygen content was observed for all samples. This decrease was observed during the three sampling time periods at an interval of 60 minutes for all lignin samples. After the addition of enzyme, the oxygen supply was continued and the oxygen content started increasing again to a constant level. In some lignin samples, abnormalities in oxygen content measurements were observed due to issues with the sensor spots which led to fluctuations in the measurements.

HWKL crude and fractionated samples

The MtL oxidation of the crude sample led to a drop of the oxygen content from 80% to 50% for 100 mg of the sample upon the addition of the enzyme. During the polymerization reaction, the oxygen consumption for MtL oxidation was high and it nearly reached the initial value of around 80% at the last hour of polymerization. The high molecular weight retentate fraction showed a drop of oxygen content from 100% to 90% during the addition of MtL. During the polymerization, the oxygen content reached the initial level of 100% and drops were only observed during the sampling time. In contrast, the filtrate fraction showed a larger drop in oxygen content to 60% and nearly reached the initial level during the last hour of polymerization with MtL. The oxygen consumption was higher for the filtrate fraction compared to the retentate fraction (figure 12). The oxygen content is measured in absolute unit O_2[%] and the scales are adjusted accordingly for better comparison and readability.

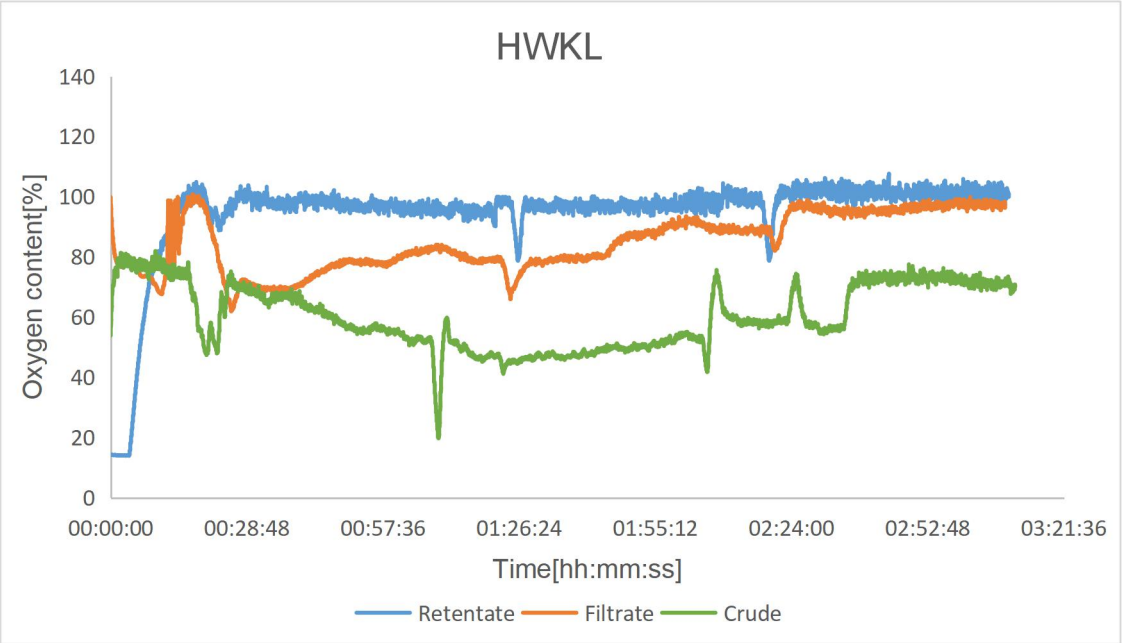

Figure 12: Oxygen profile for HWKL crude and fractionated samples. The oxygen content in all three samples were observed to decrease upon addition of MtL and during the sampling periods. The oxygen consumption was the highest for the crude sample and lowest for the retentate fraction.

SWKL crude and fractionated samples

The retentate fraction showed a drop of oxygen content from around 130% to 100% during the first sampling period and reached a constant level of 120% during the last hour of polymerization. In contrast, the filtrate fraction showed a smaller drop from 110% to 100% during the first sampling period and reached the initial level of 100% during the polymerization reaction with MtL. Additionally, due to issues with the oxygen sensor spot during the polymerization of crude sample, the oxygen content measurements were insufficient to generate a graph for comparison (figure 13).

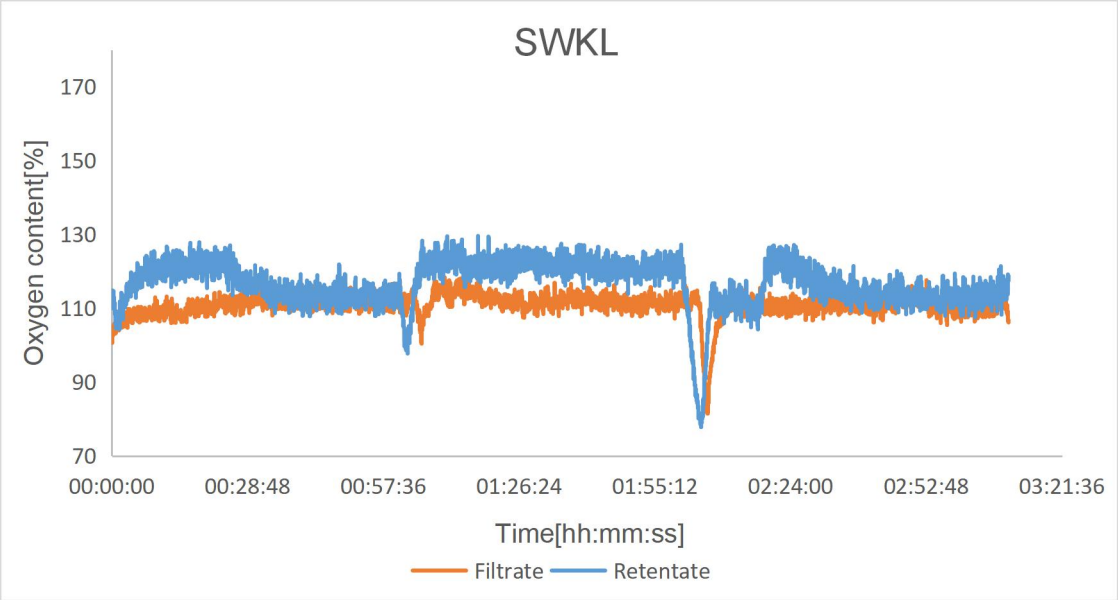

Figure 13: Oxygen profile for SWKL fractionated samples. The drop in oxygen content during the addition of MtL is not shown in the figures below because of inconsistent measurements around the time of MtL addition. The inconsistent measurements are due to problems with the sensor spots for both the fractionated samples and hence the measurements are adjusted for better comparison.

4.1.2.1.1 Comparison between HWKL and SWKL samples

The SWKL retentate fraction achieved a higher oxygen content compared to HWKL retentate fraction, indicating that the oxidizable substrates in SWKL were quickly exhausted and oxygen consumption was low for polymerization reaction compared to the HWKL retentate sample. Similarly, the SWKL filtrate fraction attained a higher oxygen saturation level during polymerization with MtL compared to the HWKL filtrate fraction. In contrast, the crude HWKL sample attained a lower oxygen saturation level indicating higher oxygen consumption and that further polymerization at extended time is possible compared to HWKL fractionated samples.

4.1.2.2 Fluorescence measurements

Fluorescence intensity was determined in order to monitor the polymerization process. During the polymerization, all samples showed decreasing fluorescence intensity due to the oxidation and modification of arylconjugated carbonyl groups and other functional fluorophore molecules in lignin by laccase [18]. The measured fluorescence intensity was observed to be decreasing in most of the lignin samples during polymerization, but the intensity never reached zero value. The fluorescence intensity is represented by the unit x1000 FU for better readability and comparison between all polymerized samples. For this reason, the scale for the fluorescence intensity is the same for all the figures. The fluorescence values of lignin samples and corresponding standard deviations are tabulated in table 3.

Table 3: Fluorescence intensity for crude and fractionated lignin samples along with their corresponding standard deviations.

SAMPLE	Time[h]	FLUORESCENCE [x1000 FU] HARDWOOD KRAFT LIGNIN	STANDARD DEVIATION HWKL	FLUORESCENCE [x1000 FU] SOFTWOOD KRAFT LIGNIN	STANDARD DEVIATION SWKL
CRUDE	0	2430.0	68.24	2476.67	11.02
	1	561.67	1.53	1158.34	6.03
	2	746.67	70.21	1036.67	6.03
	3	460.0	3.61	1056.67	47.61
FRACTIONATED RETENTATE	0	886.67	4.04	1493.34	22.48
	1	715.0	3.0	1701.67	56.45
	2	660.0	9.54	1546.67	15.01
	3	773.34	34.08	1446.67	4.93
FRACTIONATED FILTRATE	0	1425.0	9.64	1665.0	24.27
	1	1198.34	67.86	1158.34	4.62
	2	988.34	2.09	985.0	8.0
	3	1135.0	15.59	2220	130.98

HWKL crude and fractionated samples

A 5.3 fold decrease in fluorescence intensity from 2430 x1000 FU to 460 x1000 FU was observed when 100 mL of crude sample containing 10% (w/v) DS was oxidized by MtL. However, for the retentate fraction containing high molecular weight monomers (>5 kDa), a 1.1 fold decrease in fluorescence intensity was observed. In contrast, the filtrate fraction containing low weight monomers (<5 kDa), showed a 1.26 fold decrease in fluorescence intensity at the end of polymerization (figure 14).

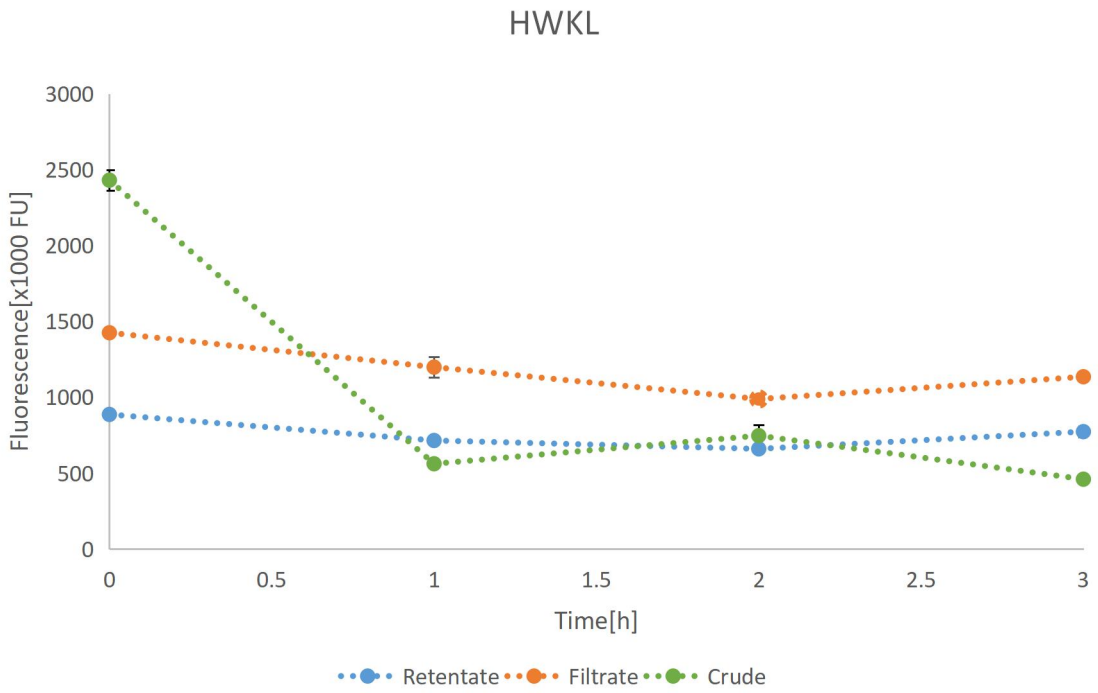

Figure 14: Fluorescence intensity profile for crude and fractionated HWKL 10% DS polymerized for 3h with MtL (792.905 U mL^{-1}). The fluorescence intensity of all three samples decreased during the polymerization.

SWKL crude and fractionated samples

The crude sample showed a 2.3 fold decrease in fluorescence intensity from 2476 x1000 FU to 1056 x1000 FU when the sample containing 10%(w/v) DS was oxidized by MtL. Interestingly, the retentate fraction containing high molecular weight monomers (>10 kDa) showed minuscule change in fluorescence intensity at the end of polymerization. The alkali soluble filtrate fraction containing low molecular weight monomers (<10 kDa) showed a 1.3 fold increase in fluorescence intensity from 1665 x1000 FU to 2220 x1000 FU (figure 15).

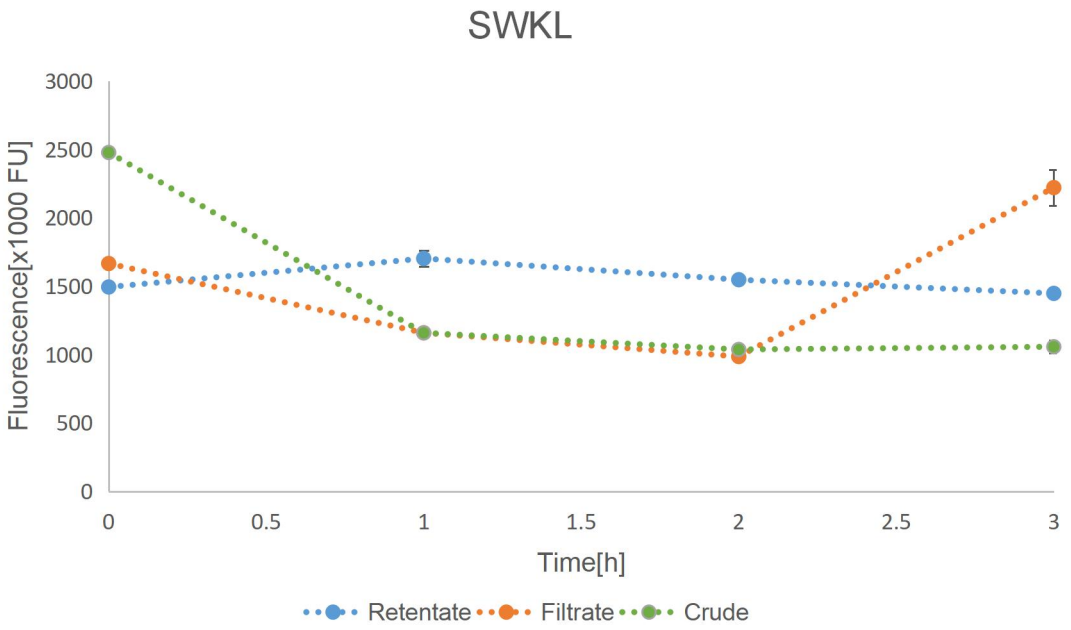

Figure 15: Fluorescence intensity profile for crude and fractionated SWKL 10% DS polymerized for 3h with MtL (792.905 U mL^{-1}). The crude sample showed decrease in fluorescence intensity whereas for the retentate fraction, the change in fluorescence intensity was very small. However, the fluorescence intensity of the filtrate fraction increased at the end of polymerization.

4.1.2.2.1 Comparison between HWKL and SWKL samples

In both HWKL and SWKL crude and fractionated samples, the largest reduction in fluorescence intensity during polymerization was observed for the crude samples. The decrease in fluorescence intensity for the retentate fractions of HWKL and SWKL were small, but the retentate fraction of HWKL had lower fluorescing moieties compared to the retentate fraction of SWKL at the end of polymerization .The increase in the fluorescence intensity for SWKL filtrate fraction may be due to depolymerization by MtL during the course of polymerization.

4.1.2.3 Phenol content

4.1.2.3.1 Calibration

For the calibration of the Folin-Ciocalteu assay vanillin standards were used. Changes in the phenol concentration of the lignin samples during polymerization occur due to the oxidation by laccase [66]. In order to compare the phenol content values of the lignin samples, the calibration values were considered in the data analysis. The absorbance of vanillin increased linearly with increasing concentration. The vanillin concentration (abscissa) was plotted against the absorbance (ordinate) and a linear function was calculated (figure 16).

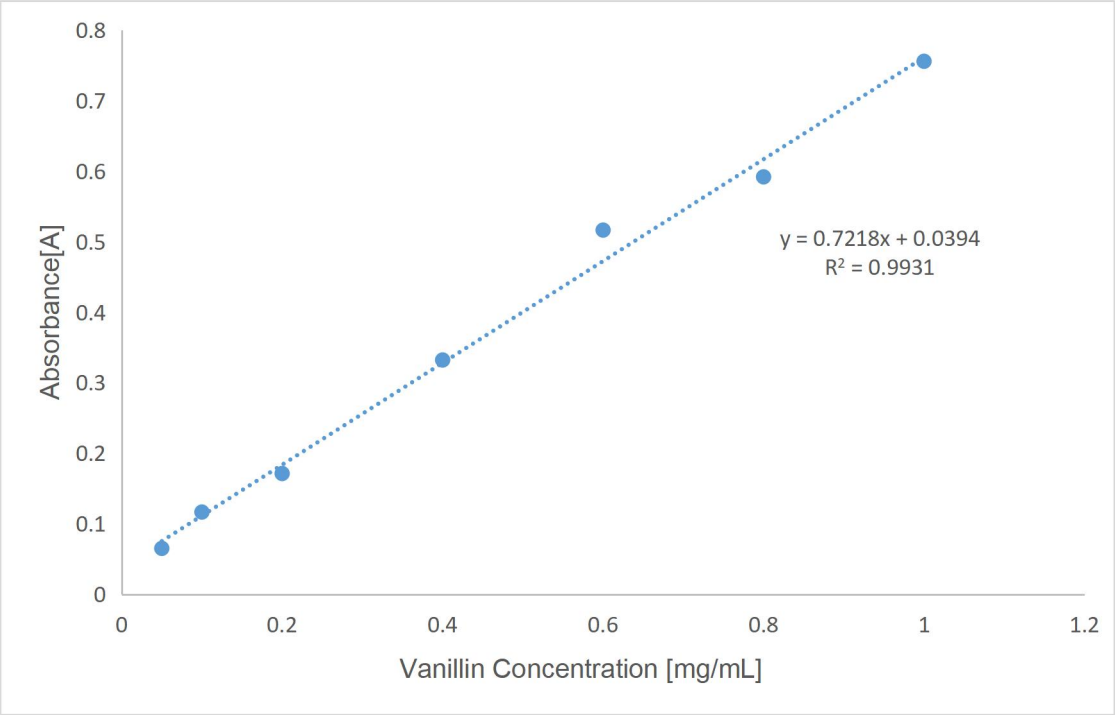

Figure 16: Vanillin Calibration curve for measurements of phenol content of lignin samples. Absorbance (ordinate) increases linearly with increase in vanillin concentration (abscissa).

4.1.2.3.2 Phenol content for polymerized samples

Phenol content was determined in order to monitor the polymerization process. During the polymerization, all samples showed a decrease in phenolic concentration due to oxidation of phenol groups by low redox potential MtL. This decrease is attributed to radical-radical coupling of phenoxyl radicals leading to a linkage of monomeric radicals of lignin samples and radical rearrangement to various condensation products [54]. However, the measured phenol concentration was observed to be decreasing in most of the samples during polymerization but the phenol concentration never reaches zero value. The phenol content is expressed in concentration units (mg/mL) and a similar scale is utilized for all figures for better comparability and readability. The phenol concentration values [mg/mL] and their corresponding standard deviations calculated for polymerized lignin samples are shown in table 4.

Table 4: Phenol concentration for crude and fractionated lignin samples along with their corresponding standard deviations.

SAMPLE	TIME [h]	PHENOL CONCENTRATION [mg/mL] HARDWOOD KRAFT LIGNIN	STANDARD DEVIATION HWKL	PHENOL CONCENTRATION [mg/mL] SOFTWOOD KRAFT LIGNIN	STANDARD DEVIATION SWKL
CRUDE	0	48.09	0.0023	32.53	0.0011
	1	31.49	0.0137	27.96	0.0039
	2	29.61	0.0057	27.18	0.0044
	3	19.93	0.0031	26.90	0.0123
FRACTIONATED RETENTATE	0	45.59	0.0044	30.39	0.0203
	1	28.05	0.0071	28.36	0.0184
	2	36.02	0.0082	33.25	0.0087
	3	27.02	0.0043	29.06	0.0118
FRACTIONATED FILTRATE	0	18.38	0.0015	15.26	0.0018
	1	17.44	0.0057	11.06	0.0022
	2	18.13	0.0054	10.05	0.0033
	3	13.39	0.0027	8.017	0.0015

HWKL crude and fractionated samples

The phenol content showed a similar trend like the fluorescence intensity during enzymatic polymerization of HWKL crude and fractionated samples. In this case, the decrease in phenol content was 2.52 fold for the crude sample. The retentate fraction containing high molecular weight monomers (>5 kDa) showed a 1.68 fold decrease in phenol content. In contrast, the filtrate fraction containing low molecular weight monomers (<5 kDa) showed a smaller, namely a 1.37 fold decrease in phenol content at the end of polymerization by MtL (figure 17).

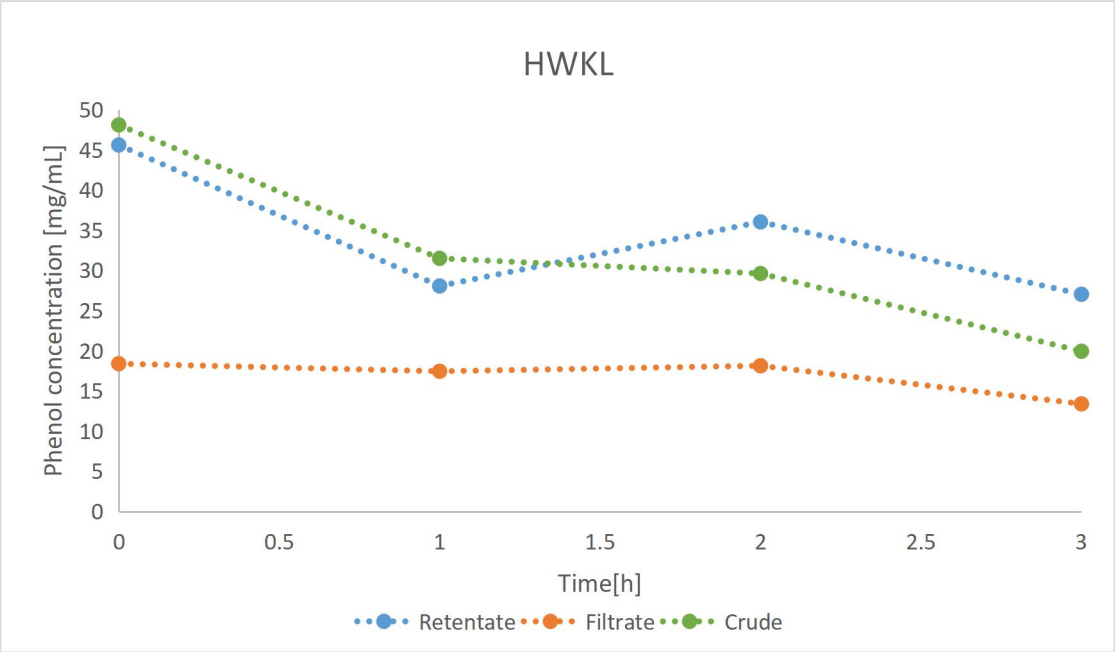

Figure 17: Phenol content of HWKL crude and fractionated samples polymerized by MtL along with the corresponding standard deviations. The phenol content of all three samples decreased during the polymerization.. The phenol content of retentate fraction was the highest and the lowest phenol content was observed in filtrate fraction.

SWKL crude and fractionated samples

The phenol content trend was similar to fluorescence intensity during enzymatic polymerization of SWKL crude and fractionated samples. The crude sample showed a 1.2 fold decrease in phenol content. Interestingly, the retentate fraction, containing high molecular weight monomers (>10 kDa), showed minuscule decrease in phenol content, similar to minuscule decrease in fluorescence intensity for retentate fraction. The alkali soluble filtrate fraction containing low molecular weight monomers (<10 kDa) showed a 1.9 fold decrease in phenol content at the end of polymerization (figure 18).

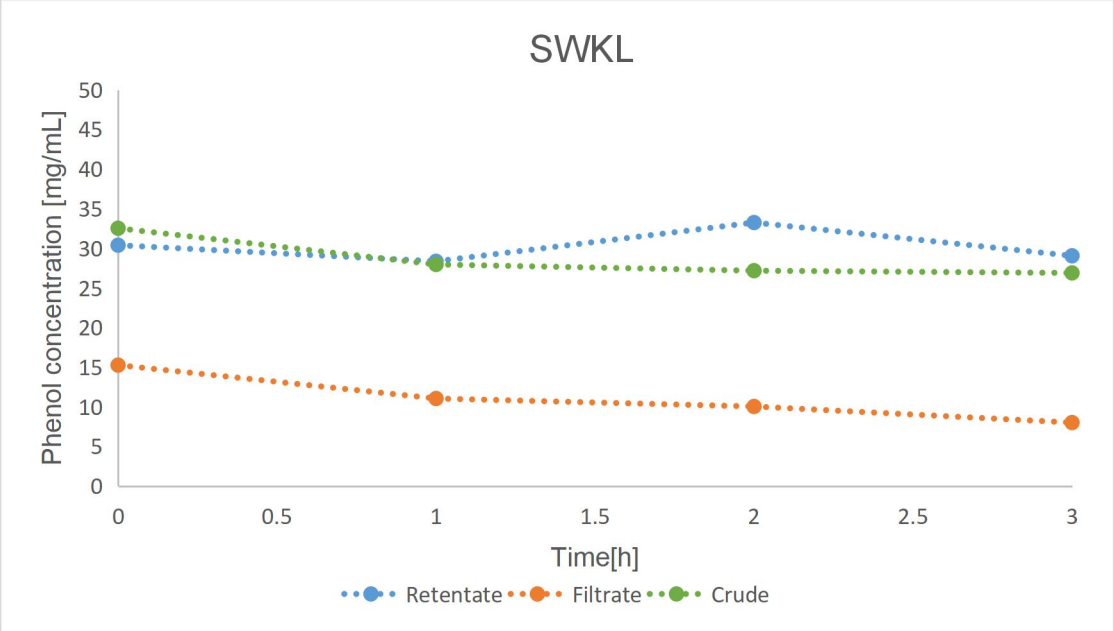

Figure 18: Phenol content of SWKL crude and fractionated samples polymerized by MtL along with the corresponding standard deviations. The phenol content of all three samples decreased during the polymerization. The phenol content of retentate fraction was the highest and the lowest phenol content was observed in filtrate fraction.

4.1.2.3.3 Comparison between HWKL and SWKL samples

The HWKL crude sample showed a larger reduction in phenol content compared to the SWKL crude sample during polymerization. A lower reduction in phenol content was observed for SWKL retentate fraction compared to HWKL retentate fraction which showed a higher reduction in phenol content. The filtrate fractions of both HWKL and SWKL samples showed a decrease in phenol content. The phenol content of SWKL filtrate fraction decreased during polymerization whereas the fluorescence intensity increased, suggesting that the trend is differing in this particular case.

4.1.2.4 Viscosity measurements

Viscosity of lignin samples was measured in order to monitor the polymerization process. During polymerization with MtL, all samples showed an increase in viscosity. The increase is due to oxidation of lignin by MtL leading to formation of radicals and subsequent coupling which leads to cross linking of lignin molecules [54]. The viscosity of the lignin samples increases as does the resistance to flow. Viscosity is measured in millipascal seconds (mPa*s) and the same scale is used for better readability and comparability. The viscosity values of lignin samples and corresponding standard deviation are shown in table 5.

Table 5: Measured viscosity in mPa*s of crude and fractionated lignin samples along with their corresponding standard deviations.

SAMPLE	TIME [h]	VISCOSITY [mPa*s] HARDWOOD KRAFT LIGNIN	STANDARD DEVIATION HWKL	VISCOSITY [mPa*s] SOFTWOOD KRAFT LIGNIN	STANDARD DEVIATION SWKL
CRUDE	0	2.08	0.035	1.91	0.039
	1	2.30	0.035	2.02	0.032
	2	2.47	0.042	2.03	0.049
	3	3.03	0.058	2.27	0.053
FRACTIONATED RETENTATE	0	2.14	0.031	1.90	0.038
	1	2.14	0.032	2.02	0.034
	2	2.15	0.033	2.01	0.034
	3	2.16	0.043	2.29	0.383
FRACTIONATED FILTRATE	0	1.34	0.039	1.42	0.053
	1	1.37	0.033	1.42	0.032
	2	1.37	0.035	1.42	0.036
	3	1.35	0.040	1.50	0.060

HWKL crude and fractionated samples

The oxidation of lignin by MtL during polymerization of the crude sample resulted in a 1.5 fold increase in viscosity from 2.08 mPa*s to 3.03 mPa*s. The high molecular weight retentate fraction showed a minuscule increase in viscosity suggesting that the viscosity could not be further increased during the polymerization. Interestingly, the low molecular weight filtrate fraction also showed a minuscule increase in viscosity (figure 19).

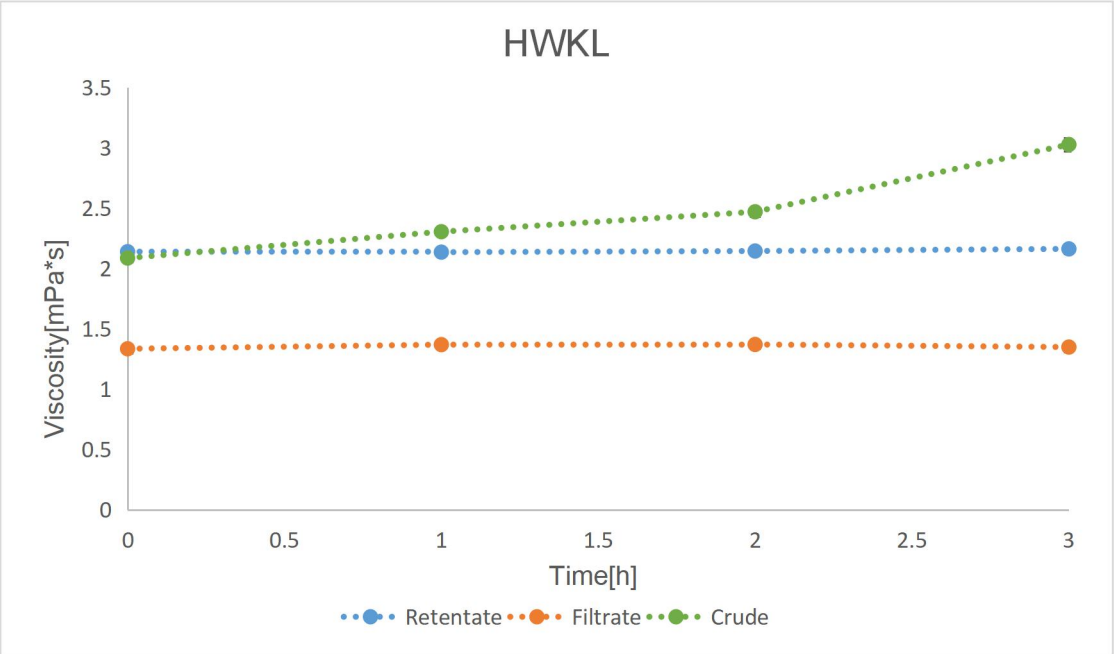

Figure 19: Viscosity profile of HWKL crude and fractionated samples. Highest viscosity value after polymerization was obtained for the crude sample. The retentate and filtrate fraction showed small increments in viscosity at the end of polymerization.

SWKL crude and fractionated samples

The crude sample showed a 1.2 fold increase in viscosity from 1.91 mPa*s to 2.27 mPa*s during polymerization. The viscosity values of the retentate fraction were similar to those of the crude sample and a 1.2 fold increase in viscosity was observed during polymerization for the retentate fraction. The low molecular weight filtrate fraction also showed minuscule increase in viscosity at the end of polymerization (figure 20).

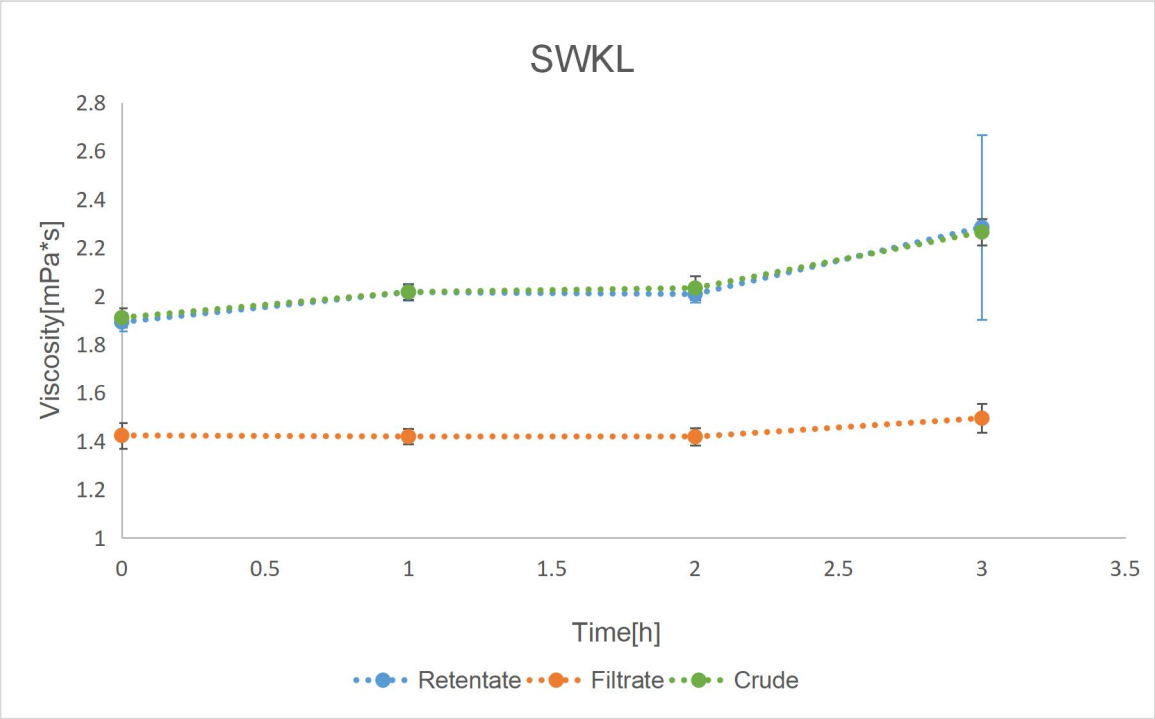

Figure 20: Viscosity profile of SWKL crude and fractionated samples. All the three sample showed minuscule increase in viscosity at the end of polymerization. The crude and retentate fraction have similar viscosity values, whereas the filtrate fraction showed only a small increment in viscosity at the end of polymerization.

4.1.2.4.1 Comparison between HWKL and SWKL samples

The HWKL crude sample showed a higher increase in viscosity during polymerization compared to SWKL crude sample. The filtrate fraction of HWKL showed a very small increase in viscosity whereas the SWKL filtrate fraction showed a higher increase in viscosity at the end of polymerization. The increase in viscosity of SWKL retentate fraction was higher than that of HWKL retentate fraction.

4.1.2.5 FTIR spectrum analysis of lignin samples

The chemical composition and functional properties of all lignin samples were estimated by FTIR. All the infrared spectra show the typical lignin patterns although some differences in the widths of the absorption bands and intensities are observed. Generally, all spectra have a strong wide band between 3650 and 3100 cm^{-1} indicating the presence of alcoholic, phenolic hydroxyl groups and water molecules [72]. Clear differences between SWKL and HWKL samples can be seen in the area of aromatic ring vibrations between 1600-1512 cm^{-1} and in the intensities of syringyl ring vibrations (1327 cm^{-1}) and guaiacyl ring (1262 cm^{-1}) vibrations. The intensity is measured in absorbance units [a.u] and the values were baseline corrected and normalized between 1600 and 1000 cm^{-1} before data analysis. The absorption intensities of S and G units of HWKL and SWKL samples along with their S/G ratio are shown in table 6. The absorption bands at different wavenumbers and their corresponding vibrations are shown in table 7 [71, 72].

Table 6: Absorption intensities of S and G units of lignin samples and their corresponding S/G ratios.

SAMPLE	HARDWOOD KRAFT LIGNIN			SOFTWOOD KRAFT LIGNIN		
	S [A] 1327 cm^{-1}	G [A] 1262 cm^{-1}	S/G Ratio	S [A] 1327 cm^{-1}	G [A] 1262 cm^{-1}	S/G Ratio
NATIVE NON MODIFIED	2.17	2.09	1.038	2.12	2.03	1.044
CRUDE	2.92	2.21	1.321	1.75	3.49	0.501
FRACTIONATED RETENTATE	3.43	2.96	1.159	1.45	2.92	0.497
FRACTIONATED FILTRATE	3.23	2.33	1.386	1.59	1.19	1.336

Table 7: The absorption bands at characteristic wavenumbers and the corresponding vibrations [71, 72].

ABSORPTION BAND LOCATION [cm^{-1}]		BAND ASSIGNMENT
HWKL	SWKL	
3650 - 3100		Stretching of alcoholic and phenolic hydroxyl groups
3000 - 2840		C-H stretching in methyl and methylene groups
1710,1656		Carbonyl groups C=O stretching
1605 - 1510		Aromatic ring vibrations
1327	-	S ring vibrations and stretching of C-O bonds
1262		G ring vibrations and stretching of C-O bonds
1108		Aromatic C-H deformation of S units
1035-1030		C-O , primary alcohols

HWKL native, crude and fractionated samples

The spectrum of HWKL samples shows strong wide bands between 3650 and 3100 cm^{-1} indicating the presence of OH stretches and water. The intensity was the highest for the retentate fraction and the lowest for the native non-modified sample. The absorption bands located in the 3000-2840 cm^{-1} wavenumber range are caused by vibrations of $-CH_2$ and $-CH_3$ groups [72]. Differences in the spectra are observed in the area of carbonyl group vibrations, for example at 1710 and 1656 cm^{-1}. The crude sample and filtrate fraction had similar intensities while the intensity of the absorption band was higher for retentate fraction at both wavenumbers. The intensity of the absorption band at 1327 cm^{-1}, which corresponds to C-O stretching of the S ring, was the strongest for the retentate fraction (3.43 A) and weakest for the native non- modified sample. Similarly, the intensity of the absorption band at 1262 cm^{-1} corresponding to C-O stretching of the G ring was the strongest for retentate fraction (2.96 A) and weakest for the native non-modified sample. The S/G ratio was highest in filtrate fraction and lowest in non-modified sample (figure 21).

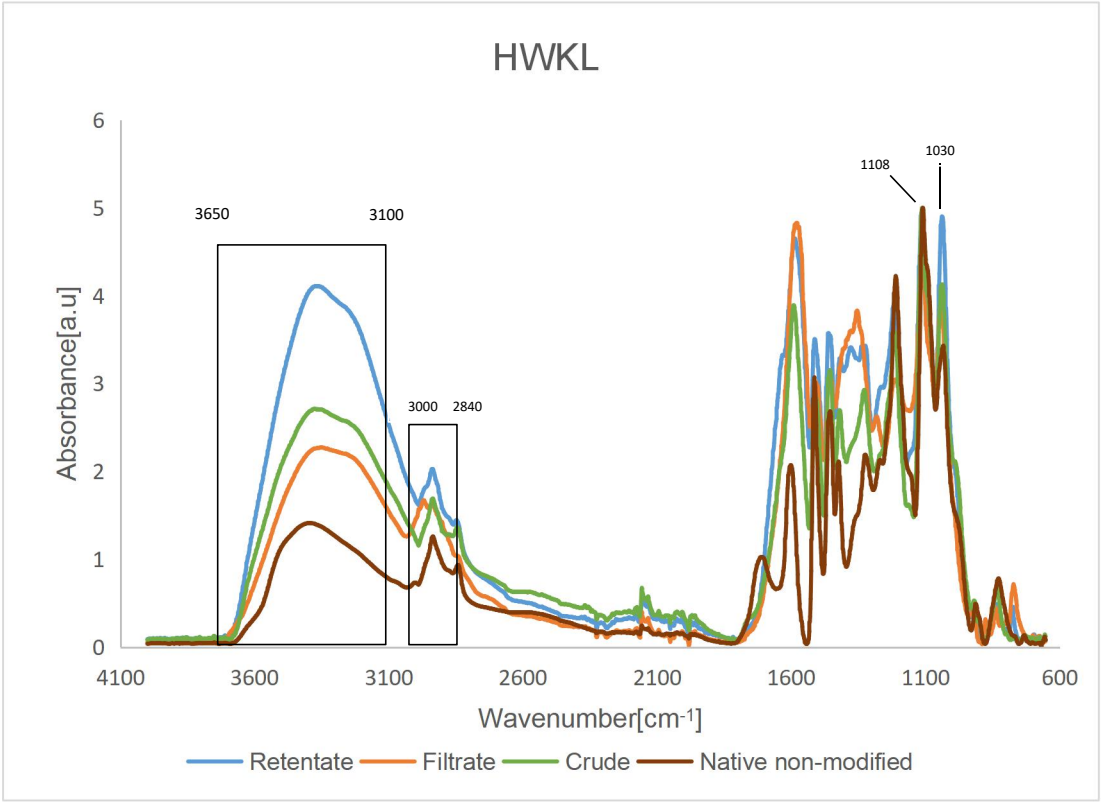

Figure 21: FTIR spectra of HWKL native non-modified and enzymatically polymerized HWKL crude and fractionated samples. The absorption bands indicating the OH stretches, C-H stretching in methyl and methylene groups and aromatic ring vibration stretches are included.

SWKL native, crude and fractionated samples

The spectrum of SWKL shows strong, wide bands between 3650 and 3100 cm^{-1} indicating the presence of OH stretches and water. The intensity was the highest for the retentate fraction and the lowest for the filtrate fraction. Between 3000 and 2840 cm^{-1}, pointier and sharper bands are seen for crude, non-modified native sample and retentate fraction, indicating asymmetric stretching of C-H bands in methyl and methylene groups, while the band is broader for filtrate fraction suggesting the presence of OH stretches [72]. The intensity of the band in the area of carbonyl group vibrations at 1710 cm^{-1} was the highest for the non-modified native sample whereas the intensity at 1656 cm^{-1} was the highest for the crude sample. The intensity of the absorption band at 1327 cm^{-1} which corresponds to C-O stretching of the S ring was the strongest for the non-modified native sample (2.12 A) and weakest for the retentate fraction. The intensity of the absorption band at 1262 cm^{-1} corresponding to C-O stretching of the G ring was the strongest for the crude sample (3.49 A) and weakest for the filtrate fraction. The S/G ratio was highest in the filtrate fraction and lowest in the retentate fraction (figure 22).

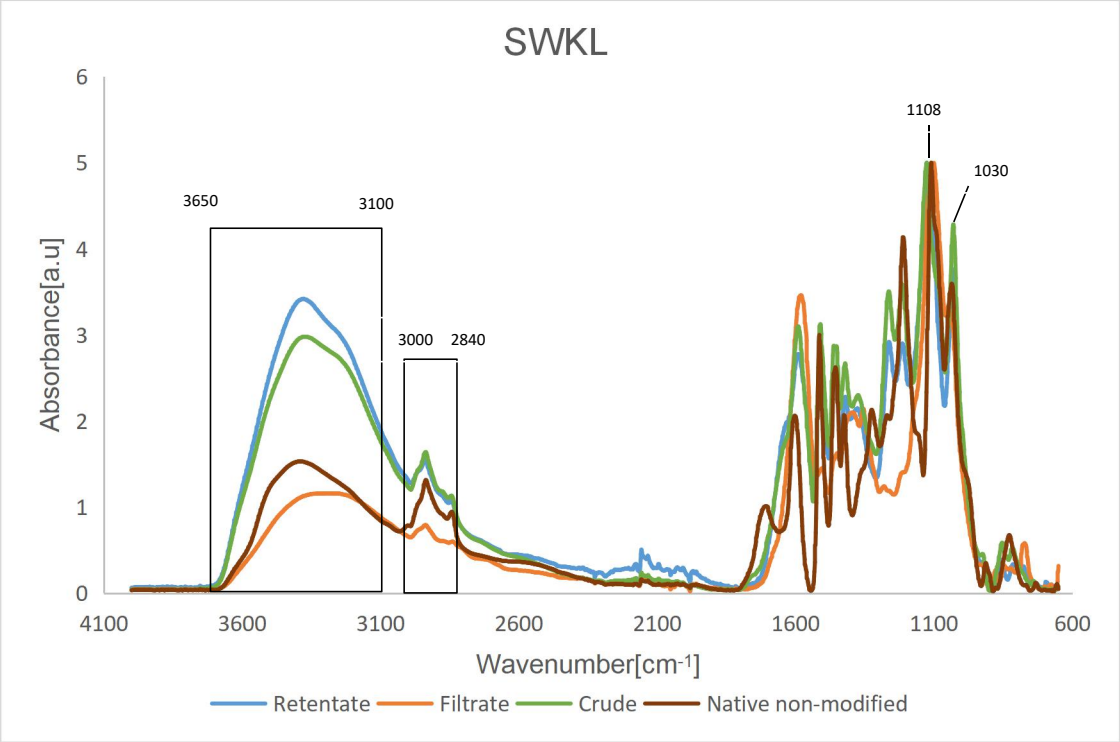

Figure 22: FTIR spectra of non-modified native SWKL sample and enzymatically cross-linked SWKL crude and fractionated samples.

4.1.2.5.1 Comparison between HWKL and SWKL samples

The HWKL samples contain more S units compared to the SWKL samples as seen in table 6. Due to a higher concentration of S units in HWKL, the S/G ratio, which indicates high delignification rate is higher for HWKL crude, retentate and filtrate samples in comparison to the respective SWKL samples. Interestingly, the non-modified native SWKL sample showed higher S/G ratio compared to the non-modified native HWKL sample. In addition, the S/G ratio increased upon polymerization with MtL for the HWKL fractionated and crude samples. In contrast, the S/G ratio was observed to decrease in the polymerized retentate and crude sample but increased for the polymerized filtrate fraction.

4.1.3 Microbial demethylation of lignin samples

4.1.3.1 Morphology of ascomycete *Aspergillus niger*

The filamentous fungus, *Aspergillus niger* formes filamented hyphae which appears like small plants when checked under the microscope. The fungal culture exhibits a cottony appearance and the colonies are initially white and gradually turn to yellow and finally black after a few days of producing conidial spores. The microscopic view of a section of colonies revealed smooth colored conidiophores and conidia. The condiophores are protrusions from the septate and hyaline hyphae and they become dark at the apex terminating in a globose vesicle. The dark brown phialides which cover the vesicles produce conidia. The conidial heads appear radial and split into columns (biseriate) [44. 45]. A microscopic view of a colony of *Aspergillus niger* is shown in figure 23.

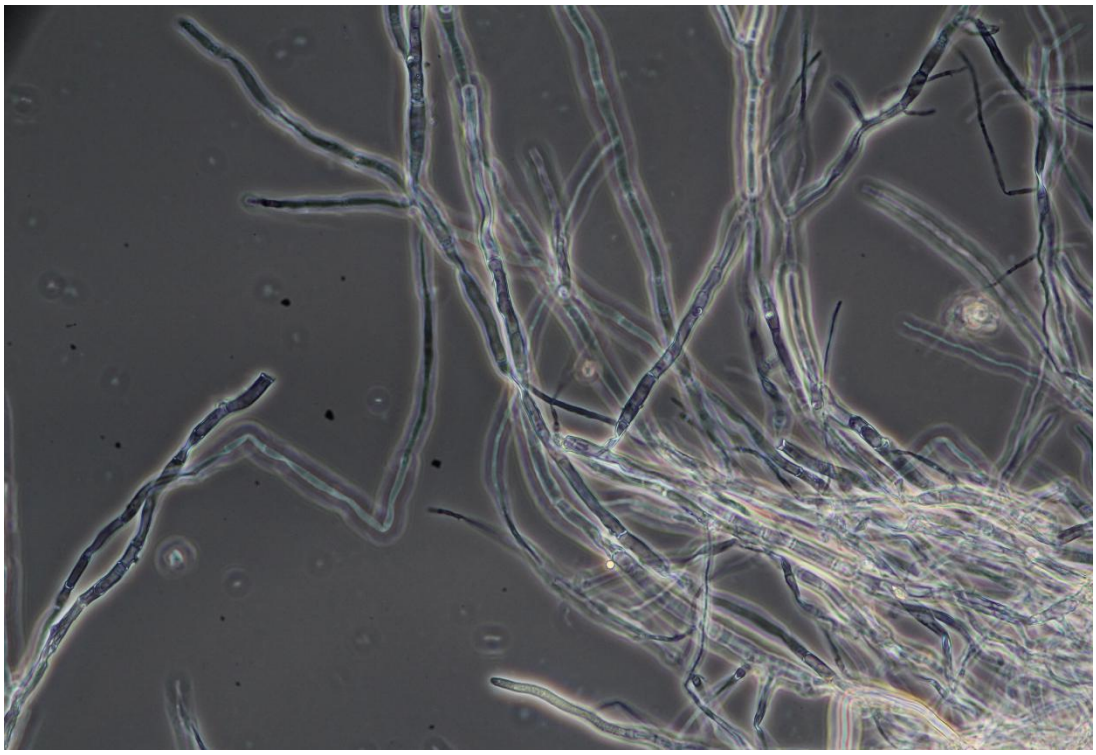

Figure 23: Microscopic image [100x] of *Aspergillus niger* pre-culture. The filamented hyphae and protruding conidiophores can be seen. A small volume of pre-culture was stained with crystal violet dye for spore counting and the structure visualization [100x] was done on a glass slide.

4.1.3.2 Pre-culture spore counting

The number of spores in 12 µL of pre-culture medium was counted in two different 4 x 4 grids of the haemocytometer chamber. The total number of spores counted in the 16 squares of the first 4 x 4 grid is 340 spores. The total number counted in the 16 squares of second 4 x 4 grid is 287 spores.

N_1 = (Total number of spores in 16 squares of first 4 x 4 grid)/16
N_1 = 340/16 = 21.3 spores
N_2 = (Total number of spores in 16 squares of second 4 x 4 grid)/16
N_2 = 287/16 = 17.9 spores
$N_A = (N_1 + N_2)/2 = (21.3 + 17.9)/2 = 19.6$ spores
$N = N_A * 10^4 = 2 * 10^5$ spores/mL.

Where, N_1 and N_2 are the average number of spores in a single square of the first and second 4x4 grid respectively; N_A is the average of N_1 and N_2; N is the average number of spores in 1 mL of pre-culture medium. Also, N is the culture inoculum utilized for microbial demethylation of HWKL and SWKL samples.

4.1.3.3 Oxygen consumption during polymerization

HWKL demethylated and demethylation control samples

The MtL oxidation of the demethylated (M+O+L) sample led to a drop of oxygen content from 60% to 38% upon the addition of the enzyme. During the polymerization, the oxygen content slowly increased and attained a saturation level at around 100%. In contrast, the demethylation control (M+O, M+L) showed a drop in oxygen content from 100% to 76% during the addition of MtL. The oxygen content increased thereafter and attained the initial level of 100% during the polymerization reaction. The demethylation control is used as a reference to analyze the extent of demethylation by microbial degradation. The oxygen consumption was higher for the demethylated sample (figure 24).

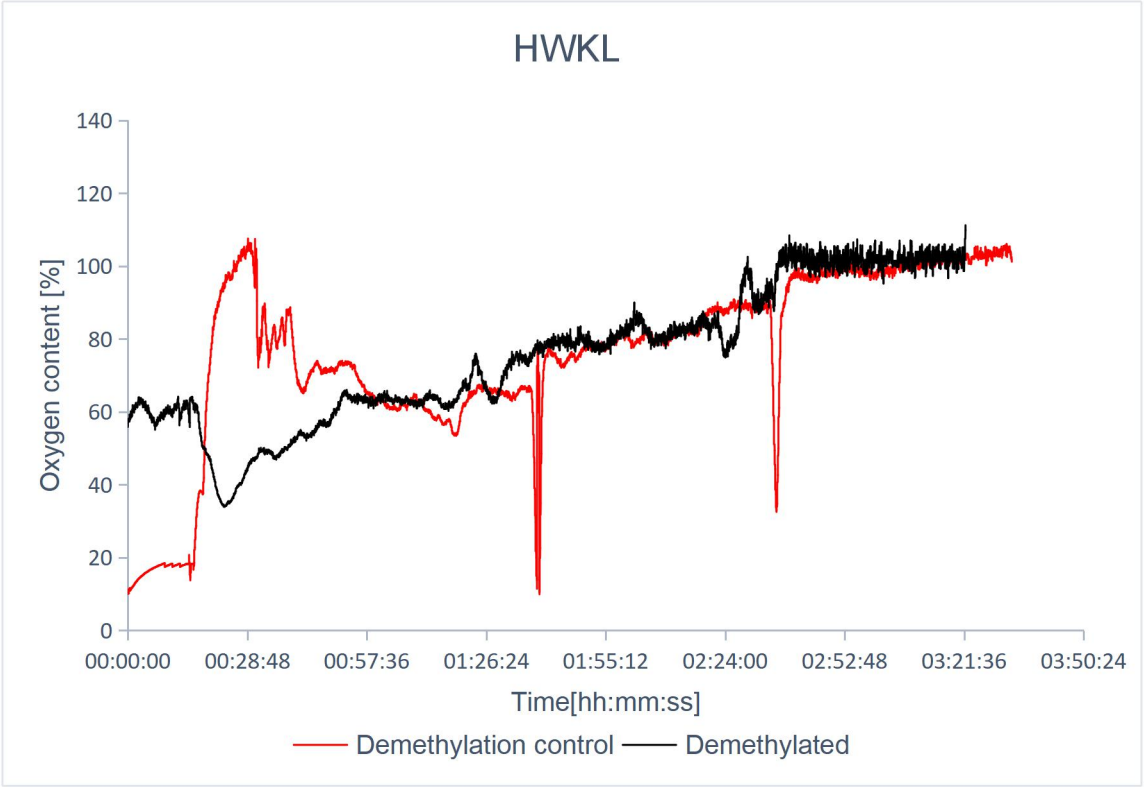

Figure 24: Oxygen profile for HWKL demethylated and demethylation control sample. Oxygen consumption was higher for the demethylated sample.

SWKL demethylated and demethylation control samples

The demethylated sample showed a drop in oxygen content from 50% to 35% during the addition of MtL. The oxygen content was observed to be decreasing due to consumption of oxygen during polymerization. The oxygen content slowly increased and attained a higher oxygen content of around 80% at the end of the polymerization reaction. In contrast, the demethylation control showed a comparatively smaller drop in oxygen content upon the addition of MtL. The oxygen content slowly increased and attained a saturation level of 110% during the polymerization reaction (figure 25).

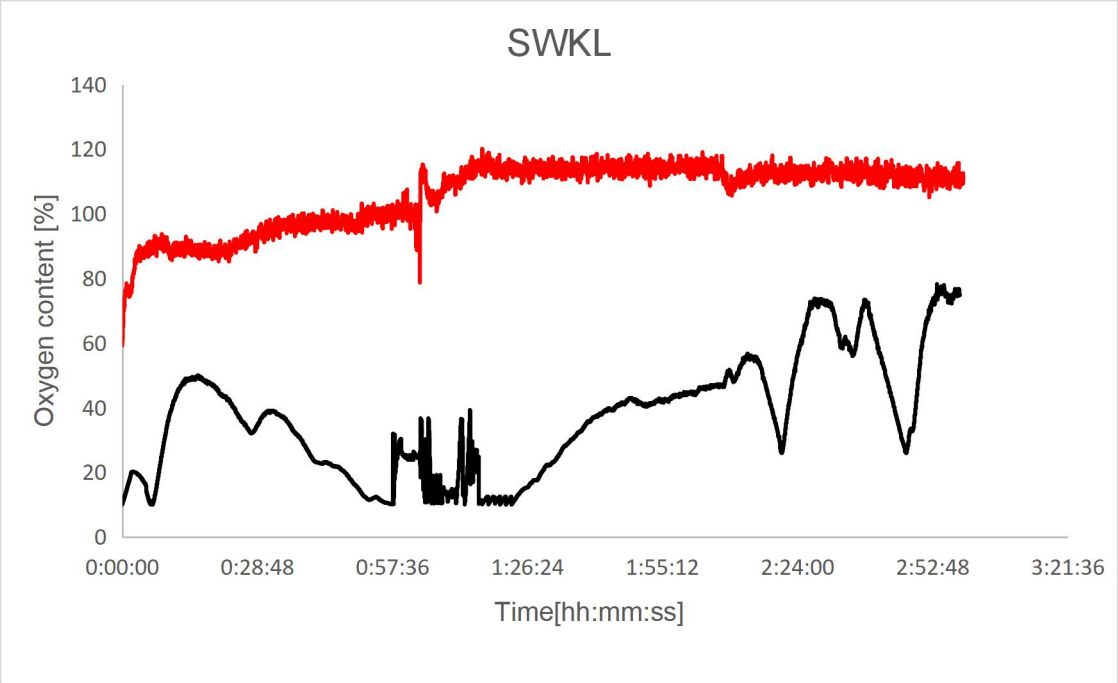

Figure 25: Oxygen profile for SWKL demethylated and demethylation control sample. Oxygen consumption was higher for the demethylated sample following the same trend as the HWKL sample.

4.1.3.3.1 Comparison between HWKL and SWKL samples

The oxygen consumption of the SWKL demethylated sample was higher compared to the HWKL demethylated sample indicating that the degree of polymerization of SWKL demethylated sample was higher than the HWKL demethylated sample. Interestingly, the oxygen consumption of HWKL demethylation control was higher than SWKL demethylation control and a higher degree of polymerization was attained.

4.1.3.4 Fluorescence measurements

The fluorescence intensity is represented by the unit x1000 FU for better readability and comparison between all polymerized samples. For this reason, the scale for the fluorescence intensity is the same for all the figures. The fluorescence values of the lignin samples and the corresponding standard deviations are tabulated in table 8.

Table 8: Fluorescence intensity for demethylated and demethylation control lignin samples along with their corresponding standard deviations.

SAMPLE	Time[h]	FLUORESCENCE [x1000 FU] HARDWOOD KRAFT LIGNIN	STANDARD DEVIATION HWKL	FLUORESCENCE [x1000 FU] SOFTWOOD KRAFT LIGNIN	STANDARD DEVIATION SWKL
DEMETHYLATED	0	1186.67	5.69	1208.34	14.98
	1	963.34	34.08	715.0	9.54
	2	776.67	2.89	756.67	18.34
	3	713.34	7.77	1603.34	56.86
DEMETHYLATION CONTROL	0	1751.67	5.86	983.34	8.39
	1	828.34	8.08	836.67	17.01
	2	675.0	20.07	996.67	24.38
	3	551.67	10.21	2293.34	46.46

HWKL demethylated and demethylation control samples

A 1.7 fold decrease in fluorescence intensity from 1186 x1000 FU to 713 x1000 FU for the demethylated sample was observed during the polymerization with MtL. In contrast, a 3.2 fold decrease in fluorescence intensity from 1752 x1000 FU to 552 x1000 FU for the demethylation control sample was observed during the polymerization with MtL (figure 26).

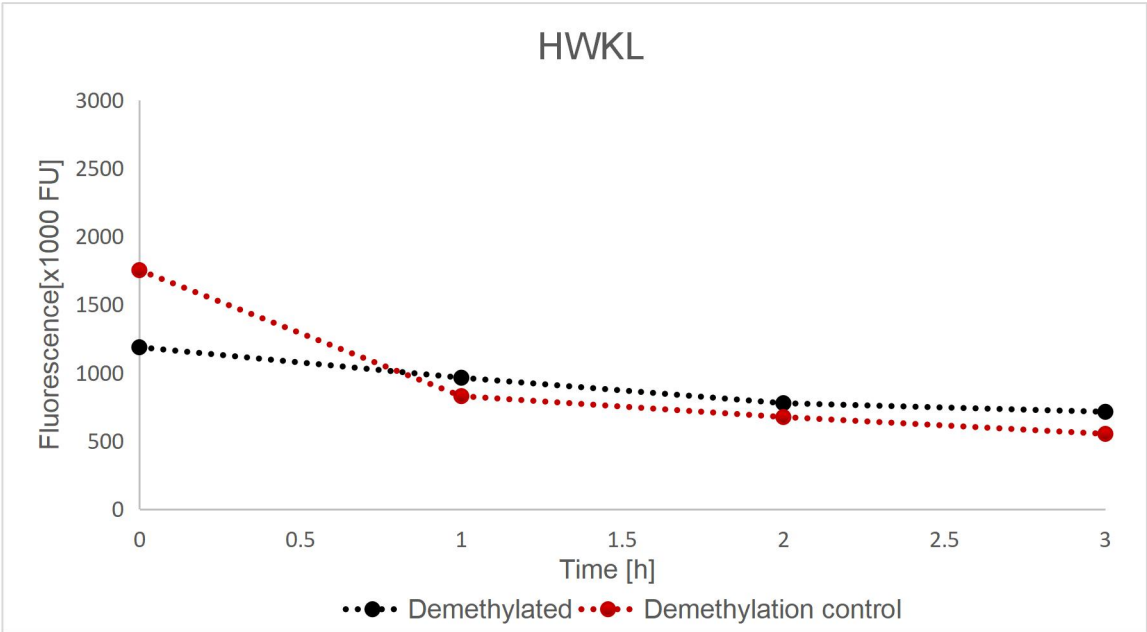

Figure 26: Decrease in fluorescence intensity for demethylated and demethylation control HWKL 10% DS polymerized for 3h with MtL (792.905 U mL^{-1}). The fluorescence intensity of both the samples decreased during the polymerization.

SWKL demethylated and demethylation control samples

A 1.3 fold increase in fluorescence intensity from 1208 x1000 FU to 1603 x1000 FU for the demethylated sample was observed during the polymerization with MtL. In contrast, a 2.3 fold increase in fluorescence intensity from 983 x1000 FU to 2293 x1000 FU for the demethylation control sample was observed during the polymerization. These anomalies can be due to experimental errors which had occurred during the sampling, over the course of microbial demethylation. As such, deviations are to be expected (figure 27).

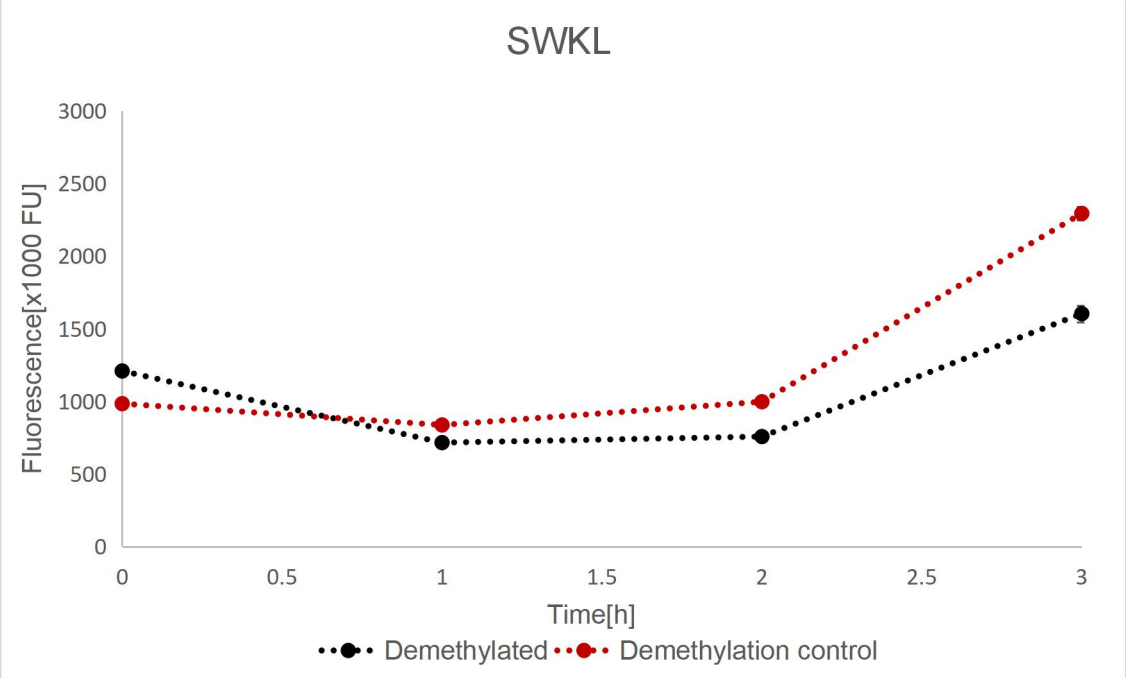

Figure 27: Increase in fluorescence intensity for demethylated and demethylation control SWKL 10% DS polymerized for 3h with MtL (792.905 U mL^{-1}). The fluorescence intensity of both the samples increased during the polymerization.

4.1.3.5 Phenol content for polymerized samples

The phenol content is shown in concentration units (mg/mL) and the same scale is used for all figures for better comparison. The phenol concentration values [mg/mL] and their corresponding standard deviations calculated for polymerized lignin samples are shown in table 9.

Table 9: Phenol concentration for demethylated and demethylation control lignin samples along with their corresponding standard deviations.

SAMPLE	TIME [h]	PHENOL CONCENTRATION [mg/mL] HARDWOOD KRAFT LIGNIN	STANDARD DEVIATION HWKL	PHENOL CONCENTRATION [mg/mL] SOFTWOOD KRAFT LIGNIN	STANDARD DEVIATION SWKL
DEMETHYLATED	0	31.27	0.0085	12.08	0.0040
	1	28.16	0.0071	9.31	0.0026
	2	18.34	0.0041	9.25	0.0059
	3	16.46	0.0061	11.30	0.0029
DEMETHYLATION CONTROL	0	40.94	0.0092	12.44	0.0009
	1	30.29	0.0082	6.76	0.0014
	2	27.39	0.0086	11.72	0.0091
	3	21.49	0.0032	13.71	0.0058

HWKL demethylated and demethylation control samples

The phenol content follows a similar trend like fluorescence intensity. A 1.9 fold decrease in phenolic content was observed for demethylated sample during polymerization with MtL. The demethylation control sample, showed a 1.9 fold decrease in phenol content which is similar to the decrease in the demethylated sample. However, the demethylated sample had lower content of phenolic hydroxyl groups compared to the demethylation control sample (figure 28).

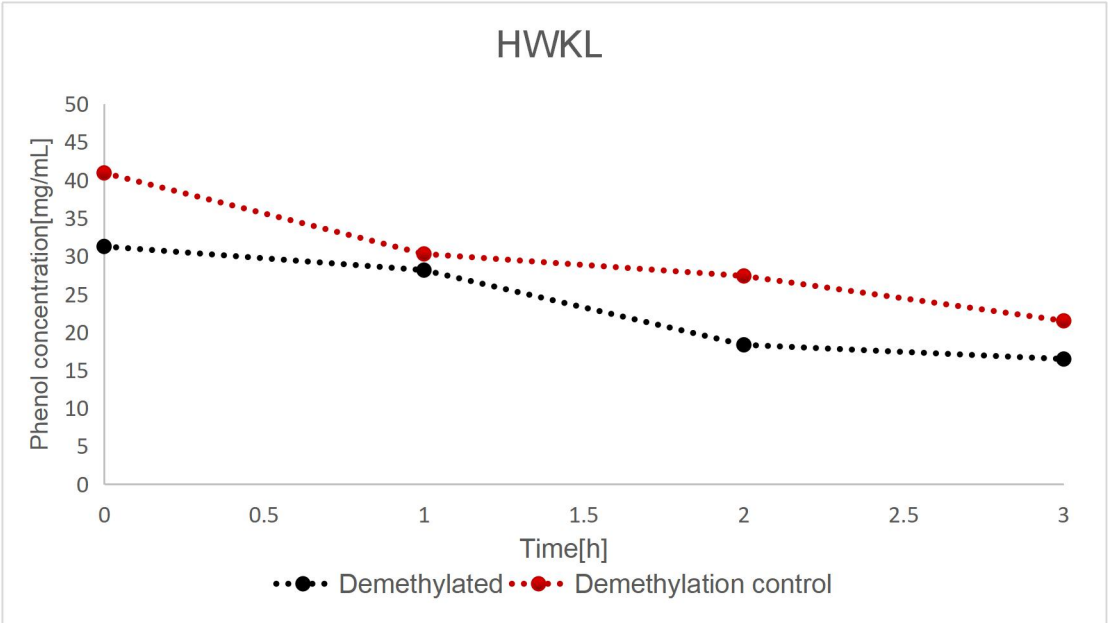

Figure 28: Phenol content for demethylated and demethylation control HWKL 10% DS polymerized for 3h with MtL (792.905 U mL^{-1}). The phenol content of both samples decreased during the polymerization reaction.

SWKL demethylated and demethylation control samples

The demethylated sample showed a minuscule decrease in phenol content at the end of polymerization with MtL. In contrast, a 1.1 fold increase in phenol content was observed for the demethylation control sample. During the microbial demethylation of the samples, some experimental errors had occurred which might had led to deviations from the expected values (figure 29).

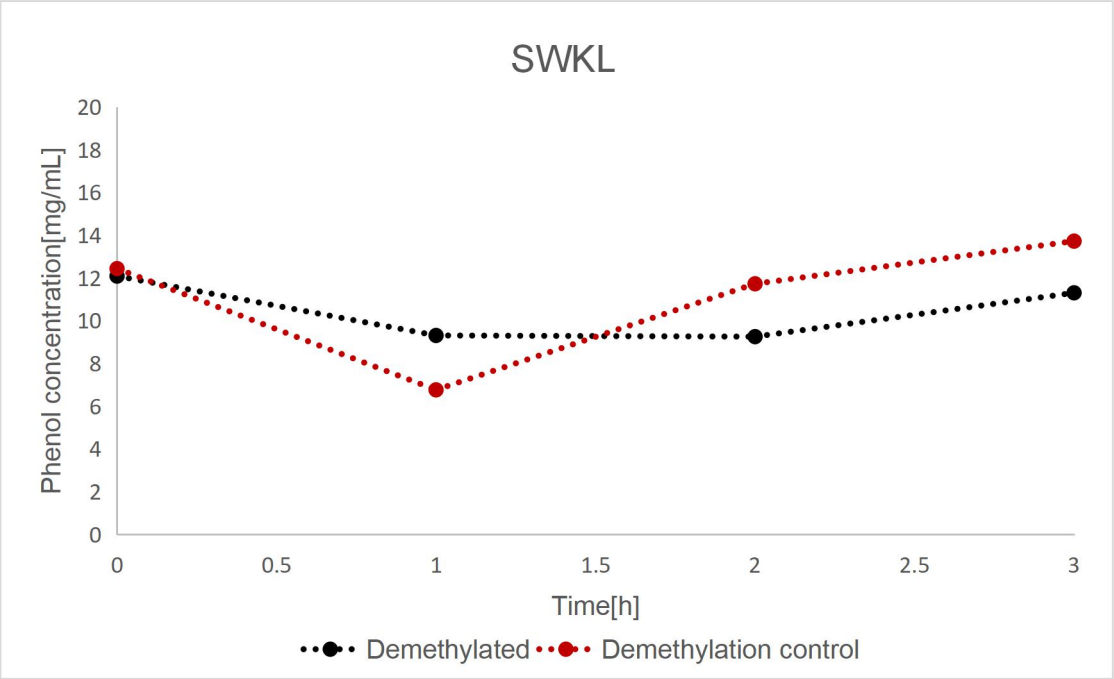

Figure 29: Phenol content for demethylated and demethylation control SWKL 10% DS polymerized for 3h with MtL (792.905 U mL^{-1}). A slight decrease in phenol content was observed for the demethylated sample and the demethylation control sample showed an increase in the phenol content at the end of the polymerization reaction.

4.1.3.6 Viscosity measurements

Viscosity is measured in milli pascal seconds (mPa*s) and same scale is used for better readability and comparability. The viscosity values of lignin samples and corresponding standard deviation are shown in table 8.

Table 10: Measured viscosity in mPa*s of demethylated and demethylation control lignin samples along with their corresponding standard deviations.

SAMPLE	TIME [h]	VISCOSITY [mPa*s] HARDWOOD KRAFT LIGNIN	STANDARD DEVIATION HWKL	VISCOSITY [mPa*s] SOFTWOOD KRAFT LIGNIN	STANDARD DEVIATION SWKL
DEMETHYLATED	0	1.57	0.077	13.21	3.797
	1	1.59	0.035	6.70	2.878
	2	1.93	0.081	6.37	0.908
	3	1.88	0.037	9.76	3.398
DEMETHYLATION CONTROL	0	1.61	0.030	2.33	0.035
	1	1.88	0.039	2.49	0.075
	2	2.49	0.064	7.99	0.152
	3	2.41	0.038	8.65	0.161

HWKL demethylated and demethylation control samples

The demethylated sample showed a 1.2 fold increase in viscosity from 1.57 mPa*s to 1.88 mPa*s during the polymerization with MtL. In contrast, the demethylation control sample showed a higher, namely a 1.5 fold increase in viscosity during the polymerization. Interestingly, both the demethylated sample and demethylation control had similar initial viscosity before the onset of polymerization (figure 30).

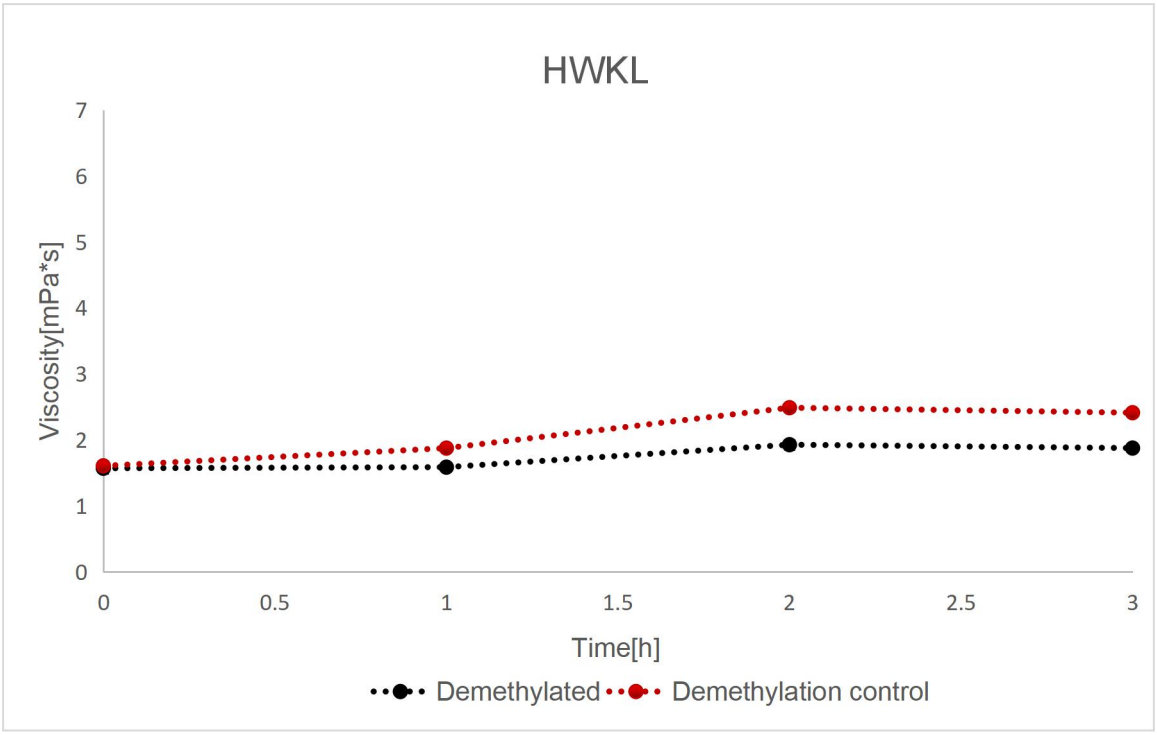

Figure 30: Viscosity profile for HWKL demethylated and demethylation control sample. Both the samples followed the general trend of increase in viscosity at the end of polymerization with MtL.

SWKL demethylated and demethylation control samples

The demethylation control sample showed a 3.7 fold increase in viscosity during the polymerization with MtL leading to an increase in the resistance to flow. The demethylated sample showed a 1.35 fold decrease in viscosity during the polymerization. The high viscosity values of the demethylated sample is due to the experimental error which had occurred during the course of microbial demethylation. As such, the results may deviate from corresponding HWKL samples (figure 31).

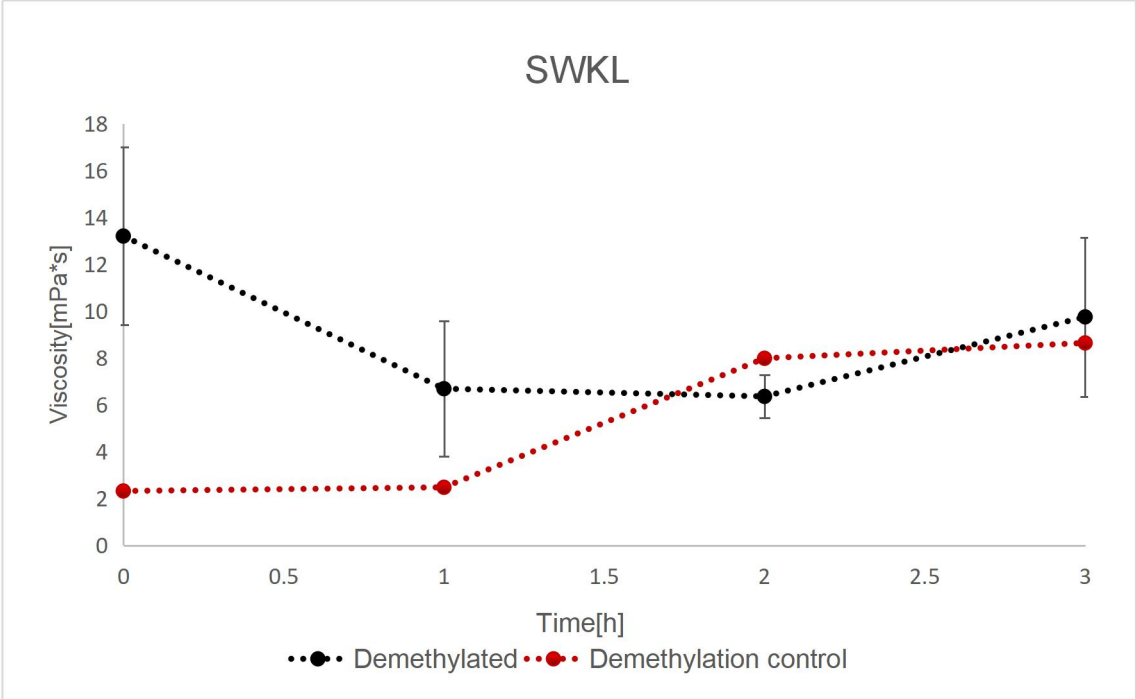

Figure 31: Viscosity profile for SWKL demethylated and demethylation control sample. The demethylation control sample showed an increase in viscosity. The viscosity of the demethylated sample decreased during polymerization.

4.1.3.7 FTIR spectrum analysis of lignin samples

The infrared spectra shows typical lignin patterns although some differences in the widths of the absorption bands and intensities are observed. The intensity is measured in absorbance units [a.u] and the values were baseline corrected and normalized between 1600 and 1000 cm^{-1} before data analysis. The absorption intensities of S and G units of HWKL and SWKL samples along with their S/G ratio are shown in table 11.

Table 11: Absorption intensities of S and G units of lignin samples and their corresponding S/G ratios.

SAMPLE	HARDWOOD KRAFT LIGNIN			SOFTWOOD KRAFT LIGNIN		
	S [A] 1327 cm^{-1}	G [A] 1262 cm^{-1}	S/G Ratio	S [A] 1327 cm^{-1}	G [A] 1262 cm^{-1}	S/G Ratio
DEMETHYLATED	3.44	2.67	1.289	2.60	4.86	0.535
DEMETHYLATION CONTROL	2.59	3.25	0.797	3.58	4.32	0.829
DEMETHYLATED NON POLYMERIZED	3.09	2.40	1.287	2.06	4.40	0.468
DEMETHYLATION CONTROL NON POLYMERIZED	2.26	2.65	0.853	-	-	-

HWKL demethylated and demethylation control samples

The intensities of the absorption bands between 3650 and 3200 cm^{-1} of polymerized demethylated and demethylation control sample are stronger compared to the respective non-polymerized samples which are used as references to show the effect of polymerization on the chemical composition and functional groups of lignin samples. The demethylation control showed higher intensity for the presence of OH stretches compared to the demethylated sample. Between 3000 and 2840 cm^{-1}, the bands corresponding to asymmetric stretching of C-H in methyl and methylene groups are pointier and sharper for all samples except for the non-polymerized demethylated sample. The intensities of the absorption band corresponding to stretching of carbonyl groups at 1710 cm^{-1} are similar for all samples but the intensities differ for the absorption band at 1656 cm^{-1} with the highest intensity observed for demethylation control sample. The intensity of the absorption band at 1327 cm^{-1} which corresponds to C-O stretching of the S ring was the strongest for the demethylated sample (3.44 A) and weakest for the non-polymerized demethylation control sample. The intensity of the absorption band at 1262 cm^{-1} corresponding to C-O stretching of the G ring was the strongest for demethylation control sample (3.25 A) and weakest for the non-polymerized demethylated sample. The S/G ratio was highest in demethylated sample and lowest in demethylation control sample (figure 32).

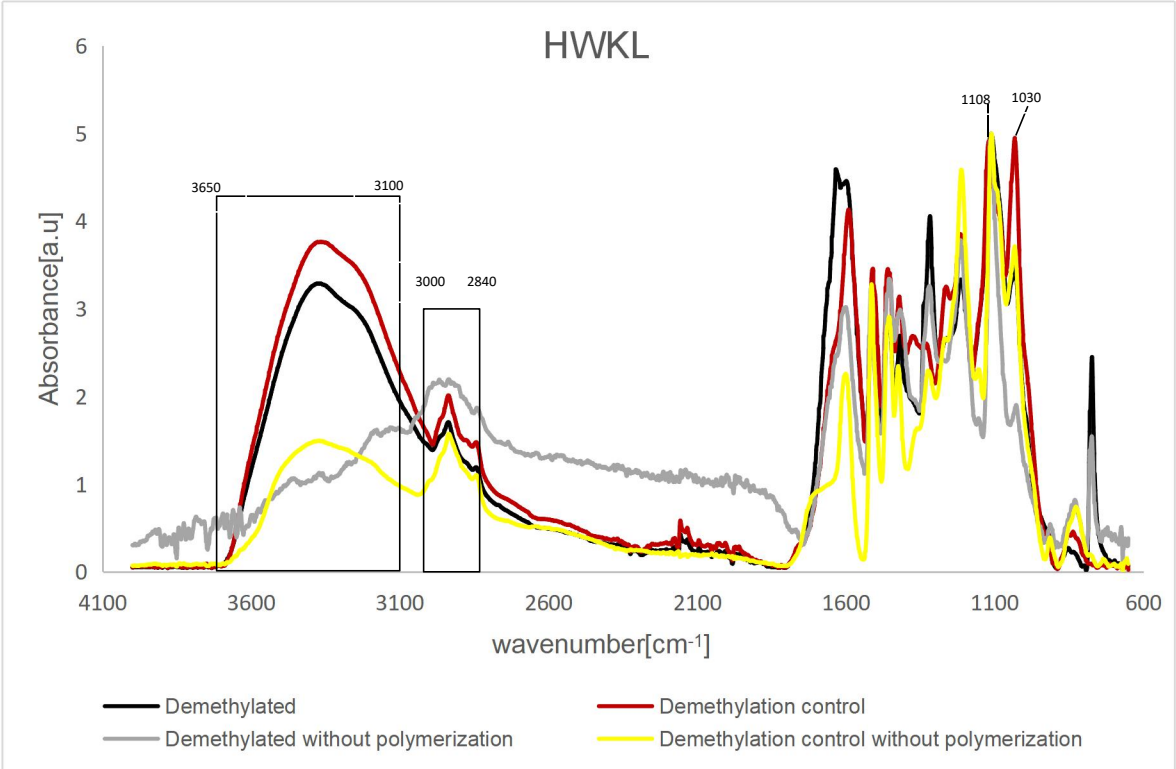

Figure 32: FTIR spectra of HWKL non-polymerized and MtL cross-linked HWKL demethylated and demethylation control samples. The absorption bands indicating the OH stretches, C-H stretching in methyl and methylene groups and aromatic ring vibration stretches are included.

SWKL demethylated and demethylation control samples

The absorption bands corresponding to OH stretches between 3650 and 3100 cm^{-1} are broader with intensities weaker compared to HWKL samples. The absorption bands indicating asymmetric C-H stretching in methyl and methylene groups corresponding to wavenumbers between 3000 and 2840 cm^{-1} are sharper for all samples. The intensity of the absorption band at 1710 and 1656 cm^{-1} which indicates the carbonyl group vibrations is strongest at both wavenumbers for demethylation control sample and weakest for non-polymerized demethylated sample. The intensity of the absorption band at 1327 cm^{-1} which corresponds to C-O stretching of the S ring was the strongest for the demethylation control (3.58 A) sample and weakest for the non-polymerized demethylated sample. The intensity of the absorption band at 1262 cm^{-1} corresponding to C-O stretching of the G ring was the strongest for the demethylated sample (4.86 A) and weakest for the non-polymerized demethylated sample. The S/G ratio was highest in demethylation control sample and lowest in non-polymerized demethylated sample. Due to low yield of demethylation control sample after microbial demethylation, FTIR measurements of non-polymerized demethylation control sample was not possible (figure 33).

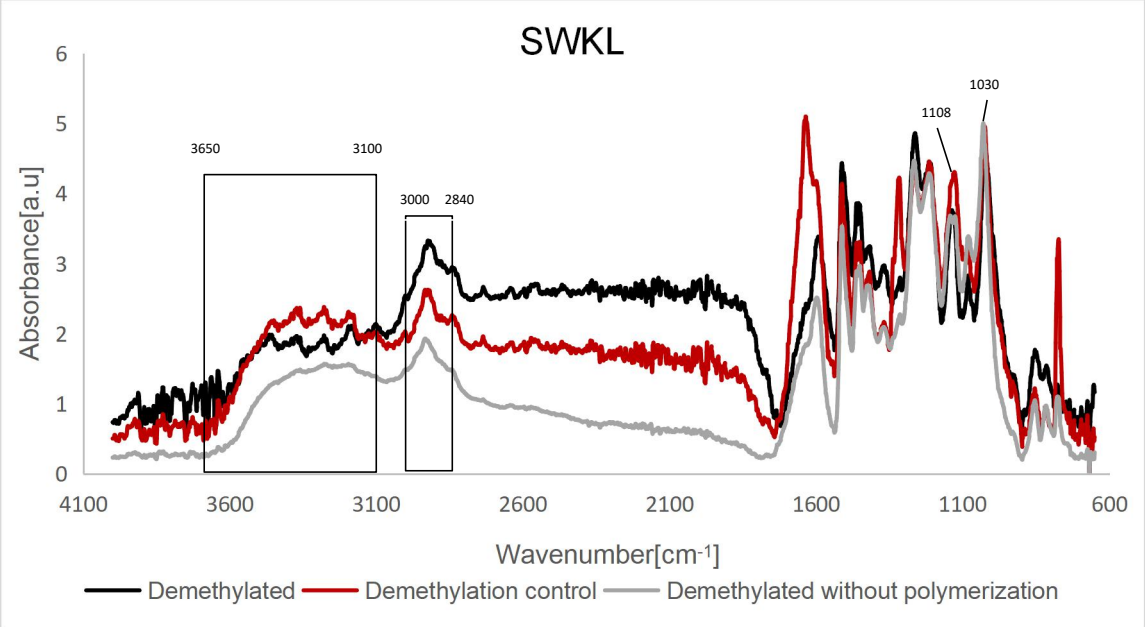

Figure 33: FTIR spectra of SWKL non-polymerized and MtL cross-linked SWKL demethylated and demethylation control samples.

4.1.3.7.1 Comparison between HWKL and SWKL samples

The HWKL samples which have more S units, have higher S/G ratios compared to SWKL samples. The S/G ratio of HWKL demethylated and non-polymerized demethylated sample is higher compared to the respective SWKL samples. However, the S/G ratio of SWKL demethylation control sample is higher than HWKL demethylation control sample. In addition, the S/G ratio increased upon polymerization of both HWKL and SWKL demethylated samples, but decreased for HWKL demethylation control sample. Due to low yield, the spectral analysis of SWKL non-polymerized demethylation control sample is not possible.

4.1.3.8 Sugar analysis of microbially demethylated lignin samples by HPLC

The fungi *Aspergillus niger* requires sugar substrates for growth, development and secretion of extracellular enzymes. These secreted enzymes are involved in modification of lignin samples such as removal of methoxy groups in order to improve the reactivity of lignin samples. The concentration of sugars such as glucose during the microbial demethylation is determined by HPLC using an ion exchange column. The glucose concentration of Medium + Organism + lignin (M+O+L) combination in both HWKL and SWKL decreased over the course of microbial demethylation. This is due to the metabolism of glucose and other sugars such as rhamnose and xylose formed during microbial demethylation in lignin samples by the organism. The glucose concentration is measured in $mg*L^{-1}$ by HPLC but due to large differences in concentrations, log function of glucose concentration is used in figures for better comparison and readability. The glucose concentration of the three combinations of both HWKL and SWKL are shown in table 12.

Table 12: Glucose concentrations (mg/L) of three combinations of HWKL and SWKL at each sampling time [d] during the course of microbial demethylation.

SAMPLE	TIME [d]	LOG [GLUCOSE CONCENTRATION] [mg/L]		
		MEDIUM + ORGANISM+LIGNIN [M+O+L]	MEDIUM + LIGNIN [M+L]	MEDIUM + ORGANISM [M+O]
HARDWOOD KRAFT LIGNIN HWKL	0	1.509441834	2.926113939	1.562253042
	3	1.309297862	2.905661932	1.050134373
	5	0.811747662	2.919979763	1.059328727
	7	1.229047212	2.942121327	1.188978423
	10	1.201348593	2.958955872	1.182241128
	11	1.199605634	2.965761274	1.185857728
SOFTWOOD KRAFT LIGNIN SWKL	0	1.591419878	3.060680594	3.09433874
	1	1.318358819	3.216966692	1.072527571
	3	3.225336272	3.219911369	0.577349693
	6	0.805612306	2.931845923	0.434040617
	9	0.932909532	0.836488686	0.511639197
	10	0.914936974	0.313853446	0.514721701

HWKL Microbial Demethylation

The medium + organism + lignin (M+O+L) sample showed a 1.3 fold decrease in glucose concentration during 11 days of microbial demethylation suggesting that the organism consumed glucose and other sugars formed during microbial demethylation in the HWKL sample. The medium + organism (M+O) control showed a 1.3 fold decrease in glucose concentration due to metabolism of glucose by the organism present in the control. In contrast, the glucose concentration of medium + lignin (M+L) control remained unchanged because of absence of a organism. Interestingly, the M+O+L sample and M+O control showed similar decrease in glucose concentration over the course of microbial demethylation (figure 34).

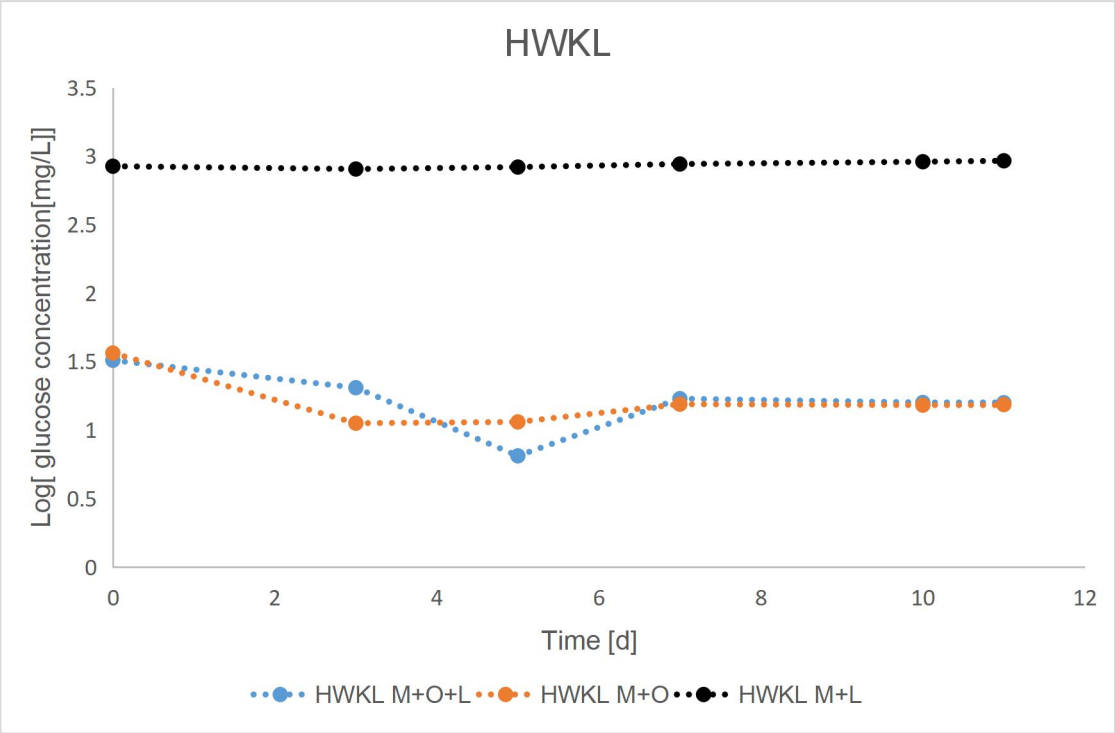

Figure 34: Glucose concentration of HWKL microbial demethylation samples. The M+O+L sample and M+O control showed similar decrease in glucose concentration while the glucose concentration of M+L control remained unchanged.

SWKL Microbial Demethylation

The M+O+L sample showed a 1.8 fold decrease in glucose concentration during 11 days of microbial demethylation. The M+O control showed a 6.0 fold decrease in glucose concentration due to metabolism of glucose by the organism present in the control. The M+L control showed a 9.8 fold decrease in glucose concentration over the course of microbial demethylation. The glucose concentration of M+L control is supposed to remain constant due to absence of a organism. This deviation is due to an experimental error which had occurred during sampling and therefore, the SWKL microbial demethylation results may be unreliable (figure 35).

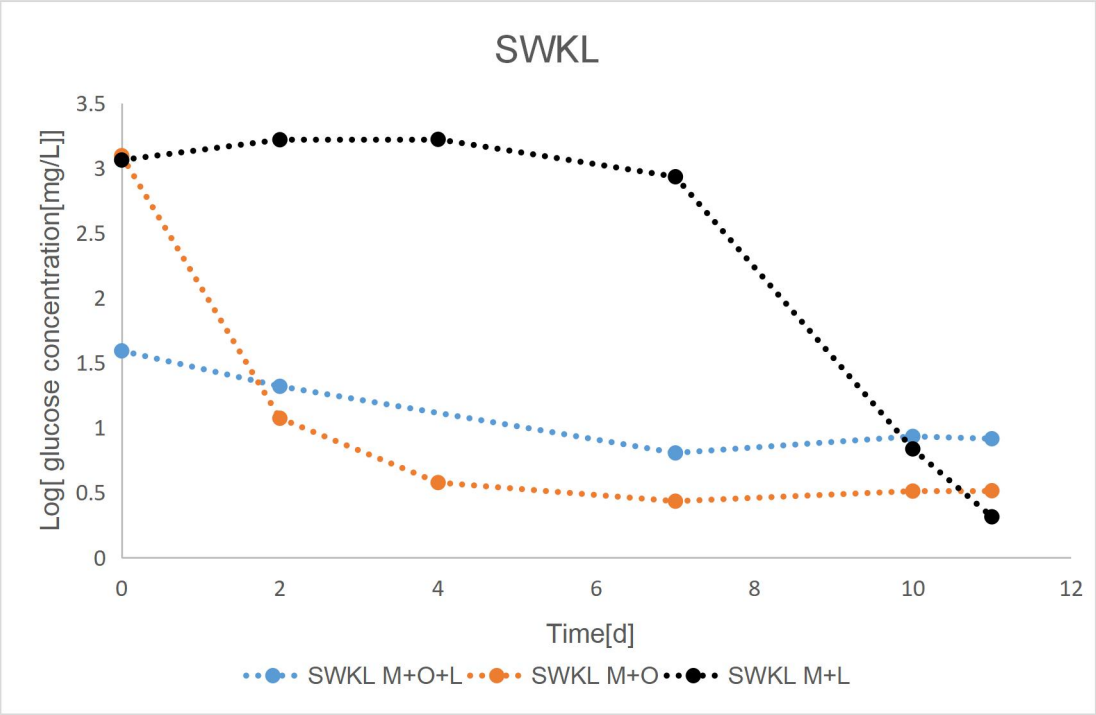

Figure 35: Glucose concentration of SWKL microbial demethylation samples. All the three combinations in this case, showed a decrease in glucose concentration. The deviation is evident for the M+L control sample which is due to an sampling error.

4.1.3.9 Determination of molecular weight of secreted proteins

The extracellular proteins secreted by the fungus *Aspergillus niger* catalyse the modifications of lignin samples. These enzymatic modifications include removal of methoxy groups on the benzene ring to increase the phenol OH content and reactivity of lignin. The molecular weight of these secreted enzymes is determined by SDS PAGE. The molecular weight of the obtained bands are estimated by comparing them to a standard PeqGold prestained protein marker IV with known molecular weights and the secreted enzyme is characterized. The bands of HWKL microbial demethylation samples obtained with SDS PAGE along with the molecular weights of standard marker are shown in figure 36. The molecular weight of the standard marker is expressed in kDa and the molecular weight of secreted enzymes is estimated for M+O+L and M+O samples. M+L is the control for the microbial demethylation of lignin samples by the organism.

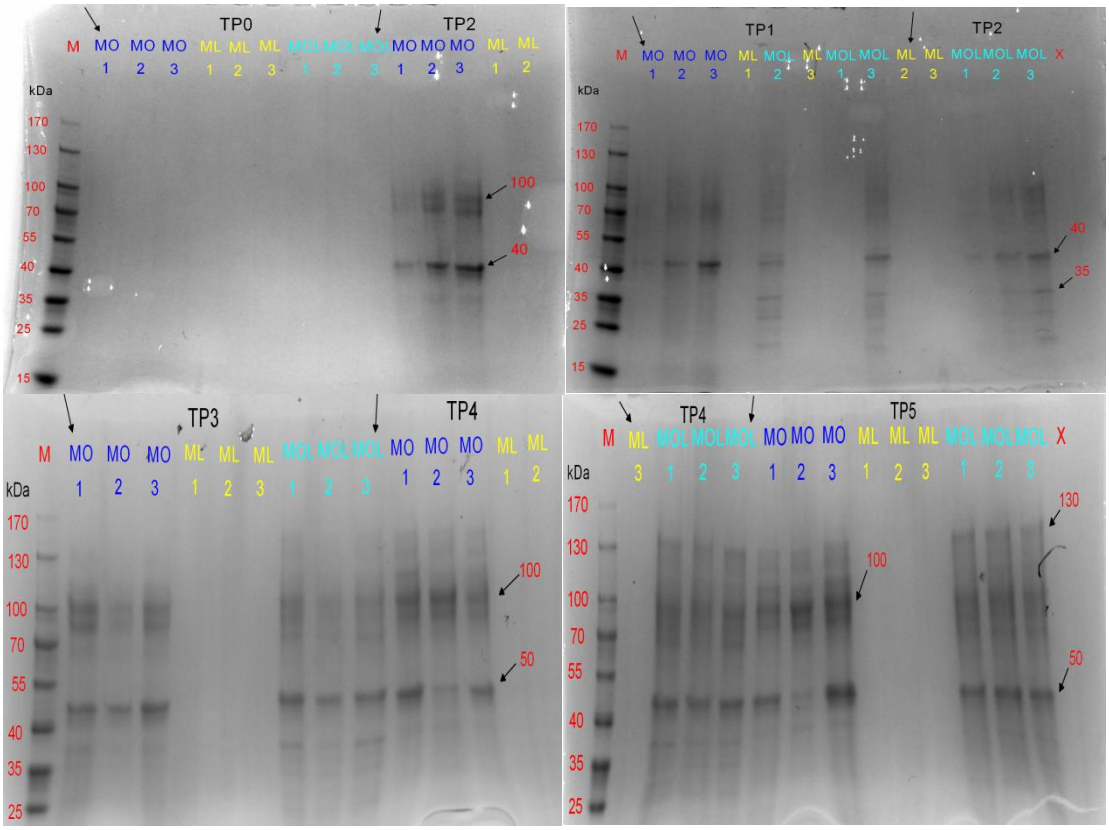

Figure 36: Molecular weight determination of HWKL microbial demethylation samples. The bands can be seen for M+O+L and M+O samples. M+L control shows no bands due to absence of organism.

Prominent bands can be seen for M+O+L sample and M+O sample over the course of microbial demethylation at different sampling time points. The dark bands of M+O+L samples corresponds to secreted proteins with molecular weights of 130, 100, 50, 40 and 35 kDa. The dark bands of M+O samples are similar to that of M+O+L sample, although lighter bands can also be seen. No bands are seen for the M+L control as no enzymes are secreted due to absence of an organism. The bands obtained for SWKL microbial demethylation samples are not shown because of the experimental error during sampling and therefore comparison cannot be made with HWKL microbial demethylation sample.

The molecular weight of the secreted enzymes by *Aspergillus niger* is estimated by using the known molecular weights of the standard marker. The enzymes corresponding to the relative molecular weight are shown in table 13 in the order of decreasing molecular weight.

Table 13: Molecular weight of the enzymes secreted by *Aspergillus niger.* [https://www.brenda-enzymes.org/index.php]

MOLECULAR WEIGHT [kDa]	SECRETED ENZYME
160	aldehyde reductase
149	β-N-acetyl glucosaminidase
121	β-glucosidase
120	α- manosidase
116.3	β-galactosidase
80-100	laccase
97	α- galactosidase
91.2	β-xylosidase
75	α- glucosidase
68.309	glucoamylase
66	acid phosphatase, phosphohydrolase
62	α-L-arabinofuranoside
52	glucanosyl transferase
45-50	manganese peroxidase
38-46	lignin peroxidase
43	chitinase
29 /132 (dimeric)	ferulic acid esterase
27-54	peroxiredoxin
19	superoxide dismutase

4.2 DISCUSSIONS

4.2.1 Oxygen consumption during polymerization

The behaviour of oxygen consumption is similar for all lignin samples. When the external oxygen is supplied in the beginning of the polymerization reaction, an increment in the oxygen content is observed. Thereafter, the oxygen content slowly decreases which can be due to oxygen consumption by lignin molecules or due to oxygen diffusion from the lignin solution. The oxygen content starts increasing gradually to a saturation level and a significant drop in oxygen content is observed upon addition of MtL. The drop is due to the consumption of oxygen by MtL during the oxidation of lignin samples. The oxygen content did not increase immediately due to rapid oxidation of lignin samples resulting in polymerization and simultaneous consumption of oxygen. The oxygen content starts increasing when most of the oxidizable lignin molecules are exhausted and substrate limitation comes into effect. The oxygen content then increases to a saturation level which does not change during the polymerization reaction except during the time points where samples are collected for analysis of lignin samples (section 4.1.2.1, section 4.1.3.3).

The enzyme from *Myceliophthora thermophila*, MtL has a low redox potential which exhibits high substrate specificity but the oxidation is slower compared to high redox potential laccases (*Trametes hirsuta* Laccase-ThL, *Trametes villosa* Laccase-TvL) [61]. During the polymerization of HWKL crude sample, the oxygen consumption by MtL was high indicating the presence of more non- oxidizable substrates compared to the fractionated samples (figure 12). The degree of polymerization of HWKL crude sample can be further increased by

extending the duration of polymerization reaction and with the addition of mediators in order to overcome the steric hindrance [53]. The point of oxygen saturation was reached much faster and occurred at higher values for the retentate and filtrate fractions, indicating that the oxidizable lignin substrates were exhausted faster.

During the polymerization of SWKL retentate fraction, the oxygen consumption by MtL was low indicating that the oxidizable substrates were exhausted and higher oxygen saturation level was attained during polymerization. The point of oxygen saturation occurred at slightly higher value for retenate fraction compared to the filtrate fraction which is 20% lower than the saturation point of retentate fraction. Due to insufficient oxygen content measurements, the graph for crude sample could not be generated and comparison between the crude sample and the fractionated samples is not possible (figure 13).

Comparing the HWKL samples to the SWKL samples, it was observed that the oxygen consumption of MtL for polymerization of SWKL fractionated samples was lower compared to HWKL fractionated samples. This can be due to the presence of syringyl units in HWKL samples which contain additional methoxy groups which sterically blocks the phenolic OH groups leading to higher oxygen consumption of MtL [22]. Overall, the fractionated samples obtained by membrane ultrafiltration exhibited a high degree of polymerization during enzymatic oxidation compared to crude sample (section 4.1.2.1.1). Implementation of fractionation methodology could be further improved by varying the polymerization reaction conditions such as changing the pH and temperature to improve the degree of polymerization.

During the polymerization of HWKL demethylated sample and demethylation control sample, the oxygen consumption by MtL was high indicating the presence of oxidizable substrates (figure 24). The oxygen consumption by MtL was higher for the demethylated sample compared to the demethylation control sample. During the polymerization, the oxygen content for demethylated sample increased slowly and attained a saturation level at around 100%. The point of oxygen saturation was similar for the demethylation control sample and the time it takes till the saturation level was reached was also similar for both samples (section 4.1.3.3).

During the polymerization of the SWKL demethylated sample, the oxygen consumption by MtL was high compared to the demethylation control sample (figure 25). The oxygen consumption was low for the demethylation control sample and the point of oxygen saturation was reached faster and occurred at a higher value indicating that the oxidizable lignin substrates in the control sample were exhausted faster. The oxygen consumption by MtL was high for the demethylated sample indicating the presence of higher amount of oxidizable lignin substrates. However, the point of oxygen saturation was reached slowly and occurred at a lower value suggesting slow oxidation reaction by MtL. The polymerization reaction could also be accelerated by using a laccase with high redox potential such as TvL and ThL.

The HWKL and SWKL samples subjected to microbial demethylation by *Aspergillus niger* showed a different oxygen content profile compared to fractionated samples. The consumption of oxygen by MtL for oxidation of SWKL and HWKL demethylated samples are higher in comparison to fractionated samples. This suggests that there are more non-oxidizable substrates in demethylated samples compared to fractionated samples and further polymerization can be achieved by extending the duration of polymerization with MtL and by addition of mediators. Demethylation was intended to increase the amount of phenolic OH groups but it did not work as expected. In addition, irregularities in the oxygen content measurements in some lignin samples occurred due to issues with sensor spots.

Overall, a higher degree of polymerization by enzymatic oxidation was achieved for the fractionated samples (figure 12, figure 13) compared to the microbially demethylated samples (figure 24, figure 25).

4.2.2 Fluorescence of lignin samples

The fluorescence of lignin is caused by the presence of fluorophores such as biphenyl, stilbene, phenylcoumarone, etc., [14]. During the polymerization, the functional groups of the fluorophores are modified and the fluorescence intensity decreases due to oxidation by laccase [18]. Also, during the oxidation of lignin by laccase, new linkages such as C-C, C-N and C-O bonds are formed [7]. However, the fluorescence intensity never reaches zero value due to the effect of steric hindrance in the lignin samples, which inhibits the MtL oxidation of small lignin fluorescing molecules. Another reason can be the presence of impurities in the enzyme solution or the lignin solution which is derived from kraft lignin extraction process. In addition, due to the low redox potential of MtL (0.45V), the oxidation of non-phenolic end groups of lignin are not to be expected [54, 61].

The fluorescence intensity was observed to be decreasing during polymerization with MtL. The HWKL crude sample showed higher reactivity to MtL oxidation compared to retentate and filtrate fraction. Consequently, the crude sample showed the highest decrease in fluorescence intensity during the polymerization reaction. The oxidation of fluorescence moieties of crude sample by MtL was more effective resulting in modifications of fluorophores which reduces the fluorescence emission at a higher quantity compared to the retentate and filtrate fraction. The retentate fraction showed minuscule decrease in fluorescence intensity which might be due to the presence of non-oxidized, high molecular weight non-phenolic end groups of lignin. The filtrate fraction showed a higher reduction in fluorescence intensity during MtL oxidation compared to the retentate fraction (figure 14).

The SWKL crude sample showed higher reactivity to MtL oxidation compared to the retentate and filtrate fraction. The lowest decrease in fluorescence intensity was observed for the retentate fraction and the highest decrease was observed for the crude sample. However, the filtrate fraction showed a significant increase in fluorescence intensity which is due to depolymerization by MtL during the reaction. The increase was observed during the third hour of polymerization indicating that polymerization had occurred during the first two hours resulting in a decrease in intensity followed by depolymerization in the third hour of polymerization (figure 15). This increase signifies the dual functions of MtL oxidation during polymerization.

Comparing the HWKL sample to the SWKL sample it was observed that the HWKL crude sample was the most reactive to MtL oxidation. The HWKL retentate fraction showed higher decrease in fluorescence intensity compared to the SWKL retentate fraction. The HWKL filtrate fraction showed a decrease in fluorescence intensity whereas depolymerization by MtL was observed for SWKL filtrate fraction resulting in an increase in fluorescence intensity at the end of the polymerization reaction (section 4.1.2.2.1). Differences in the fluorescence intensities observed for SWKL and HWKL samples are attributed to different wood origin and composition of the lignin samples. HWKL contains a mixture of G and S units whereas SWKL contains mainly G units [5]. Differences in the fluorescence intensities for HWKL and SWKL fractionated samples are attributed to the differences in molecular weights of the respective fractions.

The fungal organism *Aspergillus niger* was used primarily for removal of methoxy groups from the lignin samples in order to increase the reactivity of lignin by increasing the phenolic content. However, the demethylation of lignin did not work as expected. The fluorescence intensity of the HWKL demethylated sample was higher compared to the reactive HWKL retentate fraction at the end of polymerization (figure 14, figure 26). This indicates that the fluorescence moieties in the demethylated samples were not completely oxidized by MtL, which can be due to the presence of methoxy groups which reduces the reactivity of lignin. A similar comparison cannot be made for the SWKL demethylated sample because of the sampling error during the course of microbial demethylation with the organism (figure 27).

Overall, the fractionated samples showed higher reactivity to oxidation by MtL and exhibited lower fluorescence intensity at the end of the polymerization reaction (figure 14, figure 15) compared to the demethylated samples (figure 26, figure 27).

4.2.3 Phenol content of lignin samples

The phenol content of the lignin samples decreased during polymerization with MtL. The laccase oxidizes four molecules of lignin substrates leading to the production of four radicals while simultaneously reducing one molecule of oxygen to water. These reactive radicals either undergo a coupling reaction to form polymers through the formation of radicals, C-C, C-N and C-O bonds or they undergo degradation reactions involving cleavage of covalent bonds releasing monomeric units [7]. The phenol content of lignin decreases during polymerization with MtL because of degradation reactions which involves cleavage of covalent linkages holding the phenylpropane units which leads to further formation of free phenolic hydroxyl groups. The α-aryl and β-aryl ether linkages in phenolic lignin units and the β-aryl ether linkages in non -phenolic lignin units are cleaved leading to modification of lignin during polymerization with MtL and a reduction in phenol content is observed indicating the reactivity of lignin [63].

The phenol content of the HWKL and SWKL lignin samples decreases during polymerization but never reaches zero value indicating that the reduction of FC reagent occurs by lignin components after the polymerization reaction. This can be due to the presence of phenol groups which are inaccessible to MtL. The reduction of FC reagent can also occur by other substances in the enzyme solution or in the lignin solutions used for polymerization. Additionally, lesser oxidation reactions takes place because of the low redox potential of MtL which could possibly justify the remaining phenol content after the polymerization reaction (section 4.1.2.3.2).

The reduction in phenol content at the end of polymerization was higher for the HWKL crude sample compared to retentate and filtrate fraction. The resistance to degradation during polymerization with MtL was higher in the reactive retentate fraction which might be due to the presence of methoxy groups which sterically hinder the cleavage of ether linkages inhibiting the access to phenol groups to MtL oxidation. The filtrate fraction showed a smaller decrease in phenol content indicating low reactivity to MtL oxidation. This might be due to the presence of salts in the filtrate fraction (figure 17).

The phenol content at the end of polymerization was higher for SWKL retentate fraction compared to the crude and filtrate fraction (figure 18). The retentate fraction showed a minuscule decrease in phenol content indicating low reactivity to MtL oxidation. The highest reduction in phenol content was observed for the filtrate fraction. Softwood lignin samples are more resistant to cleavage due to the guaiacyl based structural network and exhibit low degree of depolymerization due to resistant ether linkages [25].

TThe HWKL demethylated (M+O+L) and the demethylation control (M+O, M+L) sample showed a similar 1.9 fold decrease in phenol content during polymerization with MtL oxidation (figure 28). The control sample had a higher phenol content at the end of the polymerization. The demethylated sample had a lower initial phenol content before polymerization compared to the demethylation control sample indicating that demethylation intended to increase the amount of phenolic OH groups in the lignin sample did not work as expected. The main reason for this is because of the bad choice of microorganisms used for demethylation which is not well known for modification of lignin.

The SWKL demethylated (M+O+L) sample showed a minuscule decrease in phenol content at the end of polymerization with MtL whereas the demethylation control sample showed a minuscule increase in phenol content (figure 29). The demethylated and the demethylation

control sample had low initial phenol content before polymerization, indicating that the phenolic OH content in the SWKL sample did not increase during microbial demethylation. Also, there was an experimental error during the SWKL microbial demethylation period and as such, deviations are seen.

Overall, the retentate fraction has the highest phenol content in both HWKL and SWKL samples after polymerization. The lowest phenol content after polymerization was obtained in HWKL and SWKL filtrate fractions (figure 17, figure 18). Since, higher reduction in phenol content correlates with high reactivity of lignin, the fractionation methodology was more effective to increase the reactivity of lignin compared to microbial demethylation.

4.2.4 Viscosity of lignin samples

The viscosity of all lignin samples increased during the polymerization by MtL. The oxidation of lignin by MtL generates radicals which undergo coupling reactions leading to cross linking of lignin monomers and a subsequent increase in polymer chain length [54]. During the polymerization by MtL, new bonds are formed resulting in an increase in viscosity caused by cross linking of lignin moieties.

The highest increase in viscosity of HWKL samples during polymerization was observed for the crude sample. The minuscule increment in viscosity of the HWKL fractionated samples indicates that it is difficult to increase viscosity by enzymatic oxidation by MtL alone in 3 hours which may be due to the steric hindrance of the methoxy groups. The low molecular weight filtrate fraction also showed a minuscule increase in viscosity which may be due to salts formed during the polymerization reaction which reduces the reactivity of lignin to MtL oxidation (figure 19).

The SWKL crude and retentate fraction had similar initial viscosities and the increment in viscosity during polymerization was also similar. The filtrate fraction showed a minuscule increase in viscosity at the end of polymerization (figure 20). Comparing the HWKL and SWKL samples it was observed that the highest increase in viscosity during polymerization by MtL was obtained for the HWKL crude sample. The increase in viscosity of the HWKL retentate fraction was lower than that of the SWKL retentate fraction which may be due to the presence of additional methoxy groups in the HWKL sample. The filtrate fractions of HWKL showed very small increase in viscosity whereas the SWKL filtrate fraction showed a higher increase in viscosity at the end of polymerization (section 4.1.2.4.1).

The HWKL demethylated (M+O+L) sample showed a lower increase in viscosity compared to the demethylation control sample. The demethylated sample and the demethylation control had similar initial viscosity before the onset of polymerization (figure 30). This might be due to the undesired modification of lignin and formation of microbial demethylation products which reduces the oxidation of lignin by MtL and cross linking of lignin monomers. The SWKL demethylated sample and the demethylation control samples had very high viscosity values (figure 31). This is due to experimental error during the sampling time in which the labels were mixed up and this was not noticed until the very end of the experiment. Hence, these deviations have occurred and comparison cannot be made with HWKL microbial demethylation samples.

Even though the HWKL demethylated sample showed a 1.2 fold increment in viscosity, the viscosity at the end of polymerization was still lower than for the HWKL retentate fraction. The retentate fraction has higher viscosity and a higher degree of polymerization was achieved in comparison to the demethylated sample which may be due to the presence of reactive groups in the alkali insoluble solid residue (figure 19, figure 30).

The differences between HWKL and SWKL samples in their degree of polymerization can be attributed to their different lignin content and composition [5]. The HWKL samples have lower molecular weight compared to the SKWL samples and they contain S units which induce steric hindrance for modification of lignin compared to higher molecular weight SWKL which contain G units only. A higher degree of polymerization was achieved for the fractionated HWKL and SWKL samples compared to the microbial demethylation samples, indicating that the membrane filtration was more effective in modification of lignin and the fractions were more reactive than the demethylated samples.

4.2.5 FTIR spectrum analysis

All lignin samples showed characteristic lignin patterns in their spectra. However, few differences in the absorption bands of samples are seen. The relative differences in the functional groups and composition of the HWKL and SWKL samples contribute to variations in the intensities and widths of the absorption bands [5]. All lignin samples showed a very wide absorption band between 3650 and 3100 cm^{-1}. This absorption band indicates the presence of water molecules and hydroxyl groups. Differences in the intensities are evident which are due to the composition of the lignin samples. The intensity in this area was the highest for the HWKL retentate fraction indicating the presence of high OH content (figure 21). Absorption bands at wavenumbers between 3000 and 2840 cm^{-1} were pointier and sharper for most lignin samples, indicating the asymmetric stretching of C-H in methyl and methylene groups. The filtrate fraction of both SWKL and HWKL showed a broader conformation, indicating the presence of OH stretching [72].

HWKL and SWKL samples showed differences in intensities of bands between 1605 and 1510 cm^{-1} which corresponds to aromatic ring vibrations. Differences in intensities were also evident at 1710 cm^{-1} and 1656 cm^{-1} which corresponds to carbonyl group vibrations. The HWKL samples showed significant differences in intensities of syringyl ring vibrations (1327 cm^{-1}) and guaiacyl ring vibrations (1262 cm^{-1}). The demethylated sample and the retentate fraction had similar intensities at 1327 cm^{-1} and the retentate fraction showed the highest intensity at 1262 cm^{-1} corresponding to guaiacyl ring vibrations (figure 21, figure 32). In comparison, the SWKL demethylated sample showed the highest intensity at both 1327 cm^{-1} and 1262 cm^{-1} (figure 33). However, due to the experimental error during SWKL microbial demethylation, these values may be overestimated and therefore cannot be used for comparison.

Differences between HWKL and SWKL sample are primarily attributed to the wood source and presence of syringyl units in HWKL samples [5]. Due to this, the S/G ratio which is an important lignin composition parameter is higher in HWKL samples. For the HWKL samples, the highest S/G ratio was obtained for the retentate fraction containing high molecular weight monomers. For the SWKL samples, the highest S/G ratio was obtained for the filtrate fraction containing low molecular weight monomers (section 4.1.2.5).

4.2.6 Determination of sugar content by HPLC

The fungus *Aspergillus niger* metabolized sugar substrates for physiological development and secretes extracellular enzymes in the process. The concentration of sugars such as glucose in the lignin (M+O+L) samples and the controls (M+O, M+L) is quantitatively determined by HPLC using an ion exchange column. In the HWKL M+L control, no change in the glucose concentration was observed because of the absence of a microorganism and therefore, no sugars were metabolized. In the HWKL M+O control, a 1.3 fold decrease in glucose concentration at the end of microbial demethylation was observed indicating that the organism utilized glucose for physiological development and other metabolic processes. The medium+organism+lignin (M+O+L) sample showed a similar, namely a 1.3 fold decrease in

glucose concentration during 11 days of microbial demethylation (figure 34). This suggests that the HWKL sample was not metabolized by the organism during microbial demethylation.

In comparison, the SWKL M+O+L sample showed a 1.8 fold decrease in glucose concentration during 11 days of microbial demethylation. The M+O control showed a 6.0 fold decrease in glucose concentration which is high compared to the HWKL M+O control. The M+L control showed a 9.8 fold decrease in glucose concentration over the course of microbial demethylation (figure 35). The glucose concentration of M+L control is supposed to remain constant due to absence of the organism but due to an experimental error, the samples were labelled wrongly and the microbial demethylation was continued. The error was noticed at a very late stage and therefore, such deviations are observed. However, the glucose consumption during the first two time points show similar decline as the HWKL samples.

4.2.7 Determination of molecular weight of secreted proteins

The fungus *Aspergillus niger* utilizes sugar substrates for growth, development and secretion of extracellular enzymes. During the microbial demethylation, the organism metabolizes sugars formed during microbial demethylation in the lignin samples and the secreted enzymes are involved in modification of lignin such as removal of methoxy groups from the phenylpropanoid units of lignin. The targeted modification during the microbial demethylation was demethylation to increase the phenolic OH content which would increase the reactivity of lignin samples to polymerization by MtL [41].

The secreted enzymes were estimated by their molecular weight determined by SDS PAGE.
The enzymes secreted by *Aspergillus niger* are primarily involved in degradation of plant cell wall polysaccharides. Various enzymes secreted by *Aspergillus niger* with molecular weights ranging from 170 kDa to 10 kDa were identified (figure 36). These enzymes include cellulolytic enzymes such as β-glucosidases, α-glucosidases and β-N-Acetyl Glucosaminidase; xylan and mannan degrading enzymes such as β-Xylosidase and α- Mannosidase; polysaccharide degrading accessory enzymes such as α-L-arabinofuranoside for removal of arabinose residues, α- Galactosidase and β-Galactosidase for removal of D-galactose residues, ferulic acid esterase which releases ferulic acid from oligosaccharides and starch degrading enzymes such as glucoamylase. These enzymes are typical for microorganisms involved in wood decay [73].

Lignin degrading enzymes include laccase, glucanosyl transferase, manganese peroxidase and lignin peroxidase which are primarily involved in biosynthesis and degradation of lignin [64]. The degree of demethylation by these enzymes is limited and it primarily exists as a side reaction to the mechanism of the lignin decay [39]. The enzymes known for lignin demethylation, O-demethylases were not identified in the enzyme profile. This could be one of the possible reasons for the insufficient demethylation during microbial demethylation of lignin with *Aspergillus niger.* The soft rot fungus, *Aspergillus niger* itself is not well known for wood decay and the selection of this organism for demethylation might not have been the most suitable choice.

5. CONCLUSION AND OUTLOOK

In this thesis, it was demonstrated that kraft lignin obtained from different wood sources can be modified by different biobased processes in order to increase the reactivity of kraft lignin and make it suitable for industrial applications. The first approach includes fractionation through filtration of kraft lignin samples to obtain highly reactive fractions. The second approach includes microbial demethylation of kraft lignin samples with the filamentous ascomycete *Aspergillus niger* to remove methoxy groups and increase the phenolic OH content. The fractionated and microbially demethylated samples can be further modified by polymerization with laccase. An important feature is the external oxygen supply which accelerates the oxidation and polymerization reaction of kraft lignin samples. Additionally, oxygen content measurement is an important parameter in monitoring the activity of the enzyme and the polymerization reaction.

The degree of polymerization is strongly dependent on the redox potential of the laccase. MtL has a low redox potential due to which the oxidation of lignin radicals is slower compared to high redox potential laccases such as TvL and ThL. Therefore, high redox potential laccases or bacterial laccases are recommended in order to achieve a higher degree of polymerization. Another disadvantage of polymerization with MtL is that the non-phenolic units of lignin are not oxidized due to high redox potential of non-phenolic aromatic groups or due to steric hindrance which inhibits the enzyme activity. Additionally, the pH 9.0 of the lignin solutions used in the polymerization reaction is not the optimum pH for MtL activity (pH 7.0) which could explain the low degree of polymerization. Further experiments with addition of environmentally friendly natural mediators can enhance the degree of polymerization with MtL.

The reactivity of kraft lignin to oxidation by MtL was analyzed by different characteristic methods. The fractionated samples showed significant changes in response to enzymatic modification. Significant reduction in fluorescence intensity of kraft lignin fluorophores was observed. The trend was similar in the reduction of phenol content, particularly for the reactive HWKL retentate fraction. However, the increase in viscosity was not high which could be attributed to low degree of polymerization. Considerable differences in reactivities to MtL oxidation were observed between fractionated HWKL and SWKL samples. These differences can be due to the variations in monolignol composition and molecular weight of the lignin samples.

The demethylation of kraft lignin samples with *Aspergillus niger* did not work as expected. The demethylated samples had a lower initial phenol content before polymerization which indicates that the demethylation was not successful compared to the modifications achieved by fractionation approach. The decrease in fluorescence intensity and phenol content which signifies the modifications during polymerization with MtL were less significant compared to the fractionated samples. Additionally, the profile of the secreted enzymes estimated by SDS PAGE did not contain O-demethylases which catalyze the removal of methoxy groups from highly methoxylated kraft lignin samples. Another reason for the low degree of demethylation of kraft lignin samples could be the selection of soft rot fungus *Aspergillus niger* for microbial demethylation. The ascomycete *Aspergillus niger* is not well known for lignin modification. A high degree of demethylation of kraft lignin samples possibly could be achieved by using other microorganisms such as white rot fungi, brown rot fungi or bacteria.

The fractionation process resulted in increasing the reactivity of kraft lignin to oxidation by MtL more successfully compared to the microbial demethylation process aimed at demethylating kraft lignin samples. The modification of reactive fractions could be further enhanced using bacterial laccase along with the addition of natural mediators or by varying the reaction conditions during MtL oxidation.

6. LIST OF FIGURES, TABLES AND FORMULAE

7. REFERENCES

[1] Ortner, A.; Huber, D.; Haske-Cornelius, O.; Weber, H.K.; Bauer, W.; Nyanhongo, G. S.; Guebitz, G. M. Laccase mediated oxidation of industrial lignins: Is oxygen limiting? *Process Biochem*. **2015**, 50, 1277-1283.

[2] Y. Lu, Y. C. Lu, H. Q. Hu, F. J. Xie, X. Y. Wei, X. Fan. Structural Characterization of Lignin and Its Degradation Products with Spectroscopic Methods. *Review, Hindawi, J. Spect.* **2017**, 1-15.

[3] Mahmood, Z.; Yameen, M.; Jahangeer, M.; Riaz, M.; Ghaffar, A.; Javid, I. Lignin as Natural Antioxidant Capacity. *Lignin - Trends and applications.* Ch.8 , DOI:10.5772/intechopen.73284.

[4] Liu, Q.; Luo, L.; Zheng, L. Review Lignins: Biosynthesis and Biological Functions in Plants. *Int. J. Mol. Sci*. **2018**, 19, 335.

[5] Novaes, E.; Kirst, M.; Chiang, V.; Winter-Sederoff, H.; Sederoff, R. Lignin and Biomass: A Negative Correlation for Wood Formation and Lignin Content in Trees. *Plant Physio*. **2010**, 154, 559.

[6] Kazzaz, A. E.; Feizi, Z. M.; Fatehi, P. Grafting strategies for hydroxy groups of lignin for producing materials . *Green chem*. **2019**, 21, 5714-5752

[7] Hämäläinen, V.; Grönroos, T.; Suonpää, Anu.; Heikkilä, M. W.; Romein, B.; Ihalainen, P.; Malandra, S.; Birikh, K. R. Enzymatic Precesses to Unlock the Lignin Value. *Front. Bioeng. Biotechnol*. **2018**, 6, 20.

[8] Bajwa, D. S.; Pourhashem, G.; Ullah, A. H.; Bajwa, D. S. A concise review of current lignin production, applications, products and their environmental impact. *Indus. Crops. Products.* **2019**, 139, 111526

[9] Boerjan, W.; Ralph, J.; Baucher, M. Lignin Biosynthesis. *Annu. Rev. Plant Biol*. **2003**, 54:519-46

[10] Whetten, R.; Sederoff, R. Lignin Biosynthesis. *The plant cell*. **1995**, 7, 1001-1013.

[11] Vanholme, R.; Demedts, B.; Morreel, K.; Ralph, J.; Boerjan, W. Lignin Biosynthesis and Structure. *Plant Physio*. **2010**, 153, 895-905.

[12] Fischer, A. B.; Fong, S.S. Lignin biodegradation and industrial implications. *Rev. AIMS Bioeng.* **2014**, 1, 2, 92-112.

[13] Tribot, A.; Amer, G.; Alio, M. A.; Baynast, H.; Delattre, C.; Pons, A.; Mathias, J. D.; Callios, J. M.; Vial, C.; Michaud, P.; Dussap, C. G. Wood-lignin: Supply, extraction processes and use as bio-based material. *Rev. Eur. Poly. J.* **2019**, 112, 228-240.

[14] Donaldson, L. Softwood and Hardwood Lignin Fluorescence Spectra of Wood Cell Walls in Different Mounting Media. *IAWA. J.* **2013**, 34, 1, 3-19.

[15] Radotić, K.; Kalauzi, A.; Djikanović, D.; Jeremić, M.; Leblanc, R. M.; Cerović, Z. G. Component analysis of the fluorescence spectra of a lignin model compound. *J. Photochem. Photobio B: Bio.* **2006**, 83, 1-10.

[16] Machado, A. E. H.; Nicodemb, D. E.; Ruggiero, R.; Perez, D, S.; Castellan, A. The use of fluorescent probes in the characterization of lignin: the distribution, by energy, of fluorophores in Eucalyptus grandis lignin. *J. Photochem. Photobio. A: Chem.* **2001**, 138, 253-259.

[17] Albinsson, B.; Li, S.; Lundquist, K.; Stomberg, R. The origin of lignin fluorescence. *J. Mol. Str.* **1999**, 508, 19-27.

[18] Prasetyo, E. N.; Kudanga, T.; Østergaard, L.; Rencoret, J.; Gutiérrez, A.; Rio, J. C. d.; Santos, J. I.; Nieto, L.; Jiménez-Barbero, J.; Martinez, A. T.; Li, J.; Gellerstedt, G.; Lepifre, S.; Silva, C.; Kim, S. Y.; Cavaco-Paulo, A.; Klausen, B. S.; Lutnaes, B. F.; Nyanhongo, G. S.; Guebitz, G. M. Polymerization of lignosulfonates by the laccase-HBT (1-hydroxybenzotriazole) system improves dispersibility. *Biores. Tech*. **2010**, 101, 5054-5062.

[19] Vishtal, A.; Kraslawski, A. Challenges in Industrial Applications of Technical Lignins. *BioRes*. **2011**, 6, 3547-3568.

[20] Li, T.; Takkellapati, S. The current and emerging sources of technical lignins and their applications. *Biofuel Bioprod. Biorefin.* 2018, 0, 1-32.

[21] Guadix-Montero, S.; Sankar, M. Review on Catalytic Cleavage of C–C Inter-unit Linkages in Lignin Model Compounds: Towards Lignin Depolymerisation. *Topics Cataly.* **2018**, 61, 183-198.

[22] Lourenco, A.; Pereira, H. Compositional Variability of Lignin in Biomass. *Lignin - Tren. App.* **2018**, 3.

[23] Shimizu, S.; Yokoyama, T.; Akiyama, T.; Matsumoto, Y. Reactivity of Lignin with Different Composition of Aromatic Syringyl/Guaiacyl Structures and Erythro/Threo Side Chain Structures in β-O-4 Type during Alkaline Delignifification: As a Basis for the Different Degradability of Hardwood and Softwood Lignin. *J. Agric. Food Chem.* **2012**, 60, 6471−6476.

[24] Zhu, X.; Akiyama, T.; Yokoyama, T.; Matsumoto, Y. Stereoselective Formation of β-O-4 Structures Mimicking Softwood Lignin Biosynthesis: Effects of Solvent and the Structures of Quinone Methide Lignin Models. *J. Agric. Food Chem.* **2019**, 67, 6950−6961.

[25] Ahmad, Z.; Dajani, W. W. A.; Paleologou, M.; Chunbao, X. Sustainable Process for the Depolymerization/Oxidation of Softwood and Hardwood Kraft Lignins Using Hydrogen Peroxide under Ambient Conditions. *Molecules.* **2020**, 25, 2329.

[26] Lancefield, C. S.; Westwood, N. J. The synthesis and analysis of advanced lignin model polymers. *Green Chem.* **2015**, 17, 4980.

[27] Zakzeski, J.; Bruijnincx, P. C. A.; Jongerius, A. L.; Weckhuysen, B. M. The Catalytic Valorization of Lignin for the Production of Renewable Chemicals *Chem. Rev.* **2010**.

[28] Aminzadeh, S.; Lauberts, M.; Dobele, G.; Ponomarenko, J.; Mattsson, T.; Lindström, M. E.; Sevastyanova, O. Membrane filtration of kraft lignin: Structural characteristics and antioxidant activity of the low-molecular-weight fraction. *Indus. Crop. Prod.* **2018**, 112, 200-209.

[29] Cui, C.; Sun, R.; Argyropoulos, D. S. Fractional Precipitation of Softwood Kraft Lignin: Isolation of Narrow Fractions Common to a Variety of Lignins. *ACS Sustainable Chem. Eng.* **2014**, 2, 959−968.

[30] Jiang, X.; Savithri, D.; Du, X.; Pawar, S.; Jameel, H.; Chang, H.; Zhou, X. Fractionation and Characterization of Kraft Lignin by Sequential Precipitation with Various Organic Solvents. *ACS Sustainable Chem. Eng.* **2017**, 5, 835−842.

[31] Rohde, V.; Böringer, S.; Tübke, B.; Adam, C.; Dahmen, N.; Schmiedl, D. Fractionation of three different lignins by thermal separation techniques - A Comparative study. *GCB Bioen.* **2018**, 1-12.

[32] Humpert, D.; Ebrahimi, M.; Czermak, P. Membrane Technology for the Recovery of Lignin: A Review. *Membranes* **2016**, *6*, 42.

[33] Demuner, I. F.; Colodette, J. L.; Demuner, A. J.; Jardim, C. M. Biorefinery Review: Wide-Reaching Products Through Kraft Lignin. *BioRes.* **2019**, 14, 7543-7581.

[34] Gilca, I. A.; Popa, V. I.; Crestini, C. Obtaining lignin nanoparticles by sonication. *Ultra. Sonochem*. **2015**, 23, 369-375.

[35] Azadi, P.; Inderwildi, O. R.; Farnood, R.; King, D. A. Liquid fuels, hydrogen and chemicals from lignin: A critical review. *Renew. Sustain. Energy Rev*. **2013**, 21, 506-523.

[36] Lu, H.; Cornell, A.; Alvarado, F.; Behm, M.; Leijonmarck, S.; Li, J.; Tomani, P.; Lindbergh, G. Lignin as a Binder Material for Eco-Friendly Li-Ion Batteries. *Materials* **2016**, 9, 127.

[37] Meng, Y.; Lu, J.; Cheng, Y.; Li, Q.; Wang, H. Lignin-based hydrogels: A review of preparation, properties, and application. *Int. J. Bio. Macro.* **2019**, 135, 1006-1019.

[38] Mandlekar, N.; Cayla, A.; Rault, F.; Giraud, S.; Salaün, F.; Malucelli, G.; Guan, J. An Overview on the Use of Lignin and Its Derivatives in Fire Retardant Polymer System. *Lignin - Tren. App.* **2018**, 9.

[39] Venkatesagowda, B. Enzymatic demethylation of lignin for potential biobased polymer Applications. *Fungal Bio. Rev.* **2019**, 33, 190-224.

[40] Wang, H.; Eberhardt, T. L.; Wang, C.; Gao, S.; Pan, H. Demethylation of Alkali Lignin with Halogen Acids and Its Application to Phenolic Resins. *Polymers* **2019**, 11, 1771.

[41] Bashtan-Kandybovich, I.; Venkatesagowda, B.; Barbosa, M. A.; Malek, L.; Dekker, R. F. H. Modification of kraft lignin by biological demethylation. *J. Science Tech. Forest Prod. Proc.* **2012**, 2, 4.

[42] Lang, J. M.; Shrestha, U. M.; Dadmun, M. The effect of Plant source on the Properties of Lignin - Based Polyurethanes. *Front. Energy Res.* **2018,** 6:4.

[43] Baker, S. E. Aspergillus niger genomics: Past, present and into the future. *Medical Mycology* **2006**, 44, S17-S21.

[44] Gugnani, H. C. Ecology and taxonomy of pathogenic Aspergilli. *Front. Bio.* **2003**, 8.

[45] Schuster, E.; Dunn-Coleman, N.; Frisvad, J. C.; Van Dijck, P. W. M. On the safety of Aspergillus niger – a review. *Appl. Microbiol. Biotechnol.* **2002,** 59, 426–435.

[46] Janusz, G.; Pawlik, A.; Sulej, J.; Swiderska-Burek, U.; Jarosz-Wilkołazka, A.; Paszczynski, A. Lignin degradation: microorganisms, enzymes involved, genomes analysis and evolution. *FEMS Microbio. Rev.* **2017,** 41, 941–962.

[47] Piontek, K.; Antorini, M.; Choinowski, T. Crystal Structure of a Laccase from the Fungus Trametes versicolor at 1.90-Å Resolution Containing a Full Complement of Coppers. *J. Biol. Chem*. **2002**, 40, 4, 37663–37669.

[48] Chauhan, P. S.; Goradia, B.; Saxena, A. Bacterial laccase: recent update on production, properties and industrial applications. *3 Biot.* **2017,** 7, 323.

[49] Yang, J.; Li, W.; Ng, T. B.; Deng, X.; Lin, J.; Ye, X. Laccases: Production, Expression Regulation, and Applications in Pharmaceutical Biodegradation. *Front. Microbiol.* **2017**, 8, 832.

[50] Chaurasia, P. K.; Yadav, R. S. S.; Yadava, S. A review on mechanism of laccase action. *RRBS.* **2013**, 7.

[51] Claus, H. Laccases: structure, reactions, distribution. *Micr*. **2004**, 35, 93–96.

[52] Kumar, S. V. S.; Phale, P. S.; Durani, S.; Wangikar, P. P. Combined sequence and structure analysis of the fungal laccase family. *Biotechnol. Bioeng.* **2003**, 83, 386-94.

[53] Christopher, L. P.; Yao, B.; Ji, Y. Lignin biodegradation with laccase-mediator systems. *Front. Ener. Res. Bioen. Biofuel* **2014**, 2, 12.

[54] Kudanga, T.; Nyanhongo, G. S.; Guebitz, G. M.; Burton, S. Potential applications of laccase-mediated coupling and grafting reactions: A review. *Enzy. Micro. Tech.* **2011**, 48, 195-208.

[55] Janusz, G.; Pawlik, A.; Swiderska-Burek, U.; Polak, J.; Sulej, J.; Jarosz-Wilkołazka, A.; Paszczynski, A. Laccase Properties, Physiological Functions, and Evolution. *Int. J. Mol. Sci.* **2020**, 21, 966.

[56] Mikolasch, A.; Schauer, F. Fungal laccases as tools for the synthesis of new hybrid molecules and biomaterials. *Appl. Microbiol. Biotechnol.* **2009**, 82, 605–624.

[57] Chatterjee, R.; Johansson, K.; Järnström, L.; Jönsson, L. J. Evaluation of the Potential of Fungal and Plant Laccases for Active-Packaging Applications. *J. Agric. Food Chem.* **2011**, 59, 5390-5395

[58] Couto, S. R.; Herrera, J. L. T. Industrial and biotechnological applications of laccases: A Review. *Biotechnol. Advances* **2006**, 24, 500–513.

[59] Xu, J.; Li, J.; Lin, L.; Liu, Q.; Sun, W.; Huang, B.; Tian, C. Development of genetic tools for Myceliophthora thermophila. *BMC Biotechnol.* **2015**, 15, 35.

[60] Karnaouri, A.; Topakas, E.; Antonopoulou, L.; Christakopoulos, P. Genomic insights into the fungal lignocellulolytic system of Myceliophthora thermophila. *Front. Microbiol. Micro. Physio. Meta.* **2014**, 5, 281.

[61] Ernst, H. A.; Jørgensen, L. J.; Bukh, C.; Piontek, K.; Plattner, D. A.; Østergaard, L. H.; Larsen, S.; Bjerrum, M. J. A comparative structural analysis of the surface properties of asco-laccases. *PLOS ONE* **2018**, 13, 11.

[62] Berka, R. M.; Schneider, P.; Golightly, E. J.; Brown, S. H.; Madden, M.; Brown, K. M.;Halkier, T.; Mondorf, K.; Xu, F. Characterization of the Gene Encoding an Extracellular Laccase of Myceliophthora thermophila and Analysis of the Recombinant Enzyme Expressed in Aspergillus oryzae. *Appl. Env. Micro.* **1997**, 63, 3151-3157.

[63] Huber, D.; Pellis, A.; Daxbacher, A.; Nyanhongo, G. S.; Guebitz, G. M. Polymerization of Various Lignins via Immobilized Myceliophthora thermophila Laccase (MtL). *Polymers* **2016**, 8, 280.

[64] Areskogh, D.; Li, J.; Gellerstedt, G.; Henriksson, G. Investigation of the Molecular Weight Increase of Commercial Lignosulfonates by Laccase Catalysis. *Biomacromolecules* **2010**, 11, 904–910.

[65] Areskogh, D.; Li, J.; Nousiainen, P.; Gellerstedt, G.; Sipilä, J.; Henriksson, G. Oxidative polymerisation of models for phenolic lignin end-groups by laccase. **2010**, 64.

[66] Blainski, A.; Lopes, G. C.; Mello, J. C. P. Application and Analysis of the Folin Ciocalteu Method for the Determination of the Total Phenolic Content from Limonium Brasiliense L. *Molecules* **2013**, 18, 6852-6865.

[67] Stoll, A.; Cavalcante, M. Chapter 3 - Stick-Slip Characteristics of Leather/Artificial Leather. *Auto. Buz. Squ. Ratt.* **2012**, 63-98.

[68] Ramaiah, G. B.; Bhatia, D. Structural Analysis Of Merino Wool, Pashmina And Angora Fibers Using Analytical Instruments Like Scanning Electron Microscope And Infra-Red Spectroscopy. *IJETSR* 2017, 4.

[69] Yan, X. High performance liquid chromatography for carbohydrate analysis. *Analy. Sci. Res. Dev. Amw. Cor.* **2014**.

[70] Pavlova, A. S.; Dyudeeva, E. S.; Kupryushkin, M. S.; Amirkhanov, N. V.; Pyshnyi, D. V.; Pyshnaya, I. A. SDS-PAGE procedure: Application for characterization of new entirely uncharged nucleic acids analogs. *Electrophoresis* **2017**, 0, 1–5

[71] Sammons, R. J.; Harper, D. P.; Labbé, N.; Bozell, J. J.; Elder, T.; Rials, T. G. Characterization of Organosolv Lignins using Thermal and FT-IR Spectroscopic Analysis. *BioRes.* **2013***,* 8, 2752-2767.

[72] Weiss, R.; Ghitti, E.; Sumetzberger-Hasinger, M.; Guebitz, G. M.; Nyanhongo, G. S. Lignin-Based Pesticide Delivery System. *ACS Omega* **2020**, 5, 4322−4329.

[73] De Vries, R. P.; Visser, J. Aspergillus Enzymes Involved in Degradation of Plant Cell Wall Polysaccharides. *Micro. Mol. Bio. Rev.* **2001**, 65, 497-522.

[74] Mallinson, S. J. B.; Machovina, M. M.; Silveira, R. L.; Garcia-Borras, M.; Gallup, N.; Johnson, C. W.; Allen, M. D.; Skaf, M. S.; Crowley, M. F.; Neidle, E. L.; Houks, K. N.; Beckham, G. T.; DuBois, J. L.; McGeehan, J. E. A promiscuous cytochrome P450 aromatic O-demethylase for lignin bioconversion. *Nat. Commun.* **2018**, 9, 2487.

\

STATUTORY DECLARATION

I hereby declare that I am the sole author of this thesis work, no assistance other than that permitted has been used, have not utilized any sources outside those permitted and that the sources used directly or indirectly have been cited verbatim or quoted textually in the places indicated. This written work has not been submitted in any part.

Vienna 2020 Mohammed Faraaz Ali

EIDESSTATTLICHE ERKLÄRUNG

Ich erkläre eidesstattlich, dass ich die Arbeit selbständig angefertigt habe. Es wurden keine anderen als die angegebenen Hilfsmittel benutzt. Die aus fremden Quellen direkt oder indirekt übernommenen Formulierungen und Gedanken sind als solche kenntlich gemacht. Diese schriftliche Arbeit wurde noch an keiner Stelle vorgelegt.

Wien 2020 Mohammed Faraaz Ali